WEAK LANGMUIR TURBULENCE

Sam L. MUSHER[a], **Alexander M. RUBENCHIK**[b], **Vladimir E. ZAKHAROV**[c,d]

[a]*Institute of Automation, Siberian Branch of Russian Academy of Sciences, 630090 Novosibirsk, Russia*
[b]*Department of Applied Science, University of California at Davis, and Lawrence Livermore National Laboratory, Plasma Physics Research Institute, L-418, Livermore, CA 94550, USA*
[c]*Landau Institute of Theoretical Physics, Russian Academy of Sciences, 117334 Moscow, Russia*
[d]*Department of Mathematics, University of Arizona, Tucson, AZ 85721, USA*

Weak Langmuir turbulence

Sam L. Musher[a], Alexander M. Rubenchik[b], Vladimir E. Zakharov[c,d]

[a]*Institute of Automation, Siberian Branch of Russian Academy of Sciences, 630090 Novosibirsk, Russia*
[b]*Department of Applied Science, University of California at Davis, and Lawrence Livermore National Laboratory,
Plasma Physics Research Institute, L-418, Livermore, CA 94550, USA*
[c]*Landau Institute of Theoretical Physics, Russian Academy of Sciences, 117334 Moscow, Russia*
[d]*Department of Mathematics, University of Arizona, Tucson, AZ 85721, USA*

Contents

Abstract

Weak turbulence theory presents a regular method for a statistical description of nonlinear wave interactions. The present review deals with an application of weak turbulence theory to Langmuir wave turbulence. Our main attention is devoted to a plasma with comparable ion and electron temperatures, both magnetized and unmagnetized. In this practically important situation ion-sound motions are heavily damped, which simplifies the physics of nonlinear phenomena.

We will demonstrate that the turbulence spectra are highly anisotropic and take the form of "jets" in k-space, and that the onset of a steady state is nontrivial and sometimes does not occur at all.

On the base of the jet-like spectra approach it is possible to find the turbulence spectra, to evaluate the anomalous absorption rate and to determine the comparable role of the different absorption mechanisms for a number of practical problems: the excitation of waves by powerful electromagnetic radiation or by electron and ion beams.

We demonstrate also that the range in which pure weak turbulence is valid is pretty narrow. The jet-like spectra structure stimulates a modulation instability and after that wave self-focusing and collapse. Then, weak and strong turbulence coexist.

The final part of the review deals with the turbulence of nonisothermal plasmas when additional degrees of freedom are excited. We demonstrate that the ideas, models and methods, presented in this review, give us a chance to advance greatly in the understanding of turbulence patterns.

0. Introduction

In common cases the characteristic times of the nonlinear wave interaction are sufficiently larger than their periods and one can consider the oscillations to be locally linear with slowly varying parameters. This approach permits to develop a self-consistent description of turbulence in terms of an integro-differential wave kinetic equation (Weak Turbulence Theory). Within the weak turbulence framework waves are described as quasi-particles and their interactions are the decay or scattering of long-lived quasi-particles.

The kinetic wave equation have a stationary solution, corresponding to thermodynamical equilibrium – The Rayleigh–Jeans spectrum. In the late 1960s nonequilibrium exact solutions of the kinetic equation were discovered [1-4] – the Kolmogorov spectra. There are power law isotropic solutions providing fluxes of the energy or the number of quasi-particles from the excitation zone to the dissipation range through the inertial interval.

How are these solutions related to specific cases? Do they exist under anisotropic excitation? What is the character and period of their onset? The essential advance in the understanding of all these problems was done in the last years. The linear stability of Kolmogorov spectra was studied and an exact criterion was obtained [5]. Some general results on the spectra matching with anisotropy pump are available. All these studies are summarised in a recent book [6]. But we are far from the deep understanding of the whole pattern of the weak turbulence. The present review deals with one important example of weak turbulence – the Langmuir plasma turbulence. The dominant nonlinear process is a decay of plasma wave into another plasma oscillation and ion-sound wave

$$l \rightarrow l' + s .$$ (1)

In an isothermal plasma, when the damping of ion-sound is larger than typical time of nonlinear interaction, the kinetic wave equation takes a simple form (see e.g. [7,8])

$$\partial n_k / \partial t = n_k \left(\gamma_k + \int T_{kk'} n_{k'} \, dk' \right) .$$ (2)

Here n_k is a plasmon number density in k-space, γ_k comprises wave damping and excitation. Due to the conservation of the plasmon number in the process (1) the matrix element $T_{kk'}$ is antisymmetric $T_{kk'} = -T_{k'k}$. Just the first studies of the weak Langmuir turbulence of isothermal plasma equation within Eq. (2) demonstrated quite specific features [9–11]. The turbulence happened to be strongly anisotropic had pronounced peaks in k-space, the onset of steady-state spectra was slow and took place only due to the small noise level. It was recognized [12, 13] that it is related with the general features of Eq. (2). It was shown that in the general situation the stationary distribution n_k is singular, localized on surfaces, lines or, even, at some points in k-space. A small noise regularizes solutions of (2) and defines the width of distributions. Equation (2) has a hidden Hamiltonian structure which results in a nontrivial temporal evolution of turbulence. General features of this kinetic equation are discussed in Section 1. A conception of jet-like spectra possessed the essential advance in the analytical studies of the large number of particular problems. The turbulent spectra excited by electron beams and by powerful electromagnetic waves in an isotropic plasma are described in the following sections. Then the theory of the turbulence of magnetized plasma is

developed. In this case even crude estimates of the nonlinear processes are sensitive to the details of plasmon distribution in k-space and only an exact theory can provide reliable data.

Later in the review a relation between the turbulence pattern and Kolmogorov spectra is studied. Briefly, the answer is: an average value of the exact solutions within the inertial interval coincide with the Kolmogorov ones, again demonstrating the fundamental position of the Kolmogorov–Richardson ideas.

Recently intensive and detailed experimental studies of Langmuir turbulence excited by powerful radars were done (see e.g. [14, 15]). These studies demonstrated that frequently weak turbulence breaks even for moderate pump intensities. As a result a discussion of the applicability of weak turbulence becomes important and we deal with this subject in one of the last sections. It is shown that the singularity of Langmuir spectra causes a modulational instability. It results in the local growth of the electric field and then in the Langmuir collapse or strong Landau damping switches on, increasing an efficiency of the plasma waves absorption. We show that this strong, spatially inhomogeneous turbulence inherits a lot of the homogeneous weak turbulence features and can be considered as a modified weak turbulence.

PART I. LANGMUIR TURBULENCE OF ISOTHERMAL PLASMA

1. Kinetic equation for Langmuir waves

The dispersion law for plasma Langmuir oscillations with wave vector $\vec{k}$ and frequency $\omega_{\vec{k}}$ has a form

$$\omega_{\vec{k}} = \omega_{\mathrm{p}}(1 + \tfrac{3}{2}k^2 r_{\mathrm{D}}^2) \tag{1.1}$$

for wavelengths larger than the Debye radius $k^2 r_{\mathrm{D}}^2 \ll 1$. It means that all Langmuir waves have close frequencies although their wavelengths can differ by several orders. This narrowness of the frequency spectrum can be used as a small parameter significantly simplifying description of nonlinear interactions. Namely, we can use an averaging method which is based on the fact that the harmonic oscillations with frequency near ω_{p} are the quickest type of motion (see [16, 17]). The plasma motions can be divided into two types: high-frequency electron oscillations and low-frequency ones involving ions. The interaction of high-frequency oscillations will be neglected, which allows us to describe them using the linearized hydrodynamical equations for an electron gas

$$(\partial/\partial t)\delta n_{\mathrm{e}} + \nabla \cdot (n_0 + \delta n) v_{\mathrm{e}} = 0 , \tag{1.2}$$

$$(\partial/\partial t) v_{\mathrm{e}} + 3 v_{T_{\mathrm{e}}}^2 \nabla(\delta n_{\mathrm{e}}/n_0) = -(e/m)E . \tag{1.3}$$

These equations can be supplemented by Maxwell's equations from which the magnetic field

$$(\partial^2/\partial t^2)E + c^2 \nabla \times \nabla \times E - 4\pi e(n_0 + \delta n)(\partial/\partial t)v_{\mathrm{e}} = 0 \tag{1.4}$$

is eliminated. In (1.2)–(1.4) the electron density is imagined in the form

$$n = n_0 + \delta n_{\mathrm{e}} + \delta n , \quad \delta n_{\mathrm{e}}, \delta n \ll n_0 . \tag{1.5}$$

Here δn and δn_e are the density variations connected with low-frequency and high-frequency motions, respectively. In (1.2)–(1.4) the terms of the order $(\delta n_e/\delta n)v/v_e$ are eliminated. From the continuity equation it is seen that as to order of magnitude this is the ratio of the phase velocities of the low- and high-frequency motions $c_s k/\omega_p \sim kr_D\sqrt{m/M} \ll 1$. Before making further considerations, it should be noted that in the nonlinear terms and the terms describing the thermal dispersion, the linear relations can be used for connecting $\delta n_e, v_e$. Taking this into account, it is not difficult to reduce (1.2)–(1.4) to the equation

$$(1/c^2)((\partial^2/\partial t^2) + \omega_p^2)E + \nabla \times \nabla \times E - (3v_{T_e}^2/c^2)\nabla\nabla\cdot E + (\omega_p^2\delta n/c^2 n_0)E = 0 . \tag{1.6}$$

In the linear approximation, when $\delta n = 0$, it describes Langmuir and electromagnetic waves with the dispersion laws

$$\omega_L^2 = \omega_p^2 + 3k^2 v_{T_e}^2 ; \qquad \omega_t^2 = \omega_p^2 + k^2 c^2 . \tag{1.7}$$

Now let us consider oscillations with a frequency close to the plasma one (for the Langmuir oscillations this means $kr_D \ll 1$, and for electromagnetic ones $kc \ll \omega_p$) and imagine the electric field in the form

$$E = \tilde{E}\exp(-i\omega t) + \text{c.c.} . \tag{1.8}$$

Here $\tilde{E}$ is a slowly varying quantity $\partial\tilde{E}/\partial t \ll \omega_p\tilde{E}$. Substituting (1.8) into (1.6) and neglecting the second derivative, finally the following expression is obtained:

$$-2i\omega_p\partial\tilde{E}/\partial t + c^2\nabla \times \nabla \times \tilde{E} - 3v_{T_e}^2\nabla\nabla\cdot\tilde{E} + (\omega_p^2/n_0)\delta n\tilde{E} = 0 . \tag{1.9}$$

Eq. (1.9) is convenient for describing oscillations with a frequency close to the plasma frequency. Taking into account the intrinsic electron nonlinearities in (1.2), (1.3) could lead to the excitation of oscillations at double plasma and zero frequencies which could lead, in turn, to the appearance of terms of the type $r_D^2 \nabla^2(EE/nT)$ in (1.9). They are negligibly small if the characteristic time of the nonlinear processes following from (1.9) satisfies a rather soft condition.

$$1/\tau \gg \omega_p\tilde{E}^2/mnv_{ph}^2 \sim \omega_p(\tilde{E}^2/8\pi nT)(kr_D)^2 , \tag{1.10}$$

here v_{ph} is a characteristic phase velocity. Besides, it should be noted that in (1.9) the quantity $(vT_e^2/c)^2$ is a small parameter allowing the separation of potential and nonpotential oscillations. Assuming that $\tilde{E} - \nabla\psi$ and taking the divergence of both parts of (1.9) we obtain

$$\nabla^2\left(i\frac{\partial}{\partial t} + \frac{3}{2}\frac{v_{T_e}^2}{\omega_p}\nabla^2\right)\psi = \frac{\omega_p}{2}\nabla\cdot\frac{\delta n}{n_0}\nabla\psi . \tag{1.11}$$

Eq. (1.11) conserves the integral $I = \int |\nabla\psi|^2\,d\vec{r}$ coinciding apart from a multiplying factor, with the number of Langmuir plasmons. Eq. (1.9) conserves the analogous integral $\int|\tilde{E}|^2\,d\vec{r}$ having the meaning of the total number of Langmuir and electromagnetic plasmons. To close (1.11) it is necessary to find another connection between δn and $\tilde{E}$. For this purpose it should be noted that the phase velocities of the electrons taking part in low-frequency motions are considerably less than

the thermal velocities, and they can be described in hydrodynamical terms and considered stationary:

$$\overline{(v_e \, \nabla)v_e} = \frac{e}{m} \, \nabla\varphi_{el} - \frac{e}{mc} \, \overline{[v \times H]} + \frac{T_e}{m} \, \frac{\nabla n}{n_0} \; . \tag{1.12}$$

Here the bar means averaging over time, and φ_{el} is the electrostatic potential of the low-frequency motions. Using the identity $(v\nabla)v = \frac{1}{2}\nabla v^2 - [v \times \nabla \times v]$ and the Maxwell equation $(1/c)(\partial H/\partial t) = -\nabla \times E$ we obtain

$$\overline{(v_e \, \nabla)v_e + \frac{e}{mc} \, [v_e \times H]} = \frac{1}{2} \, \overline{\nabla v_e^2} = \frac{e^2}{4m^2\omega_p^2} \, \nabla|\tilde{E}|^2 = \frac{1}{m} \, \nabla\phi \; . \tag{1.13}$$

Thus, it is evident that high-frequency oscillations lead to the appearance of force having a potential ϕ (Miller's force), and pushing out the electrons from the region of the electric field localization. It should be noted that this force acts on electrons only (the corresponding force acting on ions is m/M times smaller. As regards (1.12), it describes the Boltzmann distribution of electrons,

$$\delta n/n_0 = (1/T_e)(e\varphi_{el} - \phi) \; , \tag{1.14}$$

for which a thermodynamical equilibrium has time to be established due to slowness of the low-frequency motions. The ion distribution function obeys Vlasov's equation in the potential φ_{el}:

$$\frac{\partial f_i}{\partial t} + (v\nabla)f_i - \frac{e}{M}\left(\nabla\varphi_{el}\frac{\partial f_i}{\partial v}\right) = 0 \; . \tag{1.15}$$

The quasi-neutrality condition

$$\delta n_i = \int f_i \, dr - n_0 = \delta n = (n_0/T_e)(e\varphi_{el} - \phi) \tag{1.16}$$

allows φ_{el} to be determined and thus the system of equations (1.9), (1.15) to be closed. Eq. (1.15) takes into account a nonlinear interaction of low-frequency waves which in the majority of cases can be neglected. After linearization of (1.15) the variation of the density δn can be expressed linearly by the high-frequency force potential $\phi(r, t)$. This connection can be expressed in terms of the dielectric tensor; however, it is more convenient to introduce a plasma Green function $G_{k,\Omega}$, defining it by the relations between Fourier transforms

$$\delta n_{k\Omega} = (n_0/T_e)G_{k\Omega}\phi_{k\Omega} \simeq (n_0/T_e)\phi_{k\Omega}((\varepsilon_e/\varepsilon) - 1) \; . \tag{1.17}$$

Here ε is the longitudinal part of a dielectric tensor, and ε_e is the electron contribution to it. For $G_{k,\Omega}$ from (1.14), (1.15) it follows that

$$G_{k\Omega} = \frac{T_e}{Mn_0} \frac{L_{k\Omega}}{1 - (T_e/Mn_0)L_{k\Omega}} \; , \quad L_{k\Omega} = \int \frac{k\partial f_{0i}/\partial v}{kv - \Omega} \, dv \; . \tag{1.18}$$

The Green function possesses obvious properties analogous to those of ε:

$$G_{k\Omega} = G^*_{k-\Omega} = G_{-k\Omega} \; . \tag{1.19}$$

What is more, since it is expressed through ε, $G_{k\Omega}$ it is also analytical in the upper half-space of the variable Ω. In some cases the system of equations (1.9)- (1.17) can be considerably simplified. If the characteristic times of all the processes are rather great $\tau^{-1} \ll kv_{T_i}$, the ion distribution in the low-frequency electric field can be considered as a Boltzmann distribution:

$$\delta n/n_0 = - e\varphi_{el}/T_i \ll 1 \ . \tag{1.20}$$

With the help of a quasi-neutrality condition from (1.13) it follows

$$\delta n/n_0 = - \phi/(T_e + T_i) = |\tilde{E}|^2/16\pi n_0(T_e + T_i) \ . \tag{1.21}$$

In the potential case Eq. (1.11), within the framework of the above-mentioned "static" approximation, is of the form

$$\nabla^2(\mathrm{i}\psi_t + \tfrac{3}{2}\omega_p r_D^2 \nabla^2\psi) + (\omega_p/32\pi n_0(T_e + T_i)) \nabla\cdot| \nabla\psi|^2 \nabla\psi = 0 \ . \tag{1.22}$$

From this equation the following estimate follows:

$$1/\tau \sim \omega_p(W/nT) \sim \omega_p k^2 r_D^2 \ , \quad W \sim \tilde{E}^2/8\pi \ . \tag{1.23}$$

From the applicability conditions for (1.22) follow:

$$W/nT \ll mT_i/MT_e \quad (kr_D)^2 \ll (mT_i/MT_e) \ . \tag{1.24}$$

In the opposite limiting case $\tau^{-1} \gg kv_{T_i}$ for low-frequency motions the following hydrodynamical description is valid:

$$((\partial^2/\partial t^2) - c_s^2 \nabla^2)\delta n = (1/16\pi M) \nabla^2|\tilde{E}|^2 \ , \quad c_s^2 = (T_e + \tfrac{5}{2}T_i)/M \ . \tag{1.25}$$

In the nonisothermal plasma $T_e \gg T_i$ (see later) (1.25) is applicable at all amplitudes of the field; in the long-wave limit $k^2 r_D^2 < (m/M)T_i/T_e$ for small intensity of oscillations $W/nT < (m/M)T_i/T_e$ the static equation (1.22) follows from (1.25). In an isothermal plasma $T_i \sim T_e$ Eq. (1.25) is valid for describing turbulence with a high level $W/nT > (m/M, k^2 r_D^2)_{max}$, when the plasma motion becomes supersonic under the pressure of a high-frequency field. In this case the term $c_s^2 \nabla^2\delta n$ in (1.25) can be neglected. The simple asymptotics $G_{k\Omega}$ correspond to the simplified equations (1.22), (1.25). First of all, it should be noted that $G_{k\Omega}$ is a function of the parameter $\zeta = \Omega/kv_{T_i}$. In the limit $\zeta \ll 1$ or $\Omega \ll kv_{T_i}$ we have

$$G_{k\Omega} = - T_e/(T_e + T_i) \ . \tag{1.26}$$

In the hydrodynamical limit $\zeta \gg 1$ or $\Omega \gg kv_{T_i}$ $G_{k\Omega}$ has a pole corresponding to ion-sound waves. Expanding (1.18), we obtain

$$G_{k\Omega} = k^2 c_s^2/(\Omega^2 - k^2 c_s^2 + 2\mathrm{i}\gamma_s\Omega) \ . \tag{1.27}$$

When compared with (1.25), the Green function accounts for the sonic wave damping

$$\gamma_s = kc_s\sqrt{\pi m/8M} \ . \tag{1.28}$$

In (1.27) only Landau damping on electrons is directly taken into account; however, within the framework of the above-mentioned scheme it is not difficult to account for the ion Landau damping. The system (1.22), (1.25) was widely used in studies of strong Langmuir turbulence during

the last years (see e.g. [17–21]). Recently some attempts had been made in order to modify this system by taking into account a finite ion temperature. Also a straightforward including of Landau damping was done in some early papers devoted to numerical plasma experiments (see Refs. [17-21]). A modification of Eq. (1.25) using a more accurate approximation of Green function (based on the ideas suggested in [22]) was considered in [20, 23]. It follows, however, from the results of these papers that this simulation of an isothermal plasma with including a large damping is not adequate, it is impossible to improve somehow such an approach by the modification (1.25). Therefore, only an exact structure of the green function must be considered. We will show later that Langmuir spectra are quite sensitive to the structure of Green function $G_{k,\Omega}$ and its proper approximation is necessary for reliable numerical simulations. Finally, in the last variant of the simplifications of the dynamical equations valid for a sufficiently strong damping of ion-sound oscillations we can consider low-frequency motions as forced. Relation (1.18) can be rewritten in the form

$$\delta n_{k\Omega} = (n_0 e^2 (2\pi)^{-2}/4m\omega_p^2 T_e) \int G_{k_1 - k_2, \Omega} (\tilde{E}_{k_1, \omega_1} \tilde{E}^*_{k_2, \omega_2})$$

$$\times \delta(k_1 - k - k_2)\delta(\omega_1 - \omega_2 - \Omega) dk_1 dk_2 d\omega_1 d\omega_2 . \tag{1.29}$$

It is obvious that at a low level of nonlinearity we have $\tilde{E}_{k,\omega} \simeq \tilde{E}_k \delta(\omega - \omega_k)$, here ω_k is the law of wave dispersion reckoned from the plasma frequency. With this accuracy the inverse Fourier time transform can be made in (1.29):

$$\delta n_k(t) = ((2\pi)^{-3/2}/16\pi n T_e) \int G_{k_1 - k_2, \omega_1 - \omega_2} (\tilde{E}_{k_1} \tilde{E}^*_{k_2})\delta(k_1 - k - k_2) dk_1 dk_2 . \tag{1.30}$$

Considering the oscillations to be potential, let us introduce the variable

$$a_k = i(8\pi\omega_p)^{-1/2} \psi_k , \qquad E_k = -ik\psi_k , \tag{1.31}$$

determined in such a manner that the value $\int \omega_k |a_k|^2 dk$ coincides with the total energy of Langmuir oscillations. Substituting (1.30) into (1.11), we obtain finally

$$(\partial a_k/\partial t) + (\omega_k + i\gamma_k)a_k = i \int T_{kk_1 k_2 k_3} a^*_{k_1} a_{k_2} a^*_{k_3} \delta(k + k_1 - k_2 - k_3) dk_1 dk_2 dk_3 , \tag{1.32}$$

where

$$T_{kk_1 k_2 k_3} = \frac{\omega_p^2}{(2\pi)^3 4n T_e}$$

$$\times \left[\frac{(kk_2)(k_1 k_3)G((\omega_1 - \omega_3)/|k_1 - k_3|) + G((\omega_1 - \omega_2)/|k_1 - k_2|)(kk_3)(k_1 k_2)}{kk_1 k_2 k_3} \right] . \tag{1.33}$$

The plasma oscillations damping which can be considered to be collisional $\gamma_k \simeq \nu_{ei}$ is included in (1.32). The matrix element $T_{kk_1 k_2 k_3}$ in (1.33) possesses the symmetry properties following from the symmetry relations for the Green function:

$$T_{kk_1 k_2 k_3} = T^*_{k_2 k_3 kk_1} , \tag{1.34}$$

when

$$\omega_k + \omega_{k_1} = \omega_{k_2} + \omega_{k_3} \,.$$ (1.35)

It should be noted that in the above-considered static approximation

$$T_{kk_1k_2k_3} = \frac{\omega_p^2}{(2\pi)^3 4n(T_e + T_i)} \left[\frac{(kk_2)(k_1k_3) + (kk_3)(k_1k_2)}{kk_1k_2k_3} \right] \,.$$ (1.36)

The real and imaginary parts of the Green function $G_{k\Omega}$ quickly decreases if $\Omega \gg kv_{T_i}$. Therefore, when $kr_D \gg \sqrt{m/M}$ (1.33) shows that only oscillations with close wave vectors interact with one another. The condition $(\omega_{k_1} - \omega_{k_3})/|k_1 - k_3| \sim 1$ gives $|k_1| - |k_3| \sim r_D^{-1}\sqrt{mT_i/MT_e} \equiv k_{dif}$. Here the quantity k_{dif} is introduced which has the meaning of a characteristic size of the matrix element. For the validity of (1.32) it is necessary that the nonlinear corrections in the argument of the Green function would be negligibly small. In the region of the spectrum $k^2r_D^2 < m/M$, when Langmuir oscillations cannot excite ion-sound, this condition is of the form

$$1/\tau \sim \omega_p(W/nT) \sim (kr_D)^2\omega_p < kv_{T_i} \,.$$ (1.37)

That is, in this case (1.32) makes the static approximation equations more precise. When $k^2r_D^2$, for the validity of (1.32) it is necessary that all the sonic oscillations would be forced, that is, all characteristic times τ would exceed the ion-sound damping time $\gamma_s\tau > 1$. Using the expression (1.27) for the Green function in a hydrodynamical approximation, from (1.32) we obtain for a characteristic time of a nonlinear process $\tau^{-1} \sim \omega_p(\tilde{W}/nT)(\omega_s/\gamma_s)$. Here $\tilde{W}$ is the energy density within the interval of wave vectors of the order of the Green function size. If the noise density is uniformly distributed over the scale k, then $\tilde{W} \simeq W\,k_{dif}/k$, the applicability condition takes the form

$$(W/nT)(k_{dif}/k) \ll kr_D\sqrt{(m/M)}(\gamma_s/\omega_s)^2 \,.$$ (1.38)

In particular, for an isothermal plasma, where $\gamma_s \sim \omega_s$, condition (1.38) is in the form $W/nT < k^2r_D^2$. We assume later that in the case to be considered the interaction of such a great number of monochromatic waves takes place that is necessary to describe these phenomena statistically. In this description the information on interacting wave phases is lost and the wave field is described using the language of mean quadratic amplitudes, pair correlation function of complex amplitudes a_k. Then for the correlation function $\langle a_k a_{k'}^* \rangle$ we have

$$\langle a_k a_{k'} \rangle = n_k \delta_{k-k'} \,.$$ (1.39)

To derive a closed equation for n_k – kinetic equation – we assume that the wave field is a close Gaussian stochastic process and the fourth-order correlation function can be split into pair ones [25–27]:

$$\langle a_k^* a_{k_1}^* a_{k_2} a_{k_3} \rangle = n_k n_{k_1}(\delta_{k-k_2}\delta_{k_1-k_3} + \delta_{k-k_3}\delta_{k_1-k_2}) \,.$$ (1.40)

This assumption is valid if the nonlinearity is small enough, and the relative rotation of the phases cannot be correlated by nonlinear interactions. A detailed consideration of an applicability of the weak turbulence approach is given in Section 9. A more rigorous derivation of weak turbulence equations can be done also by the usage of a diagram technique (see [28]).

Multiplying (1.32) by a_k^*, subtracting the complex conjugate expression and taking into account formula (1.39)–(1.40), we obtain

$$(\partial n_k/\partial t) + 2n_k\left(\gamma_k - \int T_{kk'}n_{k'}\,\mathrm{d}k'\right) = 0 \,, \tag{1.41}$$

where $T_{kk'} = -T_{k'k} = \operatorname{Im} T_{kk',kk'}$.

One can see that Eq. (1.41) have an isotropic solution n_k = const. It is a Kolmogorov-type turbulence spectrum corresponding to a constant flux of the number of Langmuir plasmons towards small k region.

We will show later that very often in (1.41) a small noise term f_k has to be included

$$(\partial n_k/\partial t) + 2n_k\left(\gamma_k - \int T_{k,k'}n_{k'}\,\mathrm{d}k'\right) = f_k \,, \tag{1.42}$$

which represents the small thermal noise or small terms, omitted during the derivation of (1.41). As was told above, Eq. (1.32) is not valid when the damping of the ion-sound waves is not small enough. In this situation a corresponding equation must describe the evolution of ion-sound oscillations besides Langmuir waves. If simultaneously with the substitution (1.31) we change to the normal variables [24]

$$\delta n_k = \sqrt{(kn_0/c_s)}(b_k + b_k^*) \,, \qquad v_k = -\mathrm{i}k\sqrt{(c_s/2kn_0)}(b_k - b_k^*) \tag{1.43, 1.44}$$

for the ion-sound and Langmuir oscillations, the system of equations (1.22), (1.25) is reduced to an equation for high-frequency waves

$$(\partial a_k/\partial t) + \mathrm{i}\omega_k a_k = -\mathrm{i}\int [V_{k_1 k_2 k}b_{k_1}a_{k_2}\delta(k - k_1 - k_2)$$

$$+ V_{k_1,kk_2}^* b_{k_1}^* a_{k_2}\delta(k + k_1 - k_2)\,\mathrm{d}k_1\,\mathrm{d}k_2 \,, \tag{1.45}$$

and an equation for low-frequency waves

$$(\partial b_k/\partial t) + \mathrm{i}\Omega_k b_k = -\mathrm{i}\int V_{kk_1,k_2}^* a_{k_1}^* a_{k_2}\delta(k + k_1 - k_2)\,\mathrm{d}k_1\,\mathrm{d}k_2 \,, \tag{1.46}$$

here $\Omega_k = c_s k$ is the frequency of ion-sound waves and V_{kk_1,k_2} is the corresponding matrix element

$$V_{kk_1,k_2} = \frac{1}{(2\pi)^{3/2}}\frac{\omega_p}{2\sqrt{2Mnc_s}}\sqrt{k}\frac{(k_1 k_2)}{k_1 k_2} \,. \tag{1.47}$$

Introducing the averaged variables analogously to (1.39):

$$\langle a_k a_{k'}^*\rangle = N_k\delta(k - k') \,, \qquad \langle b_k b_{k'}^*\rangle = n_k\delta(k - k') \,, \tag{1.48}$$

we obtain for the description of the decay processes

$$\omega_k = \omega_{k_1} + \Omega_{k_2} \,, \quad k = k_1 + k_2 \,, \tag{1.49}$$

the following kinetic equations:

$$(\partial N_k/\partial t) + \gamma_k N_k = \int (R_{k_2|kk_1} - R_{k_2|k_1k}) \, \mathrm{d}k_1 \, \mathrm{d}k_2 \,, \tag{1.50}$$

$$(\partial n_k/\partial t) + \Gamma_k n_k = - \int R_{k|k_1,k_2} \, \mathrm{d}k_1 \, \mathrm{d}k_2 \,, \tag{1.51}$$

where

$$R_{k_2|kk_1} = 2\pi |V_{k_2kk_1}|^2 [N_{k_1}n_{k_2} - N_k n_{k_2} - N_{k_1}N_k]\delta(k - k_1 - k_2)\delta(\omega_k - \omega_{k_1} - \Omega_{k_2}) \,. \tag{1.52}$$

If Γ_k is large enough, $n_k \ll N_k$ and Eqs. (1.50), (1.51) are reduced to (1.41) with $T_{k,k'}$:

$$T_{k,k'} = - T_{k',k} = 2\pi \frac{(kk')^2}{(kk')^2} \frac{\omega_{\mathrm{p}}^2}{4nT} \left[\delta\left(\frac{\omega_k - \omega_{k'}}{c_{\mathrm{s}}|k - k'|} - 1 \right) - \delta\left(\frac{\omega_k - \omega_{k'}}{c_{\mathrm{s}}|k - k'|} + 1 \right) \right] \,. \tag{1.53}$$

One can see that (1.53) can be obtained directly from (1.41) by using instead of (1.27) the following expression:

$$\mathrm{Im}\, G_{k,\Omega} \simeq \pi \left[\delta\left(\frac{\Omega}{kc_{\mathrm{s}}} - 1 \right) - \delta\left(\frac{\Omega}{kc_{\mathrm{s}}} + 1 \right) \right] \,. \tag{1.54}$$

With the help of (1.52) one can also estimate the value of f_k. It will be done later.

Up to now we are discussing only the waves in an isotropic plasma. It is easy to take into account a weak magnetic field when the electron cyclotron frequency ω_{H} is well below ω_{p} ($\omega_{\mathrm{H}} \ll \omega_{\mathrm{p}}$). In this case it is sufficient to take into account in Eqs. (1.41) and (1.50), (1.51) the change of the dispersion law:

$$\omega_k = \omega_{\mathrm{p}}(1 + \tfrac{3}{2}k^2 r_{\mathrm{D}}^2 + \tfrac{1}{2}(\omega_{\mathrm{H}}^2/\omega_{\mathrm{p}}^2)\sin^2\theta) \,, \tag{1.55}$$

where θ is an angle between the wave vector k and the magnetic field B.

In a strong magnetic field a modification of the matrix elements takes place. There are two types of a high-frequency potential oscillations in a magnetized plasma. The first wave is the upper-hybrid mode with the following dispersion law:

$$\omega_k = \omega_{\mathrm{p}}(1 + \tfrac{1}{2}(\omega_{\mathrm{p}}^2/\omega_{\mathrm{H}}^2)\sin^2\theta) \,. \tag{1.56}$$

The main features of this mode are similar to the corresponding characteristics of Langmuir waves. For fusion applications low-hybrid waves are more important:

$$\omega_k = \omega_{\mathrm{p}}|\cos\theta| \,. \tag{1.57}$$

Usually, the magnetized plasma of the fusion devices is an isothermal one, and the main nonlinear process is the induced scattering by particles (see [29]). In this case the dynamics of turbulence is also described by Eq. (1.41), but with more complicated matrix elements [29, 30]. In a strong magnetic field $\omega_k \omega_{\mathrm{H}} \gg \omega_{\mathrm{p}}^2$ it is possible to simplify these matrix elements up to the form

$$T_{k,k'} = \frac{\omega_{\mathrm{p}}^2}{4\pi} \frac{(k_z k_z')^2}{(kk')^2} \mathrm{Im}\, G\left(\frac{\omega_k - \omega_{k'}}{|k - k'|} \right) \,, \tag{1.58}$$

where G is the same function, as in (1.18). Another specific case of a magnetized plasma will be discussed below. Expression (1.58) looks very similar to the kernel of the corresponding equation for Langmuir waves; we will see, however, that a difference in the dispersion law changes drastically all patterns of the turbulence.

2. The weak turbulence spectra are singular

Let us consider the stationary spectra of Langmuir turbulence:

$$\left(\gamma_k + \int T_{kk'} n_{k'} \, \mathrm{d}k' \right) n_k = f_k \, . \tag{2.1}$$

It follows from this equation that

$$n_k = \frac{f_k}{\left(\gamma_k + \int T_{kk'} n_{k'} \, \mathrm{d}k' \right)} \, . \tag{2.2}$$

The following inequality takes place due to the condition $n_k \geq 0$:

$$\gamma_{\mathrm{eff}}(k) = \gamma_k + \int T_{kk'} n_{k'} \, \mathrm{d}k' > 0 \, . \tag{2.3}$$

Passing in (2.1) to the limit $f_k \to 0$ we obtain

$$\left(\gamma_k + \int T_{kk'} n_{k'} \, \mathrm{d}k' \right) n_k = 0 \, . \tag{2.4}$$

There are a lot of solutions of (2.4). We can assume, for example, that

$$n_k = \sum_{l=1}^{m} N_l \delta(k - k_l) \, , \tag{2.5}$$

where k_l is an arbitrary set of points in k-space. The spectrum (2.5) is a solution of (2.4) if the quantities N_l are solutions of the finite system of equations

$$\gamma_{k_l} + \sum_{p=1}^{m} T_{k_l, k_p} N_p = 0 \, . \tag{2.6}$$

Of course, the positiveness of the solutions is not guaranteed. In the general case the solution of (2.4) is concentrated on some set Ω which will be called later a "compact support" or simply "support". From the formal point of view, the support can be given arbitrarily. It is sufficient only that there should exist at least one solution of Fredholm's integral equation of the first kind on this set Ω:

$$\gamma_k + \int_{\Omega} T_{kk'} n_{k'} \, \mathrm{d}k' = 0 \, . \tag{2.7}$$

But we have to keep in mind the criteria (2.3). Peforming the passage to the limit $f_k \to 0$, we can check that the following inequality takes place

$$\gamma_{\text{eff}}(k) \geq 0 \,. \tag{2.8}$$

It means that the set Ω is part of the tangent points of the non-negative function $\gamma_{\text{eff}}(k)$ and the null plane. We will illustrate it by an example. Let us assume k-space to be one dimensional and

$$T_{kk'} = k - k' \,, \qquad \gamma_k = k(k-1) \,, \tag{2.9}$$

from which we get

$$\gamma_{\text{eff}}(k) = k(k-1) + kN - N_1 \,,$$

$$N = \int_{-\infty}^{\infty} n_k \, dk \,, \qquad N_1 = \int_{-\infty}^{\infty} k n_k \, dk \,.$$

The function γ_{eff} is a parabola which can contact the axis of abscissa at the only one point $k = k_0$, so $\gamma_{\text{eff}} = (k - k_0)^2$. There are $2k_0 = 1 - N$, $k_0^2 = N$; besides $n_k = N\delta(k - k_0)$, therefore $N_1 = k_0 N$. Solving the system of equations obtained, we are convinced now, that $k_0 = 0$ and obtain

$$n_k = \delta(k) \,. \tag{2.10}$$

The information about the structure of the set of the tangent points Ω can be determined in some cases from general considerations. For example, if γ_{eff} is an analytical function then the set Ω cannot include the whole parts of the three-dimensional k-space. In this case Ω must consist of lower-dimensional manifolds, i.e. surfaces, lines and separate points. The equality $\gamma_{\text{eff}} = 0$ can be fulfilled only in exceptional cases. It happens if there is a positive solution of Fredholm's equation of the first kind

$$\gamma_k + \int T_{kk'} n_{k'} \, dk' = 0 \tag{2.11}$$

over the whole range of k'. It has to be noted that the set Ω can be efficiently reconstructed at the small variation of γ_k and $T_{kk'}$. The separate lines and the surfaces in Ω must be split into separate points at the action of the disturbances of the general type. All the more, it happens in the maximally degenerate case of the coincidence Ω with the whole k-space. The unique situation of the structural stability corresponds to the case when the set Ω consists of a discrete set of points: any small variation of equation leads only to small shifts of the points.

Nevertheless, in the concrete cases considered below we will study "jet-like" spectra concentrated on lines and surfaces in k-space. These considerations are the sequences of the definite approximation – in a more precise examination the "lines" and the "surfaces" are decomposed into an aggregate of separate points. This decomposition develops a "fine structure" of the "jet-like" spectra. As a whole, those spectra will be called "singular", for which the "support" consists of the manifolds with a lower dimensionality than the dimension of k-space. Integrating (2.1) over the whole k-space, we obtain due to the antisymmetry of $T_{kk'}$:

$$\int \gamma_k n_k \, dk = \int f_k \, dk \,. \tag{2.12}$$

So we have in the tending f_k to zero

$$\int \gamma_k n_k \, \mathrm{d}k = 0 \, . \tag{2.13}$$

It is the equation of the balance of the quasi-particle numbers. It follows, in particular, from this equation that $n_k = 0$ in the case $\gamma_k \geq 0$ – the damping regions are necessary for the solution of (2.1) to exist.

Let us repeat the arguments above in a different manner. It follows from the condition $\gamma_{\mathrm{eff}} \geq 0$ that the surface γ_k is situated above the surface $- \int T_{kk'} n_{k'} \, \mathrm{d}k'$ and that they touch one another at the points on which the solution n_k is localized. It means that at the points where $n_k = 0$ damping is larger than the "driving term". It follows that the stability of the solutions is guaranteed by this circumstance. The functions γ_k and $\int T_{kk'} n_{k'} \, \mathrm{d}k'$ have a different origin and topology. It is naturally that they can touch one another only along some lines or at separate points in k-space.

Let us examine now the influence of the small noise f_k on the solutions of (2.2). It depends on the dimension of the manifold Ω, more precisely, from the co-dimension (a co-dimension is the difference between the dimensions of the whole k-space and the "support"). Up to now we assumed that the dimension of the phase space was equal $d = 3$, however, it makes sense to consider the cases $d = 1$, $d = 2$.

Let the co-dimension be equal to one $d_0 = 1$. Three cases are possible:

– the spectrum is located on a two-dimensional surface in the three-dimensional k-space;
– the spectrum is located on a line in the two-dimensional k-space;
– the spectrum is concentrated on some point in the one-dimensional k-space (as in the example considered above).

Let us assume k to be a perpendicular coordinate with respect to the support. At $f_k = 0$ we have $\gamma_{\mathrm{eff}} = \alpha k^2$, $\alpha > 0$. At the small but finite $f_k = f$ the function γ_{eff} becomes a positive parabola

$$\gamma_{\mathrm{eff}} = \alpha(k - \delta k)^2 + \beta \, , \ \beta > 0 \tag{2.14}$$

and for the spectrum we obtain

$$n_k = f/(\alpha(k - \delta k)^2 + \beta) \, . \tag{2.15}$$

The total intensity of the spectrum must be constant as the f_k tend to zero, so we have

$$\int_{-\infty}^{\infty} (f/(\alpha(k - \delta k)^2 + \beta) \, \mathrm{d}k = N \tag{2.16}$$

and we get that $\beta = 4f^2/N\alpha^2$. Thus the distribution of waves is described by a Lorentz formula with the width Δ equal to

$$\Delta = 2f/\alpha\sqrt{N} \, . \tag{2.17}$$

The small value of the shift of the distribution $\delta k \sim f$ remains uncertain, we will not take it into account later.

Let the co-dimension d_0 to be equal to two. It takes place in two cases: either the spectrum is located on a line in the three-dimensional k-space or the spectrum is located at a point in the

two-dimensional space. There are two orthogonal directions with respect to the support k_1, k_2 and we have

$$\gamma_{\text{eff}} = \alpha_1 k_1^2 + \alpha_2 k_2^2 + \beta , \qquad n_k = f/(\alpha_1 k_1^2 + \alpha_2 k_2^2 + \beta) ,$$

while

$$\int f/(\alpha_1 k_1^2 + \alpha_2 k_2^2 + \beta) \, dk_1 dk_2 = N . \tag{2.18}$$

The integral in (2.18) diverges, however, and must be "cut" at the some wave number k_0. We obtain with logarithmic accuracy

$$N = \frac{\pi f}{2\sqrt{\alpha_1 \alpha_2}} \ln \left(\frac{\sqrt{\alpha_1 \alpha_2} k_0}{\beta} \right) , \qquad \beta = \sqrt{\alpha_1 \alpha_2} k_0 \exp \left(- \frac{2N\sqrt{\alpha_1 \alpha_2}}{\pi f} \right) . \tag{2.19, 2.20}$$

The distribution (2.18) is better located than (2.16) in spite of the logarithmically diverging "tail", because the characteristic width Δ of the distribution can be assumed as before

$$\Delta \simeq \sqrt{\beta/\alpha} . \tag{2.21}$$

This quantity is decreasing more quickly as $f \to 0$ than defined by formula (2.17).

At last, the co-dimension $d_0 = 3$ can be realized only for the spectrum n_k concentrated at a point in three-dimensional k-space. Then we have at $f \to 0$,

$$\gamma_{\text{eff}} = \alpha_1 k_1^2 + \alpha_2 k_2^2 + \alpha_3 k_3^2 \tag{2.22}$$

and there is an integrable singularity at $k = 0$

$$n_k = f_k/\gamma_{\text{eff}} . \tag{2.23}$$

If all the α_i are of the same order then the integration of (2.23) over the whole k-space provides the contribution $\delta N \sim f k_0/\alpha$ (tending to zero as $f \to 0$) to the integral intensity. It is the only thing to be done: to conserve the δ-shaped singularity at the point $k = 0$. Thus the "smoothing" of the singular spectrum does not occur by including the small thermal noise at the $d_0 = 3$ case. This smoothing takes place as soon as a finite, completely defined value f_k is given. The phenomenon is completely analogous to the phase transition of the second kind at the transition of liquid helium from the super-fluid state into the normal one. The singular part of the spectrum corresponds to the super-fluid component and the "smoothed" part – to the normal one. We will show now that sometimes it is enough to have a very small level of thermal noise f_k for the regularization of the singular spectra and the transforming into smooth distributions. Let us consider the simplified one-dimensional example

$$(\partial n_k/\partial t) + n_k \left(\gamma_k + \int_{-\infty}^{\infty} T(k - k') n_{k'} \, dk' \right) = f_k \tag{2.24}$$

with $T(q) = -T(-q)$. We assume also $T(\infty) = 0$ and $T(q) > 0$ at $q > 0$. Let us examine Fredholm's equation of the first kind

$$\gamma_k + \int_{-\infty}^{\infty} T(k - k') n_{k'} \, dk' = 0 \tag{2.25}$$

and try to obtain the criteria for the smooth regular solution of (2.25) to exist. We denote by δ_1 the width of the increment γ_k and by δ_2 the characteristic scale of the kernel $T(q)$. It is evident that if $\delta_2 \geq \delta_1$ we have no smooth solutions of (2.25). In this case the spectrum consists of the spectral peaks separated by the interval $\sim k_2$. We have a right to assume the regular distribution at $\delta_2 \ll \delta_1$. The formal solution of (2.25) takes the form

$$n_k^0 = (1/2\pi) \int (\gamma_\lambda/T_\lambda)\exp(-ik\lambda)\,d\lambda \,, \tag{2.26}$$

where γ_λ and T_λ are the Fourier transforms of the functions γ_k and $T(q)$, respectively. This solution is meaningless for $\delta_1 < \delta_2$ because the function γ_λ/T_λ increases at large λ. In the opposite case $\delta_1 \gg \delta_2$ the function γ_λ/t_λ decreases at large λ if γ_k is a sufficiently smooth function. Generally speaking, the smoothness of γ_k is unclear a priori. For the case of insufficient smoothness of the γ_k the stationary spectrum is the aggregate of very close spectral peaks. It is evident that only small variations of γ_k are enough to achieve the complete regularization of the solution. It can be done by including the term f_k/n_k in Eq. (2.25). Thus, the ratio of δ_1,δ_2 defines the type of the stationary spectra by taking into account the thermal noise. We will speak of the singular regime at $\delta_1 \leq \delta_2$ and at $\delta_1 \gg \delta_2$ – of the regular one. The limiting case of the complete regularization corresponds to $\delta_2 \to 0$, then it can assume $T(q) \to T_0\delta'(q)$. Eq. (2.25) takes the form

$$\gamma_k + T_0(\partial/\partial k)n_k = 0 \tag{2.27}$$

and its solution is

$$n_k = -(1/T_0)\int_{k_0}^{k} \gamma_q\,dq \,, \tag{2.28}$$

the integration is performed from the point k_0 ($\gamma_{k_0} = 0$); this expression is valid until the obtained solution n_k is positive. This solution must be merged later with the trivial solution $n_k = 0$. It is necessary to emphasize that formula (2.26) gives a true picture only if the Fourier transform T_λ has no zeroes different from $\lambda = 0$. In fact, let us assume the pair of such zeroes to be given at the points $\lambda = \pm \lambda_0$ ($T_{\pm\lambda_0} = 0$); then it is possible to add to any solution of (2.25) the oscillating term $A\cos(\lambda_0 k + \phi)$ with arbitrary A and ϕ. Furthermore, for Eq. (2.25) to be solvable the orthogonality γ_k to the functions $\sin\lambda_0 k$, $\cos\lambda_0 k$ is demanded. Generally speaking, this criterion is not fulfilled. The situation can be redeemed by taking into account the term f_k/n_k. Then the orthogonality criteria become the system of equations which determine A and ϕ:

$$\int \left\{ \gamma_k - \frac{f_k}{n_k^0 + A\cos(\lambda_0 k + \phi)} \right\} \cos\lambda_0 k\,dk = 0 \,,$$

$$\int \left\{ \gamma_k - \frac{F_k}{n_k^0 + A\cos(\lambda_0 k + \phi)} \right\} \sin\lambda_0 k\,dk = 0 \,.$$

Thus, in the presence of additional zeroes of the function T_λ the regular spectrum n_k^0 has an oscillatory structure with period $2\pi/\lambda_0$. We will see later that such oscillations are seen at the numerical modelling of the induced scattering kinetics.

3. Jets in k-space

The considerations, presented above, are very general. We now start to apply these ideas to a detailed study of Langmuir turbulence spectra. The main equation is (see (1.42)):

$$(\partial n_k/\partial t) + 2n_k \left(\gamma_k - \int T_{kk'} n_{k'} \, dk' \right) - f_k = 0 , \tag{3.1}$$

where $T_{kk'} = -T_{k'k} = \text{Im } T_{kk',kk'}$. The characteristic size of the kernel $T_{kk'}$ in (3.1) $k_{\text{dif}} \simeq (1/r_{\text{D}})$ $\times \sqrt{m/M}$ is the maximum momentum to be transfered in a single scattering act. This value plays a basic role in the theory of Langmuir turbulence. The characteristic size of the region of excitation Δk (the size of γ_k) depends on the method of pumping. In the case $\Delta k \gg k_{\text{dif}}$ one can expect (according to the results of the previous sections) an excitation of the smooth over k spectra with a typical scales much larger than the characteristic size of the matrix element $T_{kk'}$. In this case it is possible to substitute $n_{k'}$ in (3.1) as

$$n_{k'} \simeq n_k + (\partial n_k/\partial k)(|k'| - |k|) . \tag{3.2}$$

Really it is more convenient to write

$$T_{kk'} = \frac{(kk')^2}{(kk')^2} \text{Im } G \left(\frac{\omega_k - \omega_{k'}}{|k - k'|} \right) \simeq \frac{(kk')^2}{(kk')^2} \alpha \delta' \left(\frac{\omega_k - \omega_{k'}}{|k - k'|} \right) , \tag{3.3}$$

where the prime on the δ-function denotes differentiation with respect to the argument; the constant α is equal to

$$\alpha = - \int_{-\infty}^{\infty} x \, \text{Im } G(x) \, dx . \tag{3.4}$$

As was mentioned above, the function $G(x)$ is analytical in the upper semiplane and this integral can be calculated exactly with the help of dispersion relations: $\alpha = \pi$. This approximation of the matrix element $T_{kk'}$ is the so-called "differential approximation". Finally we obtain [31–33]:

$$T_{kk'} = \frac{2\pi}{9} \frac{m}{M} \frac{1}{r_{\text{D}}^2} \frac{\omega_{\text{p}}^2}{n_0 T_{\text{e}}} \cos \Omega^2 (1 - \cos \Omega) \delta'(|k| - |k'|) ; \tag{3.5}$$

here Ω is the angle between the vectors k and k', the prime on the δ-function denotes differentiation with respect to the argument. It has to be noted that (3.5) does not depend on the ratio of electron and ion temperatures. The approximation (3.5) means that the spectra are smooth functions of the moduli of the wave vectors and all singularity is concentrated in the angular behavior. For each fixed modulus $|k|$ the spectra are located on the set of tangent points of a unit sphere and the function $\gamma_{\text{eff}}(k, n)$ is defined on this sphere (here $n = k/k$). This set consists of separate points which can be fused into lines in some exceptional cases. According to this statement the spectra in k-space will be concentrated on lines or surfaces in k-space. These lines (or surfaces) will be called two-dimensional or one-dimensional "jets", respectively. We restrict ourselves henceforth to the

axially symmetrical situation. We denote by θ and θ' the angles between the chosen direction and k and k', and obtain ultimately

$$\partial N_{k,x}/\partial t = N_{k,x}\left(\gamma(k,x) + (\partial/\partial k)\int_{-1}^{1} T(x,y)N(k,y)\,\mathrm{d}y\right).$$ (3.6)

We have introduced here the notation $x = \cos\theta$, $y = \cos\theta'$, $N(k,x) = k^2 n(k,x)$ and

$$T(x,y) = \frac{\pi^2}{9}\frac{m}{M}\frac{1}{r_D^2}\frac{\omega_p^2}{n_0 T_e}(1 - x^2 y^2 + 3x^2 y^2 - 3xy + 3xy^3 + 3x^3 y - 5x^3 y^3).$$ (3.7)

We note that the kernel $T(x,y)$ if of a definite sign

$$T(x,y) \geq 0$$ (3.8)

and is symmetrical

$$T(x,y) = T(y,x), \qquad T(-x, -y) = T(x,y).$$ (3.9)

In addition

$$T(1,1) = T(-1, -1) = 0.$$ (3.10)

When the excitation of waves is strictly isotropic, the spectrum $n(k,x)$ does not depend on x and Eq. (3.6) is simplified to the form

$$(\partial n_k/\partial t) + n_k(\gamma_k - T_0(\partial n_k/\partial k)) = 0.$$ (3.11)

here

$$T_0 = \frac{\pi^2}{9}\frac{m}{M}\frac{1}{r_D^2}\frac{\omega_p^2}{n_0 T_e}$$

and the spectra are regular. In the opposite cases ($\gamma(k,x)$ is anisotropic) the spectra are singular. Let us define

$$\gamma_{nl} = -(\partial/\partial k)\int_{-1}^{1} T(x,y)N(k,y)\,\mathrm{d}y.$$ (3.12)

In accordance with all the foregoing we must seek the spectral density $N(k,x)$ of Langmuir oscillations in the form

$$N(k,x) = \sum_i N_i(k)\delta(x - x_i(k)).$$ (3.13)

Here $x_i(k)$ is the shape of the jet and $N_i(k)$ is the intensity distribution along the jet. In the axially symmetrical situation the jets are two-dimensional; the only possible type of one-dimensional jet is $x = \pm 1$, when the surfaces γ_k and γ_{nl} are tangent at their poles. Let us assume that we know the number of jets r and their shapes $x_i(k)$, $i = 1, \ldots, r$. Then, substituting (3.13) into the stationary equation $\gamma_{nl} = 0$, we obtain a system of ordinary differential equations for the determination of the intensities:

$$\gamma(k,x(k)) + \sum_j T(x_i(k), x_j(k))(\partial N_j/\partial k) - \sum_j (\partial/\partial x_j)T(x_i(k), x_j(k))(\partial x_j(k)/\partial k)N_j(k) = 0.$$ (3.14)

The number of jets and the fact of existence or absence of one-dimensional jets on the poles should be determined from geometric considerations. To determine the shape of the ith two-dimensional jet it is necessary to use the obvious relation

$$(\partial/\partial x)[\gamma(k, x) - \gamma_{nl}]|_{x = x_i(k)} = 0 \ . \tag{3.15}$$

Substituting $N(k, x)$ in (3.15), we obtain an additional set of equations which makes the system (3.14) closed. The jet transports the flux of Langmuir quanta over the spectrum into the region of small wave numbers. Let us determine the value of this flux P_k. To this end, we integrate (3.6) over angles and introduce the symbol

$$\bar{N} = \int_{-1}^{1} N(k, x)\, dx \ . \tag{3.16}$$

We have

$$P_k = \frac{1}{2} \int_{-1}^{1} \int_{-1}^{1} N(k, x) N(k, y)\, dx\, dy > 0 \ , \qquad \partial \bar{N}/\partial t = \int_{-1}^{1} \gamma(k, x) N(k, x)\, dx + \partial P_k/\partial k \ . \tag{3.17}$$

Substituting (3.13) into (3.17), we express P_k in terms of the intensities of the jets:

$$P_k = \frac{1}{2} \sum_{i,j} T(x_i(k), x_j(k)) N_i(k) N_j(k) \ . \tag{3.18}$$

It is seen from (3.18) that the spectrum cannot consist of merely one one-dimensional jet, since a single one-dimensional jet $N_j(k, x) = N\delta(x \pm 1)$ would lead to a zero flux, by virtue of the conditions $T(1, 1) = T(-1, -1) = 0$. We consider now several examples of the determination of the shape of the jets.

1. Assume that the condition $\gamma(k, x) \equiv 0$ is satisfied in a region of k-space, $k_1 < |k| < k_2$. What is realized in this region is the Kolmogorov situation, which corresponds to a constancy of the flux of Langmuir quanta. The Kolmogorov solution of (3.6) is obviously of the form

$$N(k, x) = f(x) \ , \tag{3.19}$$

where f is an arbitrary function of x. We see therefore that the trajectories of the jets on the (k, x) plane should be straight lines parallel to the k axis. The position of these lines is determined by the condition that they be joined together at $|k| = k_2$.

2. Let $\gamma(k, x)$ have a sharply pronounced maximum at $x = \pm 1$. In this case there are two one-dimensional jets

$$N(k, x) = N_1 \delta(x - 1) + N_2 \delta(x + 1) \ , \tag{3.20}$$

with

$$\partial N_1/\partial k = -\gamma(k, -1)/T(-1, 1) \ , \qquad \partial N_2/\partial k = -\gamma(k, 1)/T(1, -1) \ . \tag{3.21}$$

The condition of "external stability" (3.15) yields the necessary and sufficient criterion for the existence of two one-dimensional jets:

$$\gamma(k, x) < \frac{1}{2}\{(x^2 + x^3)\gamma(k, 1) + (x^2 - x^3)\gamma(k, -1)\} \ . \tag{3.22}$$

This criterion takes on a particularly simple form in the symmetrical situation, when $\gamma(k, x) = \gamma(k, -x)$. We then have

$$\gamma(k, x) < x^2 \gamma(k, 1) , \quad |x| < 1 . \tag{3.23}$$

It follows from the results of Section 2 that jets can possess an oscillating structure (to be "spotted"). Let us consider this phenomena for our case of two one-dimensional jets. Eq. (3.6) is reduced to the form

$$(\partial n_k/\partial t) + \left(\gamma_k + \int_0^\infty T(k - k')n_{k'}' \, \mathrm{d}k' \right) n_k = f_k . \tag{3.24}$$

The kernel $T(k - k') = T(\kappa)$ quickly decreases for $\kappa \gg k_{\mathrm{dif}}$, so we can change the lower limit of integration in (3.24) to $-\infty$. The problem of the oscillating structure of n_k is defined now by the existence of additional zeroes of the Fourier transform $Q(\xi)$ of the kernel (except for $\xi = 0$). For $T_i \ll T_e$ we can take the "hydrodynamical" approximation of the Green function and obtain

$$Q(\xi) = T_0 \exp(-(\gamma_s/\omega_s)\xi k_{\mathrm{dif}})\sin(\xi k_{\mathrm{dif}}) , \tag{3.25}$$

which corresponds to an infinite number of zeroes. For $T_i \sim T_e$ the existence of zeroes is defined by the fine structure of the ion distribution function. For most experimental parameters the plasma is usually a nonisothermal one. It means that the jets will be always "spotted". We will show later that the jet-like spectra are modulated, the characteristic size of these "spots" is close to k_{dif}.

3. Let $\gamma(k, x)$ be a symmetrical function of x and let it have a sharply pronounced maximum at $x = 0$. We consider the possible existence of one two-dimensional jet at the point $x = 0$. Putting $N(k, x) = N(k)\delta(x)$, we obtain

$$\gamma(k, 0) = - T(0, 0)\partial N(k)/\partial k . \tag{3.26}$$

Condition (3.15) yields

$$\gamma(k, x) < \gamma(k, 0)(1 - x^2) . \tag{3.27}$$

The situation with one two-dimensional jet is also characteristic of the case when $\gamma(k, x)$ has a sharp maximum at sufficiently small x.

In the general case, the problem of determining the number of jets and their shapes is quite complicated; nor is the question of uniqueness of such a distribution trivial. Some examples of the jet-like Langmuir spectra are presented in the review [34].

3.1. Influence of a weak magnetic field

Imposition of the weak magnetic field causes a modification of the dispersion law of the electrostatic plasma oscillations [35]:

$$\omega_k = \omega_p \left[1 + \frac{3}{2} k^2 r_{\mathrm{D}}^2 + \frac{1}{2} \frac{\omega_{\mathrm{H}}^2}{\omega_p^2} \frac{k_\perp^2}{k^2} \right] . \tag{3.28}$$

One can see that it leads to an effective enlargement of the inertial interval; it is caused by a decrease of the wave numbers when increasing the angle between the wave vector and the magnetic

field. Let us remind that in a plasma without external magnetic field the inertial interval is equal to

$$N \sim \omega_{\mathrm{p}}/ck_{\mathrm{dif}} \sim (v_{T_e}/c)\sqrt{M/m} \qquad (3.29)$$

"steps" of the spectral cascading. Even for thermonuclear parameters $N \sim 5$-6. It means that already at the moderate excesses above the instability threshold $\gamma_{\max}/\nu_{\mathrm{ei}} \sim N$ Langmuir spectra (smooth or singular) reach the collapse region $k \simeq 0$. The presence of the magnetic field makes the conditions for the collisional absorption of the wave energy more favorable tending to a heating of the bulk of the particles. The nonlinear effects in the case $\omega_{\mathrm{H}} \ll \omega_{\mathrm{p}}$ are the same as in a plasma without a magnetic field. The ions can be regarded as unmagnetized under the weak condition

$$8\pi n T/H^2 \gg m/M \ .$$

Therefore, it is necessary to take into account only the differences in the frequencies for the Green function $G_{k\Omega}$. It does not change the anisotropic character of the induced scattering by ions, and Langmuir spectra must be jet-like. This conclusion was first obtained in [36] (for more details see Section 6), and later such spectra were investigated, e.g. at the parametric excitation [37,38] (see also Section 7) and at the interaction of a relativistic electron beam with a plasma [39].

4. Peak-kinetics model

Assume that the characteristic size of the excitation region $\Delta k \ll k_{\mathrm{dif}}$ and that the maximum of γ_k lie in k-space near k_0, $|k_0| \gg k_{\mathrm{dif}}$. An analysis of the matrix element shows that the waves interacting most strongly with the initial ones are those located along the vector k_0 near the points $k_0 \pm k_{\mathrm{dif}}$. In this case the waves in the vicinity of the point $-k_0 + k_{\mathrm{dif}}$ will grow, and those in the vicinity of the point $\pm k_0 + k_{\mathrm{dif}}$ will attenuate. If the initial noise level is small, then a peak with width $\Delta k \ll k_{\mathrm{dif}}$ is produced near the point $-k_0 + k_{\mathrm{dif}}$. Repeating this reasoning, we arrive at the conclusion that the spectrum in k-space will comprise after a certain time a linear sequence of peaks located near the points $\pm(k_0 - nk_{\mathrm{dif}})$ [40–43]. Assuming that the intensities of all peaks differ from the noise level, we represent the distribution n_k in the form

$$n_k = \sum_{n=0}^{n_1} N_n\delta(k_0 - nk_{\mathrm{dif}}) + \sum_{n=0}^{n_2} M_n\delta(-k_0 + nk_{\mathrm{dif}}) \ . \qquad (4.1)$$

The kinetic equation now takes the form

$$\partial N_n/\partial t = N_n[\gamma_0 + T(M_{n-1} - M_{n+1})] \ , \qquad (4.2)$$

$$\partial M_n/\partial t = M_n[\gamma_0 + T(N_{n-1} - N_{n+1})] \ , \qquad (4.3)$$

where T is the largest absolute value of $T_{kk'}$. In the symmetrical case we have $M_n = N_n$ and (4.2), (4.3) reduce to the single equation

$$\partial N_n/\partial t = N_n[\gamma_n + T(N_{n-1} - N_{n+1})] \ . \qquad (4.4)$$

Eqs. (4.2)–(4.4) describe the kinetics of the peaks; the actual peak width does not enter in these equations. Nonetheless, these peaks must not be too narrow $(\delta k r_D)^2 \gg W/nT_e$, for otherwise the quasi-monochromatic peaks will experience an automodulation instability (see corresponding section of this review). In the stationary situation the number of the peaks and their intensities are possible to calculate under the assumption that

$$\gamma_k + \int_0^\infty T(k - k')n'_k \, dk' = 0 \tag{4.5}$$

at $n_k \neq 0$, or in the "peak"-approximation

$$\gamma_n + \sum_m T(k_n - k_m)N_m = 0 \tag{4.6}$$

and the criteria of the "external stability" has to be fulfilled

$$\gamma_k + \int_0^\infty T(k - k')n'_k \, dk' < 0 \tag{4.7}$$

at $n_k = 0$. The latter equation can be re-written in the form

$$\gamma'(k_n) + \sum_m T'(k_n - k_m)N_m = 0 \,, \tag{4.8}$$

here the prime denotes differentiation with respect to the argument. Eqs. (4.6), (4.8) can be simplified if we assume that only the nearest-peaks interact effectively due to the quick decreasing of the function $T(\kappa)$. Then we obtain

$$\gamma(k_n) + T(k_n - k_{n-1})N_{n-1} - T(k_{n+1} - k_n)N_{n+1} = 0 \,,$$

$$\gamma'(k_n) + T'(k_n - k_{n-1}) - T'(0)N_n - T'(k_{n+1} - k_n)N_{n-1} = 0 \,.$$

There is a solution of this system of equations in the dissipationless case:

$$k_n = n\,\Delta k \,, \qquad N_n = \text{const} \,, \qquad 2T'(\Delta k) = T'(0) \,. \tag{4.9}$$

It is a chain of equidistant peaks with the same amplitudes; the distance between the neighbours is equal to the value k_{dif} with good accuracy. It is possible also to obtain the amplitudes of peaks in the case of nonzero damping, e.g. collisional one ν_{ei}. It takes the form of a chain of linearly decreasing peaks. The amplitude of the last one is equal to $N_c = \nu_{ei}/\tilde{T}$, where $\tilde{T} = T(k_n - k_{n-1}) = -T(k_{n+1} - k_n) = T(k_{dif})$.

5. Kinetics of the induced scattering of Langmuir waves by ions

Kinetics of the induced scattering of Langmuir waves is qualitatively different from the well-known kinetics of quasi-particles in the solid state. As will be shown in this section, the behavior of weak Langmuir turbulence is defined mainly by the two remarkable features: by the existence of a Hamiltonian structure of the kinetic equation and by a "theorem of uniqueness". The structure of the equation and the behavior of its solutions are similar to the corresponding features of the equations by Lotka–Volterra [44], initially used for the description of the dynamics of fish

populations and auto-catalytic reactions. The kinetic equation in the "peak" approximation is analogous to the Lotka–Volterra equation and this was noted more than once (see e.g. [45]). So it is possible to use a general Volterra invariant in order to provide a condition of the "stability as a whole" [46].

Let us assume the stationary solution n_k^{st} to exist and examine the functional

$$I = \int n_k^{st} \left\{ \frac{n_k(t)}{n_k^{st}} - 1 - \ln \left(\frac{n_k(t)}{n_k^{st}} \right) \right\} dk \ . \tag{5.1}$$

One can see that the quantity I is positive. Let us calculate the time-derivative I; after simple transformations we obtain

$$\frac{dI}{dt} = - \int f_k \frac{(n_k(t) - n_k^{st})^2}{n_k(t) n_k^{st}} dk \ . \tag{5.2}$$

The derivative is less than zero for any distribution of Langmuir waves and is equal to zero only if $n_k(t) = n_k^{st}$. Thus, in the nonstationary regime, the quantity I must decrease with time. It means that any solution of Eq. (1.41) as $t \to \infty$ is tending to the steady state (of course, if it exists at all). It is also clear, that the stationary solution is unique [46]. Eq. (5.2) can be re-written in the form

$$\frac{dI}{dt} = - \int \gamma_{eff}(k) \frac{(n_k(t) - n_k^{st})^2}{n_k(t)} dk \tag{5.3}$$

and the quantity I is simplified too

$$I = \frac{1}{2} \int \frac{(n_k(t) - n_k^{st})^2}{n_k(t)} dk \ . \tag{5.4}$$

Thus, the characteristic time of the relaxation τ_{rel} is defined by the integral of $\gamma_{eff}(k)$ being "weighted" with $(n_k(t) - n_k^{st})/n_k(t)$, and, consequently, τ_{rel} strongly depends on the degree of deviation from the steady state. The relaxation is the slowest for disturbances near the maximum of n_k^{st} (where γ_{eff} has a minimum). As $f_k \to 0$ τ_{rel} is tending to infinity. It does not mean, however, that at $f_k = 0$ there is no relaxation at all. There occurs a change in the relaxation law from an exponential to a power-law one. Let us consider again an example (2.9) from Section 2 of the review. It is possible for this example to integrate directly the kinetic equation

$$n_k(t) = n_k(0)\exp(-k^2 t + k(t - f_1(t)) - f_0(t)) \ , \tag{5.5}$$

where

$$\partial f_1/\partial t = N_0(t) \ , \qquad \partial f_0/\partial t = N_1(t) \ , \tag{5.6}$$

and $n_k(0)$ is the initial distribution; for simplicity we will assume $n_k(0) = const = n_0$. For f_0 and f_1 we obtain

$$\partial f_0/\partial t = (2n_0\sqrt{\pi}/\sqrt{t})\exp(\tfrac{1}{4}t(1 - f_0/t)^2 - f_1) \ , \qquad \partial f_1/\partial t = -(1 - f_0/t)\partial f_0/\partial t \ .$$

Asymptotically as $t \to \infty$ there is $\partial f_0/\partial t \to 1$, so we have

$$\partial f_1/\partial t = -I \ ; \qquad \tfrac{1}{4}tI^2 - f_1 = \ln(2n_0\sqrt{\pi}/\sqrt{t}) \ , \qquad I = 1 - f_0/t \to 0 \ .$$

Finally, $f_1 \to -\ln(2n_0\sqrt{\pi}/\sqrt{t})$, $I \to 1/2t$ as $t \to \infty$ and

$$n_k(t) \to (\sqrt{6}/2\sqrt{\pi})\exp(-k^2 t + \tfrac{1}{2}k) \ . \tag{5.7}$$

The distribution (5.7) is a growing and tightening packet of waves. The width of the packet is decreasing as $1/\sqrt{t}$ and the integral intensity is relaxing the most quickly, as $1/t^2$. When $f_k \neq 0$ we would obtain "two-scale" dynamics: Eq. (5.7) would be applicable up to $t \sim 1/f_k$, then the relaxation would go according to the exponential law $\tau \sim n_k^{\text{st}}/f_k$. A sharp slowing of the relaxation at $f_k \to 0$ is explained by the fact that the kinetic equation (1.41) at $f_k = 0$ is a Hamiltonian one [47] in spite of the presence of dissipation and consequently the phase volume and other integral invariants are conserved. Let us prove it. From the meaning of the quantity n_k it is evident that $n_k > 0$, so we may introduce a new variable $z_k = \ln n_k$ determined along all of the real axis. Eq. (1.41) can be re-written at $f_k = 0$ in the form

$$\int R_{kk'}(\partial z_{k'}/\partial t)\,\mathrm{d}k' + 2(\Gamma_k - \exp(z_k)) = 0 \ , \tag{5.8}$$

where $R_{kk'}$ is the kernel of the operator inverse to the operator with the kernel $T_{kk'}$ and $\Gamma_k = \int R_{kk'}\gamma_{k'}\,\mathrm{d}k'$. It is evident that $R_{kk'} = -R_{k'k}$. Eq. (5.8) is Hamiltonian, i.e. can be written in the form

$$\int R_{kk'}(\partial z_{k'}/\partial t)\,\mathrm{d}k' = \delta H/\delta z_k^* \ , \tag{5.9}$$

where the Hamiltonian H takes the form

$$H = \int \mathrm{d}k(\exp(z_k) - \Gamma_k z_k) \ . \tag{5.10}$$

With the help of (5.8) it is easy to make sure that H is an integral of motion. When $\gamma_k = 0$, it transforms to the well-known law of the conservation of the number of quanta which is valid as was mentioned in the Section 1, yet within the framework of a dynamic description. When γ_k is not equal to zero, the Hamiltonian H is not calculated constructively, because of the difficulties of the inversion of $T_{kk'}$. However, it follows that (5.8) has no asymptotic steady stationary solutions. In reality, in a stationary state the Hamiltonian H differs, generally speaking, from that calculated from the initial data. Thus, the relaxation process to a stationary state (if it takes place) occurs only due to a small noise term which breaks the Hamiltonian structure and makes really Eq. (1.41) a kinetic one.

Let us examine briefly the time evolution of small disturbances of the stationary spectrum $n_k(t) = n_k^{\text{st}} + \delta n_k(t)$, $\delta n_k(t) \ll n_k^{\text{st}}$ in the scope of the one-dimensional approximation for the smooth distribution

$$(\partial n_k/\partial t) + n_k(\gamma_k - T_0\partial n_k/\partial k) = f_k \ ; \tag{5.11}$$

the small noise term is added to the (3.8). Linearizing (5.11) and assuming $\delta n_k \sim \exp(i\Omega t - iqk)$, we obtain the corresponding dispersion law

$$\Omega_q = T_0 n_k^{\text{st}} q + i f_k/n_k^{\text{st}} \ . \tag{5.12}$$

One can see that small disturbances of the stationary distribution are "second sound" waves moving along the spectrum with a velocity $v \simeq T_0 n_k^{\text{st}}$ towards the region of small k. These disturbances are neutrally stable as $f_k \to 0$ (in according to the results of this section).

We can consider also an evolution of small disturbances of the stationary spectrum in the "peak kinetics" model (see [48, 49, Eq. (4.4)]),

$$\partial N_n/\partial t = TN_n(N_{n-1} - N_{n+1}) + (\gamma_n - \nu_n)N_n + f . \tag{5.13}$$

Let us assume the case of the large excesses over threshold $\gamma_n \gg \nu_n$, then we can take the amplitudes of the "neighbors" to be approximately equal to $N_n^{\text{st}} \simeq \tilde{N}$. Linearizing (5.13) under approximation $\delta N_n = N_n - \tilde{N} \ll \tilde{N}$ and assuming $\delta N_n \sim \exp(\mathrm{i}\Omega t - \mathrm{i}n\delta\pi)$, we obtain

$$\Omega = 2\tilde{N}T\sin(\delta\pi) + \mathrm{i}f/\tilde{N} . \tag{5.14}$$

It follows from the results of numerical experiments [49, 50], that $\delta \simeq \frac{1}{2}$. One can see that in the singular case we have a similar picture as in the regular one – the characteristic time of the onset of the steady state is defined by the small thermal noise and the frequency of oscillations is defined by the nonlinear interaction of Langmuir waves. The same conclusions can be obtained for the three-dimensional (3-D) spectra.

The considerations presented above in this section, are valid, strictly speaking, in the idealized case of an infinite homogeneous system and also only in the case of the not large excesses over threshold of the excitation of Langmuir oscillations. Namely, there are another mechanisms of wave damping and the onset of the steady state. It appears due to the "carrying out" waves from the region of the excitation due to inhomogeneity or to the finite size of pumping (for details see Section 7). Then, as was mentioned above, the main feature of Langmuir turbulence is the existence of an energy flux toward small k-region. At the excesses over threshold $\gamma_{\text{pmax}}/\nu_{\text{ei}} > N = k_0/k_{\text{dif}}$ (after N steps of the spectral pumping from the region of the instability $k \sim k_0$) the oscillations reach the region $k \sim 0$. There is no linear damping of long Langmuir waves and there begins an accumulation of the wave energy, leading to the appearance of a "condensate" and Langmuir collapse [51]. It appears necessary to consider the interaction between the region $k \sim 0$ and the remaining turbulence. It will be considered at the end of this section; the main conclusion is: a collapse represents an effective damping of Langmuir waves for small wave vectors. This important circumstance changes the dynamics of Langmuir turbulence, leading, for example, to the deep modulations of the energy flux into the plasma from external pumping (see Section 6).

Singular and regular regimes are possible also in the nonstationary case. We consider first the regular regime [50]. Assume that initially there is in k-space a region where we can neglect the damping and the thermal noise. Eq. (1.41) or (2.24) takes in this region the form

$$\partial n_k/\partial t = 2n_k \int_{-\infty}^{\infty} T(k - k')n_{k'}\,\mathrm{d}k' . \tag{5.15}$$

We consider solutions of (5.15) in the form of waves travelling with constant velocity v towards the smaller wave numbers. We note that the kernel in (5.15) can be represented in the form

$$T(k - k') = (\partial/\partial k)S(k - k') , \qquad \int_{-\infty}^{\infty} S(k)\,\mathrm{d}k = q , \tag{5.16}$$

where $S(\xi)$ is a positive function that decreases as $|\xi| \to \infty$. We assume that $n_k \to n_0$ as $|k| \to \infty$. Making the substitution $\partial/\partial t \to v\partial/\partial k$, we integrate (5.16) ($x = (n/n_0) - 1$):

$$\ln(1 + x_k) = (2n_0/v) \int_{-\infty}^{\infty} S(k - k')x_{k'}\, dk' \, . \tag{5.17}$$

If $x_{\max} \ll 1$, the characteristic dimension of the solution in k-space is $\Delta k \gg k_{\mathrm{dif}}$, then

$$S(k - k') = q\left[\delta(k - k') + \alpha k_{\mathrm{dif}}^2 \frac{\partial^2}{\partial(k - k')^2} \delta(k - k')\right] . \tag{5.18}$$

Here α is a dimensionless parameter. Eq. (5.17) now takes the form

$$\frac{\alpha\beta}{1 - \beta} k_{\mathrm{dif}}^2 \frac{\partial^2 x}{\partial k^2} - x + \frac{x^2}{2(1 - \beta)} = 0 \, , \quad \beta = \frac{2qn_0}{v} \, . \tag{5.19}$$

Eq. (5.19) has for $0 < \beta < 1$ a solution that decreases on both sides

$$x_k = 3(1 - \beta)\cosh^{-2}\sqrt{\frac{1 - \beta}{4\alpha\beta}} \frac{k}{k_{\mathrm{dif}}} \, . \tag{5.20}$$

The solution (5.20) is a solitary wave–soliton – and is valid for $1 - \beta \ll 1$. In the same approximation, the nonstationary equation (5.15) reduces to the well-known Korteweg–de Vries equation

$$\frac{1}{v} \frac{\partial x_k}{\partial t} = (1 - \beta) \frac{\partial x_k}{\partial k} - \beta x_k \frac{\partial x_k}{\partial k} - \alpha\beta k_{\mathrm{dif}}^2 \frac{\partial^3 x_k}{\partial k^3} \, . \tag{5.21}$$

The characteristic scale of the soliton $k_{\mathrm{dif}}\sqrt{4\alpha\beta/(1 - \beta)} \gg k_{\mathrm{dif}}$ decreases with decreasing β. We consider Eq. (5.17) in the limiting case as $\beta \to 0$. The characteristic size of the soliton should now be small in comparison with k_{dif}, and Eq. (5.17) can be simplified to

$$x_k = \exp(\beta\widetilde{S}(k)N) - 1 \, . \tag{5.22}$$

Here

$$\widetilde{S}(k) = (k_{\mathrm{dif}}/q)S(k) \sim 1 \, , \qquad N = (1/k_{\mathrm{dif}}) \int_{-\infty}^{\infty} x_k\, dk \, . \tag{5.23}$$

The dimensionless parameter N is the ratio of the number of quasi-particles in the soliton to the number of "background' particles over the dimension k_{dif}. To determine N it is necessary to solve the transcendental equation

$$N = (1/k_{\mathrm{dif}}) \int_{-\infty}^{\infty} [\exp(\beta\widetilde{S}(k)N) - 1]\, dk \, . \tag{5.24}$$

Using the narrowness of the soliton, we can put in (5.24)

$$\widetilde{S}(k) = S_0(1 - k^2/k_0^2) \, , \tag{5.25}$$

where $k_0 \sim k_{\text{diff}}$. Calculating the integral, we obtain

$$N \approx \frac{1}{\sqrt{2\pi\beta N}} \frac{k_0}{k_{\text{dif}}} e^{\beta N} , \tag{5.26}$$

from which it follows, with logarithmic accuracy, that $n \sim \beta^{-1} \ln(\beta^{-1})$ as $\beta \to 0$, and the characteristic scale of the soliton is

$$\Delta k \sim k_{\text{dif}} \ln^{-1/2}(1/\beta) < k_{\text{dif}} . \tag{5.27}$$

Since the real parameter of this approximation is the quantity $\ln^{-1/2}(1/\beta)$, it is valid only for very small β. Nonetheless, a comparison of the two limiting cases allows us to assume that a solution of the soliton type exists in the entire interval $0 < \beta < 1$. Then in practically the entire interval, with the exception of the vicinity of its ends, the soliton dimension is $\Delta k \simeq k_{\text{dif}}$. Inasmuch as $\beta \sim 1/v$, we can state that the soliton dimension depends slightly on the velocity. However, the soliton intensity does depend on the velocity in an essential manner. There exists a minimal velocity $v_0 = 2qn_0$; as $v \to v_0$ we have $N \sim \sqrt{(v/v_0) - 1}$, and at $v \gg v_0$ we get $N \sim (v/v_0)\ln(v/v_0)$. Expressing the velocity in terms of the maximum soliton amplitude and the noise amplitude, we obtain

$$v \sim 2q\, n_{\text{max}}/\ln(n_{\text{max}}/n_0) . \tag{5.28}$$

Actually the dependence of the velocity on the thermal noise is weaker, since n_{max} (if $n_{\text{max}} \gg n_0$) is also proportional to $\ln n_0$. Therefore, in fact the velocity is determined only by the parameters of the growth rate: $v \sim \gamma_{\text{inst}} k$. The soliton can manage to become attenuated by the collisions before reaching the region of small k, if $\gamma_0 k_0 > v$, which coincides with the criterion for the existence of a stationary solution of (5.15). When the soliton is damped, it is slowed down and ultimately the soliton is stopped. Within the framework of the Korteweg–de Vries equation, the solitons are repelled (see e.g. [52]); this probably takes place also within the framework of the more exact Eq. (5.16). The onset of the stationary state can therefore be represented as the result of slowing down of solitons. In the opposite case $\gamma_{\text{inst}} > \gamma_0 k_0/\Delta k$, the soliton does not have time to slow down and is absorbed only in the collapse region. Then there are no grounds for expecting a stationary state to be established; this conclusion is confirmed (see below) by results of numerical experiments. In the case of a narrow instability growth rate and when a condition inverse to the applicability of (5.15) is satisfied, a nonstationary singular regime described by a corresponding equation from the Section 4 is realized. It was shown in [53] that Eq. (4.4) has at $\gamma_{\text{inst}} = 0$ an exact solution in the form of a soliton that travels along a chain of peaks:

$$N_n(t) = F(Tt - n/s - \tau_0) , \tag{5.29}$$

where

$$F(\xi) = N_0 \left(1 + \frac{a}{1 - b + b\cosh\delta\xi} \right) . \tag{5.30}$$

The quantities δ, b and s are obtained from the equations

$$\delta[(1 - b)^2 + b^2 \sinh^2(\delta/s)] = 2N_0(1 - b)(1 - b + a)\sinh(\delta/s) ,$$

$$\delta(1 - b) = N_0(2 - 2b + a)\sinh(\delta/s) , \quad \delta = 2N_0 \sinh(\delta/s) .$$

For $a \gg 1$ we have approximately

$$\delta = N_0 a , \qquad b^2 = 1/2a , \qquad s = \delta/\ln a . \tag{5.31}$$

The soliton has a velocity

$$v = TN_0 a \, k_{\mathrm{dif}}/\ln a , \qquad N_0 \sim n_0 k_{\mathrm{dif}} . \tag{5.32}$$

We note that, as was shown in [54], Eq. (4.4) with $\gamma_{\mathrm{inst}} = 0$ is a perfectly integrable dynamic system, within the framework of which one can obtain exact formulas describing soliton collisions. It is shown by the same token that the solitons are repelled by one another. The same (at $\gamma = 0$) is true for the systems (4.2) and (4.3). For $\gamma_{\mathrm{inst}} \gg \gamma_0 \, k/k_{\mathrm{dif}}$, the nonstationary regime constitutes a successive detachment of the solitons from the instability region. Let us estimate the parameters of this process. To this end we consider the interaction of two peaks,

$$\partial N_1/\partial t = N_1(\gamma_{\mathrm{inst}} - TN_2) , \qquad \partial N_2/\partial t = TN_2 N_1 , \tag{5.33}$$

of which the first is in the instability region and the second is at a distance k_{dif} from this region. At $t = 0$ we have $N_1 = N_2 = N_0$. The system (5.33) has an integral

$$N_1 + N_2 - 2N_0 = (\gamma_{\mathrm{inst}}/T)N_2/N_0 . \tag{5.34}$$

The maximum amplitude is reached when the intensities of both peaks are comparable; for $N_{1,2}/N_0 \gg 1$ we obtain with logarithmic accuracy

$$N_{\mathrm{max}} \sim \tfrac{1}{2}(\gamma_{\mathrm{inst}}/T)\ln(\gamma_{\mathrm{inst}}/2TN_0) . \tag{5.35}$$

The characteristic time of the process is

$$\tau \sim \gamma_{\mathrm{inst}}^{-1}\ln(\gamma_{\mathrm{inst}}/2TN_0) . \tag{5.36}$$

The average energy flux to the plasma

$$N_{\mathrm{max}}/\tau \sim \gamma_{\mathrm{inst}}^2 \omega_{\mathrm{p}}/2T \sim \gamma_{\mathrm{inst}}^2 n T_{\mathrm{e}}/\omega_{\mathrm{p}} \tag{5.37}$$

does not depend on the thermal-noise level. Strictly speaking, formula (5.35) contains also factors of the type $\ln \ln \gamma_{\mathrm{inst}}/2TN_0$, which are set equal to unity in order of magnitude.

5.1. Coexistence of weak turbulence and Langmuir collapse

One can see, however, that the kinetic pattern, presented above, is not complete and self-consistent. The matter is that spectral cascading due to induced scattering is directed towards the small k-range from the pumping region and it results in the condensation of plasmons in the state $k = 0$ at the sufficiently large excesses above threshold $\gamma_{\mathrm{nl}}/\gamma_{\mathrm{damp}} > k/k_{\mathrm{dif}}$. Let us remind ourselves briefly what occurs later on (see for example [55]). A condensation of Langmuir waves brings into a development of a modulational instability and the appearance of high local maxima of the electric field. An arising ponderomotive force is pushing out the plasma and is creating "cavities". The nonlinear stage of the modulational instability results in the compression of the cavities accompanied by kinetic effects – phenomena called "Langmuir collapse". This phenomena is well investigated now by various numerical simulations (see e.g. [56, 58]) and confirmed experimentally [57–59]. In the final stage of the collapse practically all energy, trapped in the cavities, is transferred

to the particles. Hence, there occurs an effective nonlinear mechanism of dissipation in the plasma. The compression of the cavities is a self-accelerated process and arising as a result of compression the Langmuir spectrum drops quickly towards large k numbers. The main part of the energy is concentrated at $k \leq \Delta k$, $(\Delta k r_{\mathrm{D}})^2 \simeq W/n_0 T$, where W is the density of the condensate energy. Usually Δk is sufficiently smaller than the characteristic wave number of the excited plasmons k_{ex} and therefore Langmuir collapse can be considered as a sink of the wave energy at $k \simeq 0$. It can be modelled, for example, by absorbing boundary conditions at small k. Absence of a real interaction between collapsed cavities and weak turbulence spectra is quite natural. Namely, during the developed stage of Langmuir collapse the cavities have a characteristic size l, which is smaller than the mean distance between the cavities $\sim (\Delta k)^{-1}$ and their evolution in time is very fast. Therefore, only a few "weak turbulent" plasmons can interact with the cavities. The value of Δk can be estimated as follows. The energy, trapped in the cavity, is transferred to the particles during a time interval τ, which is the "longest" time of Langmuir collapse phenomena, precisely, an inverse growth rate of the modulational instability $\gamma_{\mathrm{mod}}^{-1}$. For a low level of condensate $W/n_0 T \leq m/M \gamma_{\mathrm{mod}} \sim \omega_{\mathrm{p}} W/n_0 T$; if $W/n_0 T > m/M$ (supersonic collapse [55]) $\gamma_{\mathrm{mod}} \sim \omega_{\mathrm{p}} \sqrt{(m/M) W/n_0 T}$. The rate of the energy dissipation via collapse Q_{ab} can be written as

$$Q_{\mathrm{ab}} \sim \gamma_{\mathrm{mod}} W .$$

On the other hand, in the common situations a zone of the pump localization is far from the collapse range $k_{\mathrm{ex}} \gg \Delta k$ and the energy flux into the plasma can be calculated within the scope of weak turbulence. For small linear damping

$$Q \simeq Q_{\mathrm{ab}}$$

and the value of Δk can be obtained from this relation. Let us note that for $Q < \omega_{\mathrm{p}}(m/M)^2$, when the collapse is subsonic, $\Delta k \leq k_{\mathrm{dif}}$, and collapse really does not affect the weak turbulence spectra. For a stronger pump we have

$$\omega_{\mathrm{pi}}(W/n_0 T)^{1/2} W = Q .$$

With increasing of the pump Δk grows and, when Δk is approaching k_{ex}, the "naive" weak turbulence description is not valid.

Strictly speaking, considerations presented above on the coexistence of weak turbulence and Langmuir collapse, are valid for broad and smooth distributions. The singular structure of Langmuir spectra enhances the role of the modulational instability and the weak turbulence approach have to be modified. In more detail it will be discussed in Section 9.

6. Dynamics of weak turbulence spectra

In this section we shall consider the nonstationary behavior of weak Langmuir turbulence. The detailed theory of the steady-state spectra is developed in previous sections; it turned out to be possible to obtain only in general results about the onset of these spectra. We shall be concerned now with both the realization of such spectra and the dynamics of their onset. Reliable and long-term numerical simulation will be used as a constructive method to prove the existence and stability "as a whole" of the energy distributions over scales and to study the evolution of spectra.

Excitation of Langmuir waves by a relativistic electron beam, by an external electromagnetic wave at a frequency near the plasma frequency and the mutual evolution of the electromagnetic and Langmuir oscillations will be taken as physical examples of the developed theory; sometimes we shall discuss also results of numerical experiments with some model growth rates to consider a more general situation. It has been shown above that two different types of spectra can be expected – a smooth and a spike-like one. Qualitatively we have been known already the main parameters defining a transition from the regular spectra to singular. However, in the many interesting cases only a numerical experiment can demonstrate what type of spectra is realized. For example, in the case of parametric excitation with a frequency near the plasma one there is an intermediate situation (see Section 8): the size of the growth rate region is $\Delta k \sim \frac{1}{2} k_{\text{dif}}$, and a qualitative analysis cannot give the definite answer on the type of spectral distributions. We shall represent at first the results of simulation in the differential approximation and within a "peak-kinetics" model, then we shall discuss the numerical solution of the exact equations (1.41). At the end of the section we can examine the applicability of simplified models and evaluate quantitatively the degree of deviations from exact results.

6.1. Instability of relativistic electron beam

We have shown that the structure of Langmuir spectra is sensitive to the scale of the excitation region. We will be able to consider the "narrow" and "wide" regime of the wave excitation by changing the parameters of an electron beam. As was noted in [60], the principal mechanism that limits the growth of Langmuir oscillations is induced scattering by ions, which leads to a transfer of energy from the instability zone ($k > \omega_{\text{p}}/c$) into the region of smaller wave numbers. The characteristic time of the onset of the quasi-stationary spectrum of oscillations then turns out to be significantly smaller than the time of the variation of the distribution function of the electron beam. Thus, the distribution function of the beam electrons can be regarded as specified in the problem of determining the spectrum. We denote by E the energy of an individual electron, by $\Delta\theta$ and ΔE the angle and the energy spreads of the particles, and by n_{b} the beam density. If the angular spread $\Delta\theta$ is not too small,

$$\Delta\theta > (n_{\text{b}}mc^2/n_0 E)^{1/4} , \qquad (6.1)$$

then the instability is kinetic, i.e. the beam does not influence the wave dispersion law, and determines only the growth rate. If in addition

$$\Delta\theta > (mc^2/E)\sqrt{\Delta E/E} , \qquad (6.2)$$

then the spread of the beam electrons relative to the absolute value of the velocity can be neglected in the calculation of the growth rate, and we can put $v = cp/|p|$, where p is the electron momentum. The only oscillations that can interact with the beam are those whose wave vectors satisfy the Cherenkov resonance condition

$$\omega_{\text{p}} - \boldsymbol{k}\boldsymbol{v} = 0 \qquad (6.3)$$

or

$$|(\omega_{\text{p}}/c) - k_{\|}| \sim (\omega_{\text{p}}/c)(\Delta\theta)^2 + k_{\perp}\Delta\theta , \qquad (6.4)$$

where $k_\parallel$ and k_- denote the longitudinal and transverse (with respect to the beam axis) components of the vector $\boldsymbol{k}$. The instability growth rate $\gamma(k, x = \cos\theta)$ is given by the formula (see [61]):

$$\gamma(k, x) = \pi\omega_p \frac{n_b}{n_0} \left(\frac{\omega_p}{kc}\right)^3 \int_{x_1}^{x_2} \frac{dy}{\sqrt{(y - x_1)(x_2 - y)}} \left\{ -2g - \left(y - \frac{kcx}{\omega_p}\right)\frac{\partial g}{\partial y} \right\},$$

$$x_{1,2} = \left(\frac{\omega_p}{kc}\right)\left[x \pm \sqrt{1 - x^2}\sqrt{(1 - x^2)\left(\frac{k^2 c^2}{\omega_p^2} - 1\right)} \right], \qquad g(y) = mc\int_0^\infty f(p, y)p\, dp \qquad (6.5)$$

(f is the beam distribution function). For the maximal (at fixed k) value of the growth rate, which is reached for $x \sim \omega_p/kc$, the following estimate holds true

$$\gamma \sim \omega_p \frac{n_b}{n_0} \frac{mc^2}{E} \frac{1}{(\Delta\theta)^2} \frac{\omega_p^2}{k^2 c^2}. \tag{6.6}$$

Eq. (6.5) shows that for a beam with a monotonic distribution function $g(x)$ the growth rate is positive in the right half of the resonance region and negative in the left. A plot of $\gamma(k, x)$ for fixed k is shown in Fig. 6.1. The function $\gamma(k, x)$ has a narrow maximum with a width of the order of $\Delta\theta$. This circumstance greatly simplifies the problem of finding the stationary spectrum of the oscillations in the case when the angle spread of the beam is small enough ($\Delta\theta \ll 1$) (see [62]).

When $k \gg \omega_p/c$, the maximum of the function $\gamma(k, x)$ lies close enough to the point $x = 0$. In accordance with the results of the Section 3, in this case the spectrum should consist of one two-dimensional jet, the position of which coincides, accurate to $\Delta\theta$, with the position of the maximum of the growth rate. Therefore, in the region $k \gg \omega_p/c$ the spectrum takes the form [62]
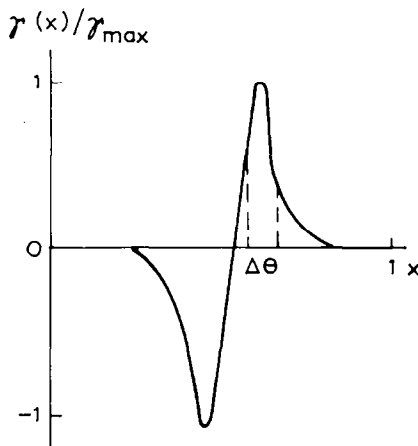
$$N(k, x) = N(k)\delta(x - \omega_p/kc), \tag{6.7}$$

Fig. 6.1. Plot of the instability growth rate of a relativistic electron beam against the angle ($x = \cos\theta$) for a fixed value of the wave vector.

where the intensity $N(k, x)$ can be obtained from the formula (3.11) by using (6.6):

$$N(k) = (T(x_0(k), x_0(k)))^{-1/2} \int_k^\infty \gamma(q)(T(x_0(q), x_0(q)))^{-1/2} \, dq \, , \qquad (6.8)$$

where $x_0(k) \equiv \omega_p/kc$. Calculations show that at $k \le 1.6\omega_p/c$ the spectrum (6.7) does not have "external stability": it is unstable relative to the excitation of waves outside the "jet" $x_0(k)$. Consequently, formula (6.7) holds true only for $k \ge 1.6\omega_p/c$. From the fact that $\gamma(k, x)$ is a polynomial of third order in x (see (6.5) and Fig. 6.1), we can see that in addition to the initial jet (6.7), there can appear in the region $k \le 1.6\omega_p/c$ not more than two additional jets; in the case of two jets, one of them must be one-dimensional.

All the foregoing calculations are based on the use of the differential approximation. Strictly speaking, this is possible only for beams with not too small angle spreads:

$$(\Delta \theta)^2 > \frac{1}{3} \frac{1}{r_D} \sqrt{\frac{m}{M}} \frac{c}{v_{T_e}} \, . \qquad (6.9)$$

It is obvious, however, that when the condition

$$(1/r_D)\sqrt{m/M} \ll \omega_p/c \, (v_{T_e}/c \gg \sqrt{m/M}) \qquad (6.10)$$

is satisfied for sufficiently large wave numbers

$$k - \omega_p/c \gg (1/r_D)\sqrt{m/M} \qquad (6.11)$$

the condition for the applicability of the differential approximation is satisfied independently of the angular width of the beam. Thus, a jet structure is always obtained in the region of large wave numbers (see later).

6.2. Numerical modelling in the case of the differential approximation

To verify the ideas concerning the jet-type of the spectrum and to investigate the dynamics of their onset, the kinetic equation describing the process of nonlinear Landau damping (induced scattering by ions) was solved in [62]. Specifically, the following equation was considered:

$$\partial V(q, x)/\partial \tau = V(q, x)\left\{ \Gamma(q, x) + (\partial/\partial q) \int_{-1}^1 R(x, y)V(q, y)\,dy \right\} + \varepsilon_d \partial^2 V(q, y)/\partial q^2 \, , \qquad (6.12)$$

where τ, q, V, Γ, R and ε_d are dimensionless quantities determined by the relations

$$\tau = \gamma_{max} t \, , \qquad q = (\omega_p/c)k \, , \qquad \Gamma = \gamma_{max}^{-1} \gamma \, , \qquad V(q, x) = \gamma_{max}^{-1} \frac{\pi^2}{9} \frac{m}{M} \frac{1}{r_D^2} \frac{c\omega_p}{n_0 T_e} N(k, x) \, ,$$

$$R(x, y) = 1 - x^2 - y^2 - 3xy + 3yx^3 + 3xy^3 + 3x^2y^2 - 5x^3y^3 \, ,$$

$$\varepsilon_d = \frac{c^2}{\gamma_{max} \omega_p} (m/M)^{3/2} \frac{1}{(kr_D)^3} \frac{1}{(r_D)^2} \left(\frac{W}{n_0 t_e} \right)^2 \, ,$$

where γ_{max} denotes the maximum instability growth rate. The term corresponding to the thermal noise was not introduced directly in explicit form in (6.12), but it was assumed in the calculations that $V(q,x)$ has a lower bound $N_0 \sim 10^{-3}$–10^{-2}. The "diffusivity" term $\varepsilon_d \partial^2 V(q,x)/\partial q^2$ was introduced in order to provide an applicability of the differential approximation and to prevent "breaking" of waves in k-space. The diffusion coefficient ε_d had to range from 2.5×10^{-4} to 5×10^{-3}. One applied to Eq. (6.12) a difference scheme of the Crank–Nicholson type uncondi-tionally stable and of second order of accuracy in time (see [64]). To integrate with respect to the cosine of the angle x in (6.12), Gaussian quadratures of suitable order of accuracy (with the nodes that "condense" toward the points $x = \pm 1$) were used, thus ensuring the best accuracy for the solutions of the type of jets. In typical variants, the number of points was 100 for the modulus of the wave vector and 32 for the angle. The initial conditions corresponded to a minimal level of oscillations $V(k,y) = N_0$. The instability zone was located at $2 > q > 1$; for small $q < 0.2$ one introduced linear damping that increased towards $q = 0$ and ensured a "sink" for the energy. Thus, one expected the realization of the Kolmogorov regime in the region $0.2 < q < 1$. In addition to the usual methods of verifying the difference scheme, one monitored the conservation of the total number of quasi-particles at $\Gamma(q,x) \equiv 0$ up to $\tau = 100$. One considered the case of not too small total angle spread $\Delta\theta \sim 15°$. The development of the instability is illustrated by Fig. 6.3. We see, that a stationary spectrum of the jet-type develops as time passes. In the inertial interval ($q < 1$) there are two one-dimensional jets, and in the region of large wave numbers ($q > 1.5$) there is one two-dimensional jet, as predicted by the theory. In the intermediate region ($1 < q < 1.5$), two two-dimensional jets are formed, and they "stick" at $x = 1$ to the ends of the interval $|x| = 1$ and are transformed into one-dimensional ones. The development of the nonlinear instability picture proceeds as follows. At first the oscillations grow exponentially in the region where the increment is positive, and the first two-dimensional jet is formed. Then, at $x = -1$, a "germ" of the second two-dimensional jet and one of one-dimensional jets is produced. The development of the one-dimensional jet recalls the propagation of the shock waves in k-space [65] in the region of small wave numbers. The thickness of these shock waves increased with increasing "diffusion" coefficient ε_d. The complete steady-state picture is established within the time of order of 30–40 reciprocal increments, and a stationary flux of the number of quasi-particles is produced in this case in the inertial region. The character of the establishment of the flux at the point $q = 0.70$ is shown in
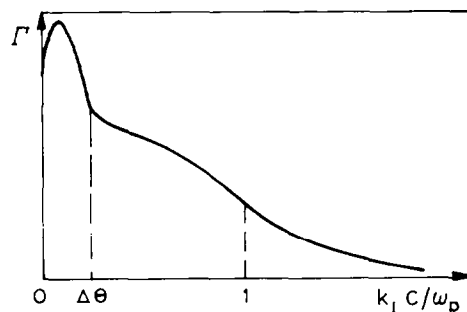

Fig. 6.2. Plot of the instability growth rate of a relativistic electron beam as function of $k_\perp$ for a fixed value of the modulus of the wave vector.

Fig. 6.4 (it shows the instant at $\tau = 10$ arrival), and the dependence of the steady-state flux on k is shown in Fig. 6.5. The value of the flux in the region of small wave numbers, $P_k = 0.06$, which is expressed in terms of dimensionless variables, agrees with the estimate $P_k \sim (\Delta k/k)^2$ (see (3.14)) with an effective width of the increment $\Delta k/k \sim 0.25$ for $\Delta\theta \sim 15°$.

It is worth to note that the nonlinear theory of the relaxation of a relativistic electron beam (REB) in a plasma (see corresponding review [60]) is founded mainly on the theory developed in Sections 3 (differential approximation) and 6.
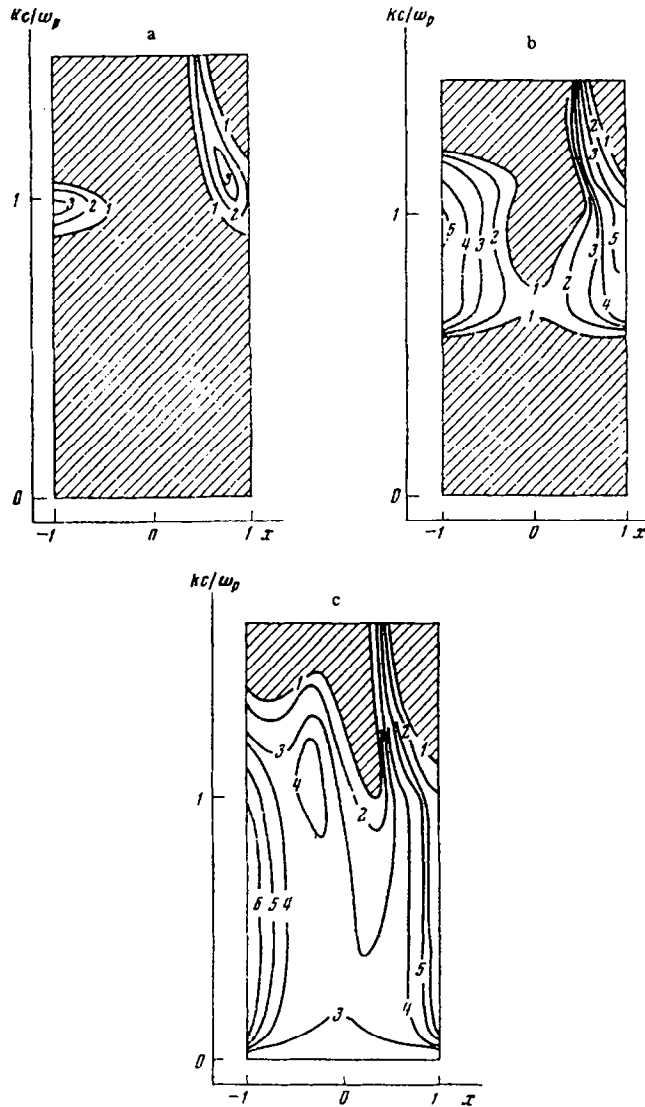

Fig. 6.3. Level lines of the function $\ln(N(k,x)/N_0)$ at different instants of time: $a - t = 8$, $b - t = 20$, $c - t = 100$. The lines are marked with the values of the function. In the shaded region where $N(k,x) = N_0$.
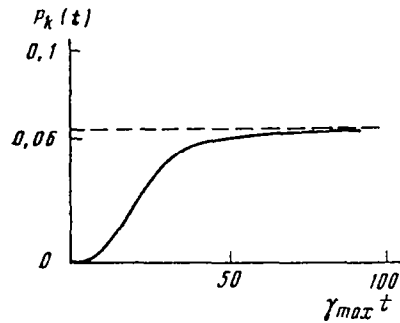
Fig. 6.4. Time dependence of the flux of Langmuir plasmons for $k = 0.7$.

The representation of Langmuir spectra as a set of "jets" in k-space (one- or two-dimensional ones) is based essentially on the "external stability"—namely, stability of jets relative to the excitation of waves outside the jets. These results are obtained in Section 3 within the scope of differential approximation which is valid, strictly speaking, for regular, "smooth" distributions. It can be shown, however, that the singular spectra represented by a sequences of δ-shaped peaks are unstable (for example, one-dimensional jets with equidistant sequence of peaks are unstable with respect to the excitation of oscillations at large angles to the jet). Therefore, in order to ascertain the limits of applicability of the differential approximation and "peak kinetics" model, a numerical simulation of the exact equations (1.41) are highly desirable.

6.3. Numerical modelling of the exact equations (1.41)

We will start with the simulation of the exact equations (1.41) in the axially symmetrical case (corresponding, for example, to the interaction of a plasma with a powerful electromagnetic wave or a beam of charged particles) [63, 66, 67]. In typical variants, the number of points was 100–150 in modulo k and 32–64 with respect to angle. A numerical solution of such equations is a time-consuming one, therefore a special fast method was developed [67], based on the ideas of "splitting" the calculations. The Crank–Nicholson difference scheme of second order of accuracy in time was applied to Eq. (1.41). In the integration over angle θ one used the quadratures of an appropriate order of accuracy, which took into account the possible singularity of the spectra.

The first series of the numerical experiments corresponded to the excitation of Langmuir waves by a relativistic electron beam (REB) (for the growth rate see (6.5), (6.6); one added also a damping of the waves equal to the frequency of an electron–ion collisions ν_{ei}). The distribution of oscillations excited by REB with an angle spread $\Delta\theta = 10°$ at large excesses above threshold $\gamma_{max} \gg \nu_{ei}$ is shown in Fig. 6.5. We see that in the inertial region, $k < \omega_p/c$, there are two quasi-one-dimensional jets $(\theta < 15°, \pi - \theta < 15°)$ that are sufficiently well described by the one-dimensional model. The characteristic width of the "instability zone" over modulus k is $\Delta k \sim (\omega_p/c)(\Delta\theta)^2$ (see (6.4)), therefore the regular regime in the inertial interval is accessible only for beams with a very large angle spreads:

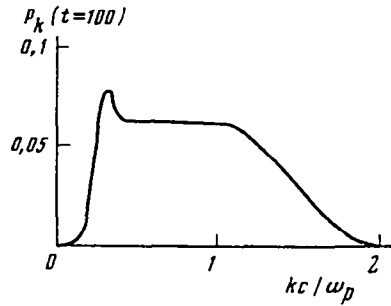$$(\Delta\theta)^2 > \sqrt{\frac{m}{M}}\frac{c}{v_{T_e}}.$$
(6.13)

Fig. 6.5. Plot of the flux of Langmuir plasmons against the modulus of the wave vector for $t = 100$.

It was shown also by the numerical experiments that in the opposite case a singular regime was established and quasi-one-dimensional jets were split into $N \sim \omega_p/k_{dif}c$ separate "spots". At sufficiently large excesses above threshold $\gamma_{max}/\nu_{ei} > N$ the steady state was not reached and there occurred a successive detachment of the solitary impulses and their moving toward the region of small k. Their length, velocity and other parameters are well described by the results of Sections 3 and 4 (see also the last part of Section 6). We see that a slight spreading of the peaks over angle θ is sufficient for the spectra to conserve a jet-like character independently of the "width" of the growth rate in modulus of k. There occurred also that a characteristic time of the onset of Langmuir spectra was close to the estimates (5.12) or (5.14)

$$\tau_{st} \sim (1/\gamma_{max})(n_{st}/n_{noise}) \,, \tag{6.14}$$

and it practically did not depend on the detailed structure of the solutions.

Let us examine now the region $k > \omega_p/c$, where the situation is quite complicated. One can obtain preliminary considerations from Fig. 6.2 where γ_b is shown as a function of $k_\perp$ for a fixed value of k_z. It is seen that there is a sharp maximum (its width is approximately equal to the angle spread of REB $\Delta\theta$) and a gently sloping "foot". As appears from the results of the above sections the spectra would consist of regular and singular parts simultaneously. Therefore, it is impossible to describe it neither by differential approximation (Section 3), nor by the "peak kinetics" model (Section 4). Numerical experiments [63, 70] confirmed these assumptions. The distribution of oscillations along the two-dimensional jet $k \cos \theta = (\omega_p/c)$ (see Fig. 6.5) looks like a pedestal with sharp peaks on it. We present also a plot of the energy flux (see Fig. 6.7) as a function of the wave vector

$$Q_k = \int \omega_p \gamma_b n_k d \cos \theta \,. \tag{6.15}$$

The sharp maxima at distances $\sim k_{dif}$ along this jet show that in spite of the smooth variation of the oscillation amplitude the width of the jet pulsates strongly. These pulsations are caused mainly by successive "birth" of solitons in the region of the maximal growth rate $k \sim \omega_p/c$ and their moving towards small k (see Sections 4 and 5).
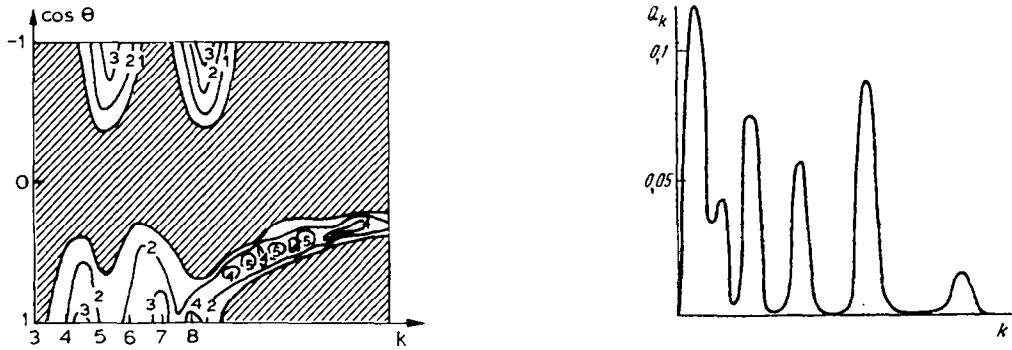
Fig. 6.6. Level lines of the function $\ln(N(k, x)/N_0)$ for the case of excitation of waves by a relativistic electron beam (a consideration of the exact equations) with the following parameters ($\gamma_0 t = 20$, $\Delta\theta = 15°$, $\gamma_{inst}/\gamma_0 \gg 1$).

Fig. 6.7. Plot of the function Q_k (at $k \geq \omega_p/c$) for the case of excitation by a REB ($\gamma_0 t = 20$).

6.4. Fine structure of one-dimensional jets

We see, that the numerical experiments are confirming the basic conclusion of Sections 2 and 3 on this jet-like structure of Langmuir turbulence. It is natural to consider a fine structure of the jets. To check on the considerations developed in Sections 3 and 5, concerning the structure of the one-dimensional spectra, one performed a special series of numerical experiments. Specifically, one considered the equation (see (2.24))

$$\partial N_\kappa/\partial\tau = N_\kappa \left(\Gamma_\kappa + \int G(\kappa, \kappa')N_{\kappa'}\mathrm{d}\kappa' \right) + f , \tag{6.16}$$

where $\kappa, \tau, \Gamma, G(\kappa, \kappa'), f$ are dimensionless quantities defined by the relations

$$G(\kappa, \kappa') = T_{k,k'}/T_{max} , \qquad \kappa = 2k/3k_{dif} , \qquad \tau = \gamma_{max}t ,$$

$$\Gamma = \gamma_k/\gamma_{max} , \qquad N_\kappa = n_k T_{max}/\gamma_{max} .$$

In typical variants, the number of points in modulus k was 200 (one "diffusion interval" k_{dif} spanned 15 points), and the noise level was 10^{-2}–10^{-4}. For the growth rate one chose the model expression

$$\gamma_k = \gamma_0 \exp(-(k - k_0)^2/\delta^2) - 1 . \tag{6.17}$$

At the first stage of experiments δ was chosen to be much larger than k_{dif} – a "broad" growth rate. For large excesses above threshold ($\gamma_0 \gg 1$), a periodic detachment of the solitons takes place (see (5.20)), with a characteristic width of the order of k_{dif} (see Fig. 6.8). For small excesses above threshold, a stationary regular distribution was established. The character of the onset coincides with that described in Section 4. Fig. 6.9 shows stationary spectra for different δ. It is seen that the envelope of these distributions is described sufficiently well by a differential approximation, and the distribution itself is deeply modulated in accordance with the results of Sections 2 and 3.
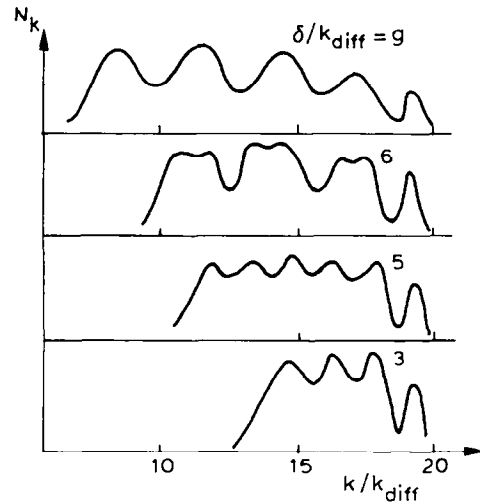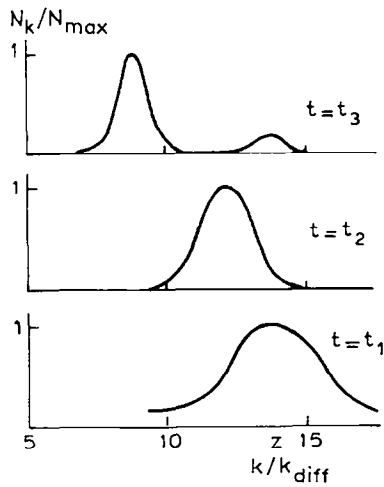
Fig. 6.8. Distribution of N_k for the case of a "broad" growth rate in the one-dimensional model for an infinite excess over the instability threshold at three successive instants of time; the point marked z is the point of the maximum growth rate increment.

Fig. 6.9. Distribution of N_k for small excesses over the instability threshold for growth rates with different ratios δ/k_{dif}.

In the case of a "narrow" growth rate ($\delta < k_{\text{dif}}$), the distribution of the oscillations in modulus k is practically independent of the exact value of δ and has a singular character. Fig. 6.10 shows the stationary distribution of the oscillations at $\gamma_{\max}/\gamma_0 = 4.37$. The width of peaks is determined by the noise level and we can obtain an estimate

$$\Delta k/k_{\text{dif}} \sim \sqrt{n_0/n_{\max}} \, , \tag{6.18}$$

which is in a good agreement with the results of Sections 2 and 4.

6.5. Spectra of parametric turbulence

Let us examine the parametric instability of a plasma placed in a homogeneous oscillating electric field with frequency $\omega_0 = \omega_p + \Omega$, $\Omega \ll \omega_p$. Eq. (1.41) can be easily generalized to include this case. The external electric field can be considered as a part of Langmuir spectra with $k = 0$, it corresponds to the following change of the variable in the dynamic equation (1.41)

$$n_k \to n_k + E_0^2/8\pi n_0 T \, .$$

It leads to the appearance in the kinetic equation (1.41) of a growth rate of the parametric instability

$$\gamma_p(k, x) = (\omega_p |E_0|^2/8\pi n_0 T_e) x^2 \operatorname{Im} G_{k, \Omega - \omega_k} \, . \tag{6.19}$$
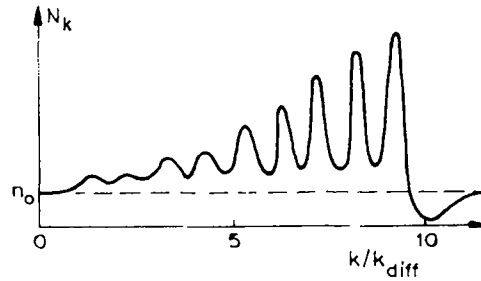
Fig. 6.10. Stationary distribution of N_k for $\gamma_0 t = 100$; the excess over threshold is 4.37.

Section 8 contains the detailed discussion of the validity of such a description (including the important problem of the "anomalous" correlators $\langle a_k a_{-k} \rangle$). It follows from (6.19) that $\gamma_p(k, x) = \gamma_p(k, -x)$ and, in addition,

$$\gamma_p(k, x) < x^2 \gamma_p(k, 1) .$$

From this, in accordance with the criterion (3.23), it follows that within the framework of differential approximation the spectrum of Langmuir turbulence excited by a homogeneous oscillating electric field must consist of two one-dimensional jets at $x = \pm 1$. One can see, however, that there are no grounds to changing over to the differential approximation in $|k|$, since γ_p and the kernel $T_{kk'}$ in (1.41) vary in k-space on the same characteristic scale (namely, the "size" of (6.19) is $k_{\text{dif}}/2$); therefore numerical simulations are necessary. A typical example of the numerical solution of (1.41) with pump (6.19) is shown in Fig. 6.11, namely the stationary distribution in k-space at low excesses above threshold. It is seen that despite the angle-width of $\gamma_p(k, x)$ being of order of unity, a one-dimensional approximation describes the situation satisfactorily the angle width of the "spots" is sufficiently small $\sim 10° \text{-} 15°$.

The imaginary part of G in (6.19) describes two overlapping processes [71]:

- the conversion of an electromagnetic wave by ions and the decay of an electromagnetic wave into a plasma wave and a virtual ion-sound wave

$$\omega_0 \rightarrow \omega_k + k v_{T_i} ;   \tag{6.20}$$

- aperiodic decay instability of an electromagnetic wave into a plasma wave and a virtual ion-sound oscillation

$$\omega_0 \rightarrow \omega_k + k c_s .   \tag{6.21}$$

The corresponding equations describing the nonlinear stage of these processes with taking into account anomalous correlators and a detailed discussion of their comparative role are derived in Section 8. We shall represent here only some results of the numerical simulation of these equations which confirm in particular the possibility to neglect the process (6.21) [71]. Namely, it follows from Figs. 6.12 and 6.13, there is only a series of peaks due to the process (6.20). Well above threshold, $\gamma_{k_0}/\gamma > k_0/k_{\text{dif}}$, with the energy absorption due to plasma-wave collapse (see Fig. 6.13), no steady state is established. The energy evolved at $k \sim k_0$ is transferred by pulses to the longwave
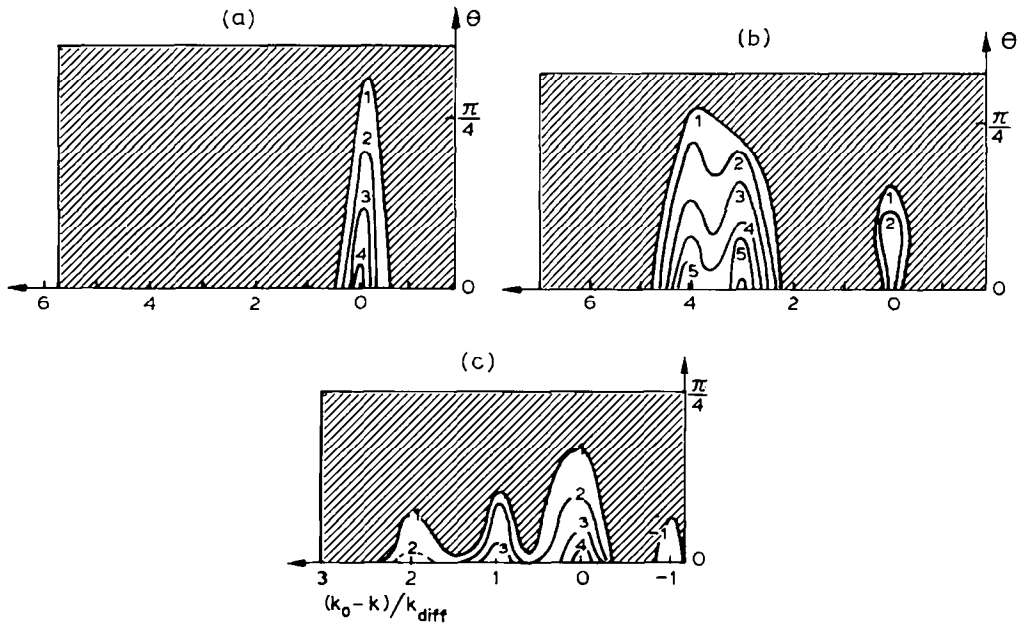
Fig. 6.11. Level lines of the function $\ln(n(k, x)/n_{\text{noise}})$ for a parametric excitation of Langmuir oscillations. The shaded region corresponds to $n(k, x) = n_{\text{noise}}$. a, b for large excesses above threshold at two successive instants of time; c the same level lines for a twofold excess above the parametric instability threshold ($\gamma_p t = 60$).

region. It results, of course, in the low-frequency modulations of the energy flux with a characteristic time $\gamma_{k_0} \tau \sim \ln(\gamma_{k_0}/Tf)$ (in accordance with the estimates of Section 5). It is worth to note also that these numerical experiments for large excesses above the threshold of the parametrical instability (see Fig. 6.13) clearly confirm the existence of the solitons (5.29) moving along the chain of peaks.

6.6. Mutual evolution of electromagnetic and Langmuir waves

In the previous sections a detailed theory of Langmuir turbulence was developed. Now we start to consider the influence of the additional channel of dissipation – a conversion of Langmuir waves into electromagnetic ones by ions:

$$l \to t + i , \tag{6.22}$$

$$\omega_k^l \to \omega_{k'}^t + |k - k'| v_{T_i} . \tag{6.23}$$

The matrix elements of this nonlinear interaction is of the same order as for the induced scattering by ions

$$l \to l + i . \tag{6.24}$$

The lth channel has to be taken into account for a dense plasma when the electromagnetic waves with frequencies near ω_p do not escape the plasma volume. It is possible to derive the
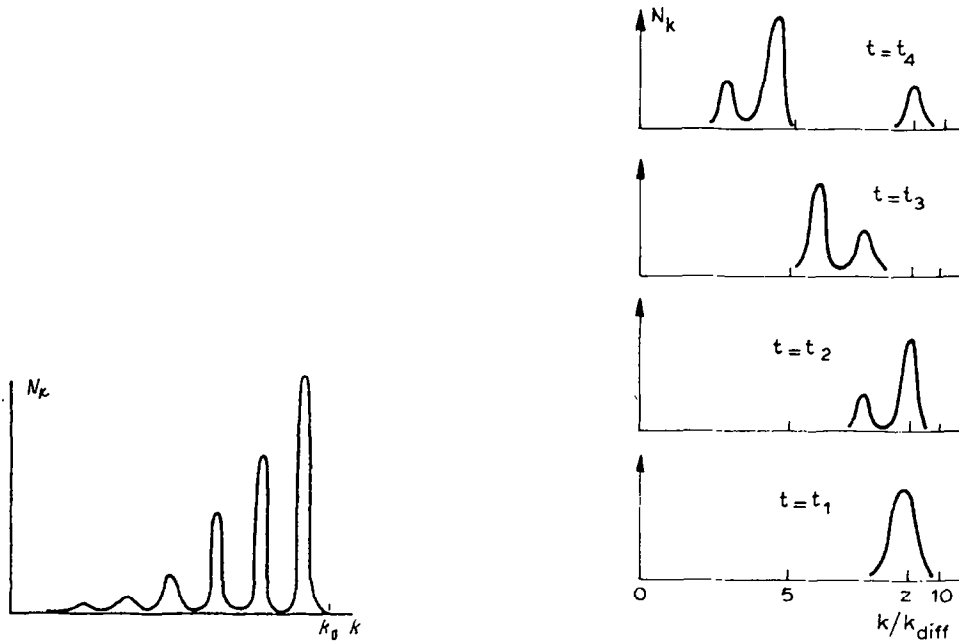
Fig. 6.12. Distribution of waves n_k in k-space for the case in which the coefficient giving the level of the pump above threshold is equal to $\gamma_k/\gamma = 3.2$.

Fig. 6.13. Wave distribution in k-space at several successive times for the case in which the pump is infinitely far above the threshold of instability.

corresponding equations similarly to the derivation of (1.32), (1.41) (see [74]). One has only to bear in mind that the frequencies of the electromagnetic waves with a different polarizations are the same. So their phases are not arbitrary, generally speaking, and it is necessary to use a description using a polarization tensor [75], (see also [76]). The resulting equations are bulky, so, for a better understanding and simplicity we will consider two limiting cases – other ones will be situated between them.

1. Let us assume that Langmuir spectra consist of two symmetrical one-dimensional jets. This is realized, e.g. under parametric RF-heating at a frequency $\omega_0 \sim \omega_p$. The electromagnetic waves appearing due to the conversion (6.23) will create also a singular distribution with the vector of electric field being parallel to the field of the Langmuir oscillations; the wave vectors of the t-waves will fill isotropically a plane which is perpendicular to the Langmuir jets. Due to the excitation of only one type of polarization the system of equations takes a simple form:

$$\tfrac{1}{2}\partial n_k^l/\partial t = n_k^l \left[\int T_{kk'} \, n_{k'}^l \, dk' + \int R_{kk'} \, n_{k'}^t \, dk' - \Gamma_k \right], \qquad (6.25)$$

$$\tfrac{1}{2}\partial n_k^t/\partial t = n_k^t \left[- \int R_{kk'} \, n_{k'}^l \, dk' - \nu_{ei} \right], \qquad (6.26)$$

where

$$R_{kk'} = \operatorname{Im} G\left(\frac{\omega_k^l - \omega_{k'}^t}{k}\right)\frac{\omega_p^2}{4\pi n_0 T_e}.$$ (6.27)

Here n_k^t is taken at the cylindrical normalization. As was shown above, the realization of the smooth or singular distribution over modulus k is defined by the ratio of the width of the excitation region δk to the characteristic size k_{dif} of the kernel $T_{kk'}$. Let us consider at first a singular case $\delta k < k_{\mathrm{dif}}$ and change to the satellite approximation. It follows from (6.23) that the distance between the electromagnetic and Langmuir peaks is $\sim k_{T_i}/2$. Therefore, the t-waves are situated between the corresponding Langmuir oscillations. Let us assume only Langmuir peaks N^l to exist and examine the stability to the appearance of the t-peaks N^t. One can see that at moderate excesses above threshold $\gamma_p/\nu_{\mathrm{ei}} < k_0/k_{\mathrm{dif}}$ (the point k_0 corresponds to the maximum of the pumping) only a solution without t-waves $N^t = 0$ is stable. At the large exceedings $\gamma_p/\nu_{\mathrm{ei}} > k_0/k_{\mathrm{dif}}$ Langmuir jet reaches a small k region and the growth rate for the excitation of t-waves becomes positive. But it is impossible to construct a stationary solution with a finite values of N^t, N^l in this case (there appears a growing condensate at $k \simeq 0$ due to the absence of longwave damping of t- and l-waves) and it is necessary to apply a numerical simulation. Summarizing its results, it can be concluded that the ratio of the total energy of t-waves to the total energy of l-waves is small for any excesses above threshold and is practically independent of the parameter $\delta k/k_{\mathrm{dif}}$.

2. In the isotropic case there is no polarization of the electromagnetic radiation

$$n_1^t(k) = n_2^t(k) \equiv \tfrac{1}{2}n^t(k)$$ (6.28)

and the corresponding kinetic equations can be written in the form

$$\tfrac{1}{2}\partial n_k^l/\partial t = n_k^l\left[\int \bar{T}_{kk'} n_{k'}^l\, \mathrm{d}k' + \tfrac{2}{3}\int R_{kk'} n_{k'}^t\, \mathrm{d}k' - \nu_{\mathrm{ei}} + \gamma_p\right] + \nu_{\mathrm{ei}} f = \Gamma^l n_k^l + \nu_{\mathrm{ei}} f,$$ (6.29)

$$\tfrac{1}{2}\partial n_k^t/\partial t = n_k^t\left[-\tfrac{1}{3}\int R_{kk'} n_{k'}^l\, \mathrm{d}k' - \nu_{\mathrm{ei}}\right] + \nu_{\mathrm{ei}} f = \Gamma^t n_k^t + \nu_{\mathrm{ei}} f,$$ (6.30)

where the kernel $\bar{T}_{kk'} = (1/4\pi)\int T_{kk'}\, \mathrm{d}\Omega$. In the case of moderate excess above threshold Langmuir waves occupy a bounded region in k; one finds analytically from (6.29), (6.30) (e.g. in the satellite approximation) that t-oscillations are not excited $\Gamma^t < 0$. In the opposite case of large excesses $\gamma_p/\nu_{\mathrm{ei}} > k_0/k_{\mathrm{dif}}$ the distribution n_k^l reaches the region $k \simeq 0$ ($\Gamma^l(0) > 0$) and the growth rate of the excitation of t-waves become positive in the whole k-interval $\Gamma^t(0) > 0$. Due to the impossibility to obtain an analytical solution of (6.29), (6.30), one performed a numerical simulation for the initial distribution $n_k^l = n_k^t = n_{\mathrm{noise}}$. The model expression $\gamma_p = \gamma_0 \exp(-(k - k_0)^2/(\delta k)^2)$ was taken for the growth rate; it turned out that all results depended slightly on the ratio $\delta k/k_{\mathrm{dif}}$. Numerical simulation showed that for small processes $\gamma_0/\nu_{\mathrm{ei}} < k_0/k_{\mathrm{dif}}$ the total energy of the electromagnetic waves Q^t was on the noise level and the distribution of Langmuir waves was practically the same, as it was without taking into account the conversion process (6.23). For large excesses there was no onset of the steady-state spectra, there was a periodical detachment of pulses from the region of instability moving to the small k region, where an accumulation of the wave energy (for l- and t-oscillations) took place. The total energies are close $Q^t \sim Q^l$, but qualitatively and quantitatively

Langmuir spectra are really the same as without lth conversion. It is worth noting and instructive that it is possible to construct within the scope of the differential approximation a stationary solution describing a different pattern of t- and l-oscillations in the isotropic case [60]. Let us discuss this problem in more detail. This solution can be characterized by the accumulation of the main part of the energy in the electromagnetic waves and the absence of an energy flux toward the small k region. One can see that it is unstable within the exact equations (6.29), (6.30) relative to the breach of the validity of the differential approximation. Namely, the amplitude of small perturbations increases while their width decreases as $\sim e^{\gamma_0 t}$. This instability takes a "floating" type and it could lead, in principle, to the only modification of the proposed stationary solution. So one can assume that (6.29), (6.30) have a stationary solution slightly differing from the one obtained in the differential approximation. One performed the following numerical test of this assumption: the mutual evolution of l–t waves was examined for the analytical solution from [60] taken as an initial condition. It was found that during a short time interval $t \sim 5 v_{ei}^{-1}$ the Langmuir spectra became the same qualitatively as at the "noise" initial conditions $n_k^t = n_k^l = n_{noise}$, Langmuir and electromagnetic condensates appeared and the energy was distributed in equal parts among t- and l-oscillations. This example confirms the conclusion that the differential approximation is applicable, strictly speaking, for the preliminary qualitative description of the kinetics of weak turbulence and one has to use it with care. It is worth to add also that this approximation gives an understatements of the values of the fluxes of energy into the plasma as compared with the exact consideration within Eq. (1.41), e.g. in the case of excitation of Langmuir waves by a relativistic electron beam considered above the difference was 10–15 times. In the work [78] one performed a detailed comparison of the satellite and differential approximations with an exact approach in the magnetoactive plasma. It follows that the satellite model is more useful for the quantitative calculations of plasma heating (it will be discussed in Section 7).

7. Weak turbulence of an isothermal magnetoactive plasma

We start now to consider the weak turbulence of the potential oscillations in a magnetoactive plasma. As was mentioned above, two high-frequency branches of the oscillations exist. The main features of the upper-hybrid waves are similar in many aspects to Langmuir ones in isotropic plasmas and were discussed in Section 3. Here we will discuss the nonlinear interactions of the lower-hybrid oscillations, which have quite a different pattern of turbulence. The dispersion law for the lower-hybrid (LH) plasmons now takes the form

$$\omega_k \simeq \frac{\omega_p \omega_H}{\sqrt{\omega_p^2 + \omega_H^2}} \frac{k_z}{k} = \frac{\omega_p \omega_H}{\sqrt{\omega_p^2 + \omega_H^2}} |\cos \theta| . \tag{7.1}$$

It is a strong function of the angle θ between the wave vector and the direction of the magnetic field and changes significantly with a variation of the wave vector. It means that the inertial interval can be larger than in a plasma without a magnetic field, the problem of the energy condensation near the "bottom" of spectra is not so severe and the applicability region of weak turbulence could be very broad. The main nonlinear process in an isothermal magnetoactive plasma is again the

induced scattering of Langmuir oscillations by ions. The evolution of the density of Langmuir plasmons is described by the same equation (1.41), but with another matrix element $T_{kk'}$.

$$\left(\frac{\partial}{\partial t} + \gamma_k\right) n_k = \int T_{kk'} n_k n_{k'} \, \mathrm{d}k' \,, \tag{7.2}$$

where

$$T_{kk'} = \frac{\omega_k \omega_{k'} \omega_p^4}{2n_0 T_e} \frac{\left| (kk') - \dfrac{\omega_H^2}{\omega_k \omega_{k'}} k_z k_{z'} + \dfrac{i\omega_H}{\sqrt{\omega_k \omega_{k'}}} [kk']_z \right|^2}{(\omega_+^2 - \omega_k^2)(\omega_-^2 - \omega_k^2) k^2 k'^2} \operatorname{Im} G\left(\frac{\omega_k - \omega_{k'}}{|k - k'|}\right), \tag{7.3}$$

and ω_+ and ω_- are the roots of the dispersion relation

$$\omega^4 - (\omega_p^2 + \omega_{H_e}^2)\omega^2 + \omega_p^2 \omega_{H_e}^2 \cos^2\theta = 0 \,. \tag{7.4}$$

The Green function $G_{k\omega}$ is in the case of unmagnetized ions ($kv_{T_i} \gg \omega_{H_i}$) the same as (1.18), while in the opposite limit ($kv_{T_i} \ll \omega_{H_i}$) it differs by the replacement of k by k_z. The term γ_k must include apart from the term γ_p corresponding to the excitation of the waves also a linear damping; it consists of the frequency of electron–ion collisions and Landau damping by electrons

$$\gamma_l = \nu_{ei} + \sqrt{\frac{\pi}{2}} \frac{\omega_k}{(kr_D)^3} \exp\left[-\frac{1}{2k^2 r_D^2} \frac{\omega_H^2}{(\omega_H^2 + \omega_p^2)}\right]. \tag{7.5}$$

At first we will give a qualitative discussion of the structure of the solutions of (7.2). In each transfer process the frequency of the Langmuir waves is changed by an amount

$$\Delta\omega_k \sim |k - k'| v_{T_i} \ll \omega_k \,. \tag{7.6}$$

The absolute magnitude of the wave vector can then either increase or decrease; an increase of the wave vector does not violate the conservation laws as it would be in the case of a plasma without a magnetic field. To understand the direction of the spectral transfer as regards the modulus k we consider how the growth rate of the instability of a narrow packet with wave vector k_0 is built up. The scattered waves are excited near the resonant surface

$$\omega_{k_0} - \omega_k = |k - k_0| v_{T_i} \tag{7.7}$$

(taking into account thermal corrections to the dispersion law does not significantly distort the resonance surface and does not introduce any changes in the results given below). The growth rate of the instability does not change along this surface and the angular width of the excited zone is of the order of magnitude of the step in the spectral transfer $\Delta x = \sqrt{(m/M)} \, kr_D$ ($x \equiv \cos\theta$); i.e. it increases with increasing k. When the larger phase volume is taken into account the oscillations are thus transferred to the region of short wavelengths. When the wavelength decreases, however, the linear Landau damping of the waves increases steeply, leading to a further transfer to the region of a large k. The energy of the oscillations therefore displays a tendency to "condense" in some point in k-space; a "jet" in a short wavelength region could be formed.

Let us go into a more detailed study of the stationary solutions of (7.2). First, we consider the case $\omega_H \gg \omega_p$ [79]. Using the fact that the spectral transfer step in a single scattering process is small,

$\Delta x \ll 1$, we simplify the kernel $T_{kk'}$, changing to a differential approximation (see Sections 1 and 3). We have for unmagnetized ions

$$T_{kk'} = \frac{\pi}{2mn_0} \frac{v_{T_i}^2}{v_{T_e}^2} |xx'| |\boldsymbol{k} - \boldsymbol{k}'|^2 \frac{\partial}{\partial |x|} \delta(|x| - |x'|) . \tag{7.8}$$

If the ions are magnetized, $kv_{T_i} \ll \omega_{H_i}$, we must change $\boldsymbol{k}$ to k_z in (7.8). We also recognize that by virtue of the symmetry in a strong magnetic field the solutions have to be axially symmetrical too. Using this we get for the quantity $N_k \equiv N(k, x) = 2\pi k^2 n_k$ the equation

$$((\partial/\partial t) + \Gamma_k)N_k = \gamma_{nl} N_k . \tag{7.9}$$

In a plasma with unmagnetized ions $(kv_{T_i} \gg \omega_{H_i})$

$$\gamma_{nl} = \frac{\pi}{2mn_0} \frac{v_{T_i}^2}{v_{T_e}^2} x \frac{\partial}{\partial x} x \int (k^2 + k'^2) N(k', x) dk' , \tag{7.10}$$

and in the opposite case

$$\gamma_{nl} = \frac{\pi}{2mn_0} \frac{v_{T_i}^2}{v_{T_e}^2} \int \left(x^3 k^2 \frac{\partial}{\partial x} x N(k', x) + xk'^2 \frac{\partial}{\partial x} x^3 N(k', x) \right) dk' . \tag{7.11}$$

It is worth to note that (in the contrast to the isotropic plasma) it is impossible to obtain analytically even an estimate of γ_{nl} without information on the turbulence spectra. At the two cases considered below—the parametric excitation and the relaxation of the ion beam, e.g. the plasmon distributions are concentrated in quite different regions in k-space and, hence, the nonlinear characteristics are different.

There is an additional advantage to change to the differential approximation in a magnetoactive plasma. It is connected with the fact that the maximum of the induced scattering is independent of k. An excitation of waves, for example, by a parametric heating by a RF-wave with frequency ω_0, produces mainly oscillations near the line

$$x_0 = \omega_0/\omega_p - kv_{T_i}/\omega_p . \tag{7.12}$$

Due to induced scattering each element of this line excites waves closely to

$$x = x_0 + (k + k_0/\omega_p)v_{T_i} , \tag{7.13}$$

and it is clear from Fig. 7.1 that the whole line simulates Langmuir waves in the whole k-space. There occurs thus a fast smoothing out of the wave distribution over angle and this gives us the additional reason for describing it in the differential approximation.

Eq. (7.9) determines the stationary solutions with a great degree of arbitrariness. This arbitrariness is removed, as was shown in Section 3, by the requirement that the stationary state must be stable under the excitation of oscillations in those regions of k-space, where $N_k = 0$, or, in "geometrical" terms: the curve Γ_k must lie above the curve γ_{nl} and touches it in those points where the oscillations are excited ($N_k \neq 0$). It is clear from (7.10) and (7.11) that the curve γ_{nl} is a parabola, $\gamma_{nl} = c_1 + c_2 k^2$. One can see that in the inertial interval of angles ($\gamma_p = 0$) it can touch the curve Γ_k only in the single point $k_0(x)$. The solution therefore in the coordinates k, x is a jet, extending
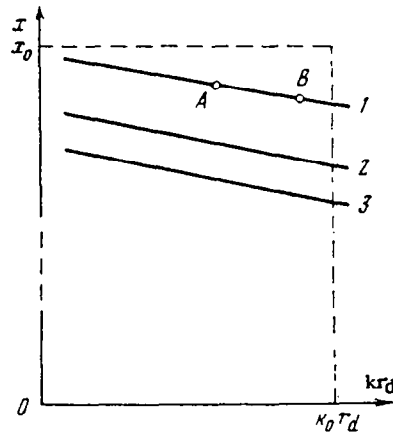
Fig. 7.1. Structure of the growth rate of the induced scattering by ions: 1 is the line on which the growth rate of the pumping due to parametric instability reaches its maximum; on the lines 2 and 3 the growth rates of the induced scattering generated by the points A and B reach their maxima. It is clear that the oscillations excited by the line 1 fill a broad region of k-space.

into the region of small x. To assess its location we put in (7.9) $N_k = N(x)\delta(k - k_0(x))$. To calculate its location let the ions be unmagnetized, in which case

$$\gamma_{\text{nl}} \propto x \frac{\text{d}}{\text{d}x} xN(x)[k^3 + k_0^2(x)] \ . \tag{7.14}$$

The point of contact $k_0(x)$ is then determined by the set of equations

$$\gamma_{\text{nl}} = \Gamma_{k_0} \ , \qquad \text{d}(\gamma_{\text{nl}} - \Gamma_k)/\text{d}k|_{k=k_0} = 0 \ . \tag{7.15}$$

We shall show below that $k_0(x)$ changes slowly with changing angle. Taking k_0 out from under the differentiation sign and dividing the first equation by the second we get the simple relation:

$$\text{d}\Gamma_{k_0}/\text{d}k_0 = \Gamma_{k_0}/k_0 \ . \tag{7.16}$$

It is clear that k_0 is independent of the shape of the spectrum and is solely determined by the linear damping. Using its explicit form we get for the contribution of the Landau damping γ_L in the point k_0

$$\gamma_L \approx \nu_{\text{ei}}(k_0 r_{\text{D}})^2 \ , \tag{7.17}$$

and the quantity $k_0 r_{\text{D}}$ is defined by the condition

$$k_0 r_{\text{D}} \approx \sqrt{1/2 \ln(\omega_{\text{p}}/\nu_{\text{ei}})} \ . \tag{7.18}$$

The value of k_0 depends slightly on the plasma parameters; when the ratio $\omega_{\text{p}}/\nu_{\text{ei}}$ changes from 10^3 to 10^5, the magnitude of $k_0 r_{\text{D}}$ changes from $\frac{1}{5}$ to $\frac{1}{7}$. It means that the linear damping of the waves is defined mainly by electron-ion collisions. The dependence k_0 on x appears only in the next order of the small parameter $k_0 r_{\text{D}}$:

$$k_0(x) = k_0(1 - \tfrac{1}{2}(k_0 r_{\text{D}})^2 \ln x) \ , \tag{7.19}$$

and this justifies the assumption made by us that $k_0(x)$ is a smooth function up to the limits of the applicability of our consideration $x \sim \sqrt{m/M}$.

The preceding calculations were performed in the assumption that the electron distribution function had a Maxwellian character. Quasi-linear effects change the nature of the Landau damping in the jet region, but one can easily check that it does not lead to a shift in it. The contribution of the collisional damping increases in that case even more. Knowing the region of wave numbers in which the oscillations are concentrated we can express the conditions that the ions are unmagnetized in terms of the parameters of the problem:

$$\omega_{\mathrm{H}}/\omega_{\mathrm{p}} \ll \sqrt{(M/m)}(k_0 r_{\mathrm{D}}) \ . \tag{7.20}$$

In the opposite limiting case of magnetized ions the jet is located near the same value k_0 and its location changes also little with changing x. However, the nature of the change $k_0(x)$ is more complicated and is determined by the shape of the spectrum. It is possible now to obtain an analytical expressions for the Langmuir spectrum from these relations for any concrete type of the wave excitation.

Then let us consider the structure of Langmuir spectra in a dense plasma $\omega_{\mathrm{H}}\omega_k \ll \omega_{\mathrm{p}}^2$. It corresponds to the practically very important case of quasi- perpendicular wave propagation. Such waves are excited for the lower-hybrid heating in tokomaks, in quasi-perpendicular collisionless shock waves, etc. It has been shown [80] that the basic nonlinear process for the electrostatic waves is again induced scattering by ions. In this case the main role in the corresponding matrix element $T_{kk'}$ is played by the third term describing the interaction of oscillations via scattering by the velocity fluctuations [81]. Making use of the smallness of the step of the spectral pumping over frequencies, $\Delta\omega_k \ll \omega_k$, we transform anologously to the above procedure to the differential approximation. The expression γ_{nl} takes the form

$$\gamma_{\mathrm{nl}} = \frac{\pi}{2n_0 m} \frac{\omega_{\mathrm{p}}^2 \omega_{\mathrm{H}}^2}{\omega_{\mathrm{H}}^2 + \omega_{\mathrm{p}}^2} \frac{v_{T_{\mathrm{i}}}^2}{v_{T_{\mathrm{e}}}^2} \frac{\mathrm{d}}{\mathrm{d}x} \int (k^2 + k'^2) n_{k'} \, \mathrm{d}k' \ . \tag{7.21}$$

It is a parabola again, therefore in the inertial frequency interval ($\gamma_{\mathrm{p}} = 0$) the steady-state Langmuir spectrum takes the form of a jet $N_k \sim \delta(k - k_0(x))$. Its location is practically the same as in the previous case.

Let us briefly discuss the turbulence in the frequency region near the lower-hybrid resonance [83, 83]. The results, obtained above, have to be modified. First of all, the dispersion law changes to

$$\omega_k^2 = \omega_{\mathrm{L}}^2(1 + z^2 + y^2) \ , \qquad z^2 = (M/m)\cos^2\theta \ , \qquad y = kR \ , \qquad \omega_{\mathrm{L}}^2 = (\omega_{\mathrm{p}}^2\omega_{\mathrm{H}}^2/\omega_{\mathrm{p}}^2 + \omega_{\mathrm{H}}^2)(m/M) \ ,$$

where

$$R^2 = \begin{cases} \left(\dfrac{3}{4} + 3\left(\dfrac{T_{\mathrm{i}}}{T_{\mathrm{e}}}\right)\right) r_{\mathrm{H}}^2 \ , & \omega_{\mathrm{H}} \gg \omega_{\mathrm{p}} \ , \\[2ex] 3\dfrac{T_{\mathrm{i}}}{T_{\mathrm{e}}} r_{\mathrm{D}}^2 & \omega_{\mathrm{H}} \ll \omega_{\mathrm{p}} \ . \end{cases}$$

The character of the induced scattering is changing too, the main process is the induced scattering by electrons in this frequency region. It is related to the fact that the ion-sound oscillations are

strongly damped by virtue of Landau damping by electrons in the angle region $\cos\theta \sim \sqrt{m/M}$. This conclusion does not depend on the ratio of T_i/T_e and the induced scattering by electrons remains the main process in a nonisothermal plasma ($T_e \gg T_i$). The corresponding matrix element $T_{kk'}$ was obtained in [82] by an averaging procedure similar to the one used in Section 1. The difference is due to the necessity to consider the low-frequency electron response by a kinetic manner too. It gives

$$T_{kk'} = \frac{\omega_H^2 \omega_p^4}{4n_0 T (\omega_p^2 + \omega_H^2)^2} \frac{[kk']_z^2}{k^2 k'^2} \operatorname{Im} G\left(\frac{\omega_k - \omega_{k'}}{|kx - k'x'|}\right), \tag{7.22}$$

where the Green function G is described by the same equation $G = (\varepsilon_e/\varepsilon) - 1$, but now the electron part ε_e includes also the kinetic effects. Let us assume that the turbulence spectra are axially symmetrical. In the region $z \gg k_0 R$ the spectral transfer proceeds, as one can see easily, in such a way that in a single scattering process $|z - z'| \ll z$. This gives a basis for changing with respect to the variable z to the differential approximation. The kinetic equations are similar to the equations of Section 3 and the present one (for a corresponding matrix element $T_{kk'}$ see Section 1). It is clear from the above results that oscillations generated due to a linear excitation close to some $z = z_p$ afterwards are transferred, due to scattering, to the region of lower frequencies and at the same time are stored rapidly in the large k-region forming these stable solutions in the shape of jets

$$N(k, x) = N(x)\delta(k - k_0). \tag{7.23}$$

The physical reason for the energy accumulation in the short-wavelength region is, as was shown above in this section, the increase of phase volume of the oscillations with increasing k.

For smaller z the transfer along the spectrum occurs in a nondifferential manner. It is then worth noting that at the same time as taking into account the fact that the transfer is nondifferential it is necessary to retain the thermal corrections to the dispersion law

$$\omega_k = \omega_L \left(1 + \frac{z^2}{2} + \frac{y^2}{2}\right), \quad y^2 = k^2 R^2 = k^2 \left(\frac{3}{4} + 3\frac{T_i}{T_e}\right) r_H^2. \tag{7.24}$$

Let us discuss the effect of the thermal corrections in (7.24) on the location of the jet-like spectra. If the waves are concentrated in the large k range, for small z the "thermal" term becomes the dominant one. The decrease in frequency in the cascading process means that the wave number k must decrease, similar to the isotropic plasma case. As a result the jet turns out to be in the small k range. On the other hand, if the angular correction in (7.24) is dominant, it follows from the arguments presented above, that cascading must increase the wave numbers. Hence, after $\cos\theta \sim \sqrt{m/M}$ in the cascading process toward the low-frequency range the jet bends and approaches the region $\omega = \omega_{LH}$ along the line $z = y$, where the thermal and angular corrections to the dispersion law are of the same order. So we can put

$$N(k, z) = N(z)\delta(k - |z|R^{-1}). \tag{7.25}$$

In the vicinity of the ω_{LH} the physical situation becomes quite similar to the isotropic plasma turbulence. The induced scattering does not change the plasmon wave numbers and, due to the small variation of the frequency, the condensation of the energy in the long wave range of the spectra takes place. As a result, modulational instability and collapse of LH-waves occur. Their

physical pattern is similar to the situation in an isotropic plasma. But many collapse features are quite different (see [90,91]). For example, the cavity structure is strongly anisotropic and both electrons and ions are accelerated as a result of LH-collapse.

At the excitation of the low branch of Langmuir oscillations in a weak magnetic field ($\omega_H \ll \omega_p$) the turbulence spectrum also takes the form of a jet and is concentrated in the region of large wave vectors $k_0 r_H \sim 1/2\sqrt{\ln(\omega_p/v_{ei})}$. One must exclude only the vicinity of the cyclotron resonance $\cos\theta > 0.6$, where the jet is turned down to the small k-region. The paper [84] was devoted to the detailed investigation of such spectra including the nontrivial problem of their isotropization.

Up to now we consider Langmuir turbulence only using the differential approximation. The fine structure of the jets can be obtained in the same way as in Sections 3–5 (see [85]). Some results of these papers [84,85] are given in Figs. 7.2–7.6; the exact kinetic equations were solved within the $\omega_H \gg \omega_p$ region. It is worth to underline one important and nontrivial conclusion of [85]. A direct comparison of the solutions of the kinetic equation with the exact matrix element $T_{kk'}$ was developed and the results obtained by means of the differential approximation and "peak-kinetics" (or "satellite") model. One demonstrated for the case of parametric excitation of waves that the satellite approximation gives a good qualitative and quantitative description of weak Langmuir spectra, while the differential approximation describes only the qualitative nature of the wave
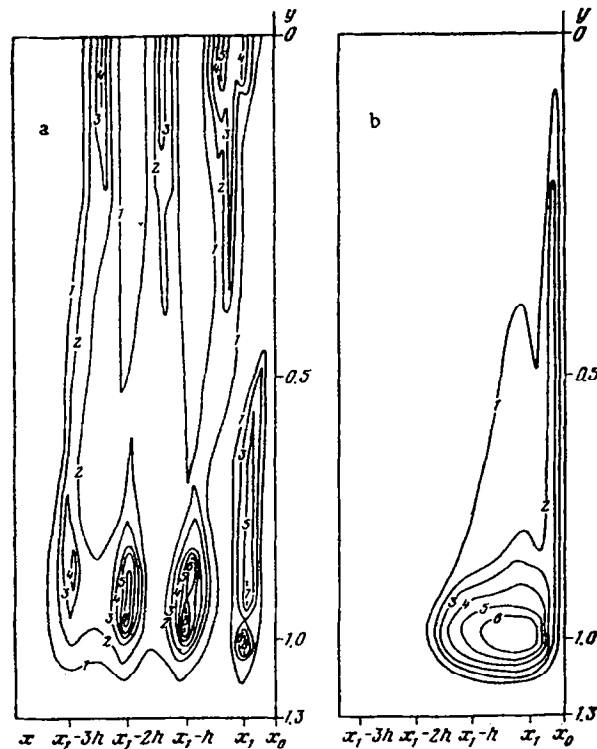

Fig. 7.2. (a) Contour of constant value of the function $\ln[N(k,x)/N_{\text{noise}}]$ for the steady-state solution of the exact kinetic equation for excess over threshold $\gamma_{\text{pmax}}/v_{ei} = 3.2$; (b) the same, but in the differential approximation.
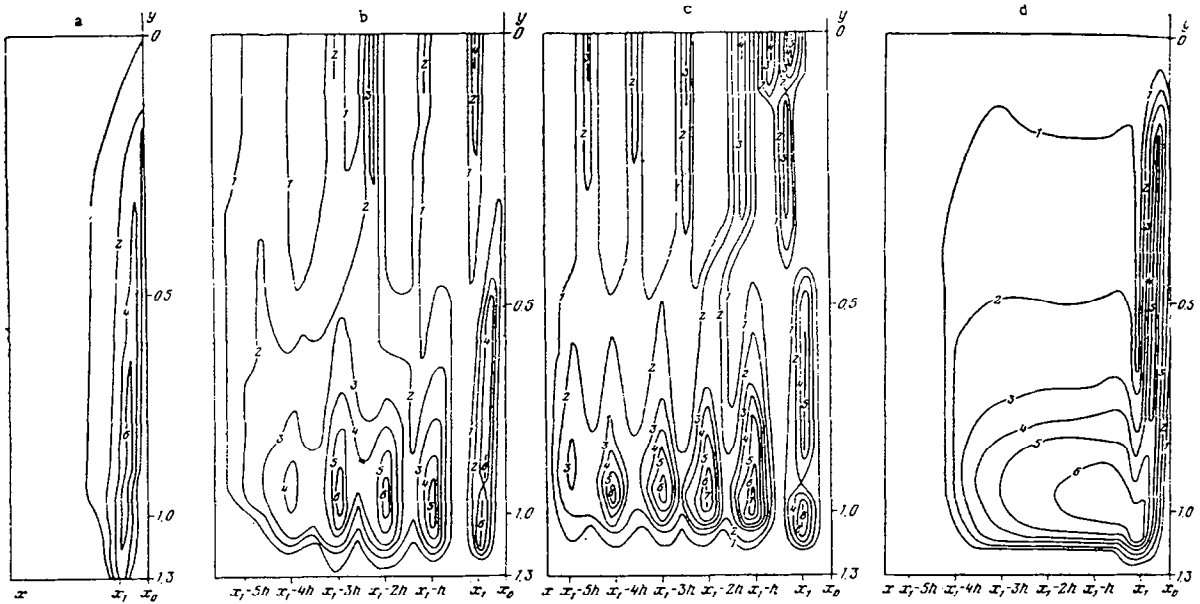
Fig. 7.3. (a)–(d) Contours of constant value of the function $\ln[N(k, x)/N_{\text{noise}}]$ for the exact matrix element at various instants with $\gamma_{\text{pmax}}/\nu_{\text{ei}} = 5.2$; $\tau = t\gamma_{\text{pmax}}^{-1}$; (a) $\tau = 6$; (b) $\tau = 80$; (c) $\tau = 560$ (the wave distribution reaches a steady state); (d) the same in the differential approximation ($\tau = 80$).
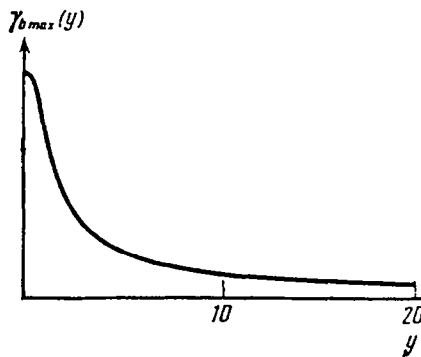

Fig. 7.4. The dependence of the maximum value γ_{bmax} of the growth rate of the beam instability on the parameter $y = \sqrt{(M/m)}\cos\theta$.

distribution averaged along the jets; it underestimates the characteristics of this averaged distribution by an order of magnitude. Another important point is that in the differential approximation it is impossible to improve the accuracy of retaining the second etc. terms in the series expansion of the kernel $T_{kk'}$. The characteristic length of the modulations occurring in the solutions of the exact equations is of the order of x_{dif} and therefore they cannot be described by any modification of the differential approximation.
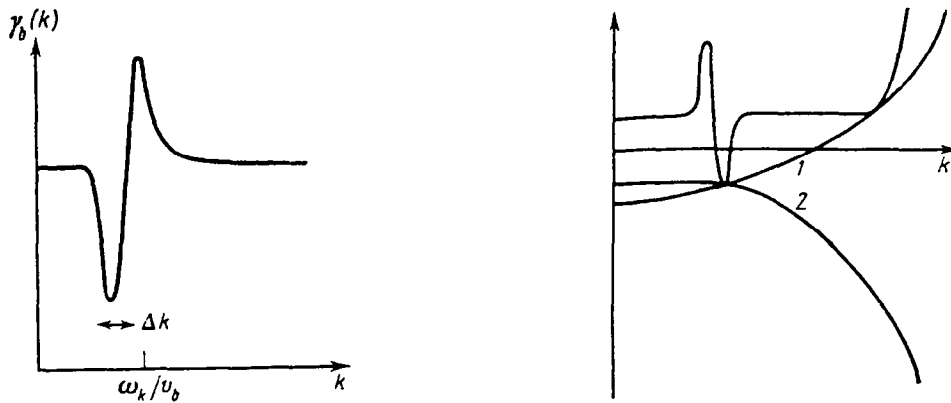
Fig. 7.5. The dependence of γ_b on the absolute value of the wave vector at a fixed value of y. The distribution function is chosen to have the form $f_b \propto \exp[-(v_\perp - v_{\text{beam}})^2/\Delta v^2]$, where $v_{\text{beam}} = 10 v_{T_i}$ and $\Delta v = 0.1\, v_{\text{beam}}$.

Fig. 7.6. The linear wave damping rate Γ_k and the damping rate γ_{nl} as functions of the wave vector at a fixed value of y. Curves 1 and 2 correspond to the two stable, stationary solutions of Eq. (7.9).

7.1. Turbulence spectra excited by ion beams

The considerations above deal with the plasmon distribution along the inertial interval which is a typical problem in parametric pumping. If the turbulence is excited by a beam of charged particles, the plasmon distributions are defined mainly by the structure of the growth rate region (similar to the isotropic plasma case). It occurs, for example, in the case of the nonlinear relaxation of ion beams propagating across a magnetic field. It is related to the problem of the structure of a transverse shock wave [88], in which the beam is created by the ions reflected from the shock front, or to the problem of anomalous plasma ionization [89] and of the nonlinear stage of the loss-cone instability. The relative motion of ions excites intense plasma oscillations with frequencies in the vicinity of the lower-hybrid one ω_{LH}, belonging to the region $\omega_{H_i} < \omega < \omega_H$. These oscillations, in turn, interact with both the beam and the plasma, giving rise to an efficient collisionless beam relaxation. We will obtain turbulence spectra excited in this case [87] as an application example of the theory developed above. Scattering by particles are the main nonlinear processes at frequencies which are not too close to ω_{LH}, it gives rise to a transfer of the wave energy to the region $|\omega_{\text{LH}} - \omega| \ll \omega_{\text{LH}}$. One can easily seen that the situation described here turns out to be very close to the one arising when Langmuir waves are excited in a plasma without a magnetic field. The accumulation of the oscillations in the long-wavelength region leads to a modulation instability and collapse. A collapse of the "lower-hybrid condensate" creates a strong effective damping, which as in the case of an isotropic plasma does not change essentially the turbulence structure and can be included phenomenologically into the kinetic equations. The lower-hybrid collapse was predicted and first investigated in [90] within the simplified model taking into account only the first angular harmonics of the electrostatic potential. Recently a detailed study was performed of this phenomena [91] with the help of a three-dimensional numerical simulation, which confirmed the results of [90] and one obtained a developed picture of the strong nonlinear

processes near ω_{LH}. Due to the narrowness of the strong turbulence region the energy transfer from the beam to the oscillations is determined usually by weak turbulence [87–89, 92]. The absorption of the wave energy does not lead to the heating plasma as a whole, but rather to the formation of "hot tails" (ion and electron) with a power-law dependence.

We will consider the frequently encountered situation in which the relaxation length greatly exceeds the ion gyroradius, so that the ion distribution function f_b is isotropic in the plane perpendicular to the magnetic field. By assuming the instability to be kinetic, it is possible to obtain expressions for the growth rate [93] γ_p (for simplicity, we will represent the corresponding dependences in graphical form in Figs. 7.4 and 7.5 and give only estimates). Let $\Delta v \ll v_b$ be the characteristic width of the beam distribution f_b, v_b is the average velocity of the beam. Then the maximum growth rate is achieved at

$$\omega/k \simeq v_b - \Delta v \simeq v_b \,, \tag{7.26}$$

and the following estimate for the maximum value of the growth rate takes place:

$$\gamma_{b,max} \sim \frac{n_b}{n} \frac{\omega_k \omega_{pi}^2}{k^2 v_b^2} \left(\frac{v_b}{\Delta v}\right)^{3/2} \simeq \frac{\omega_{pi}^2}{\omega_k} \frac{n_b}{n} \left(\frac{v_b}{\Delta v}\right)^{3/2} . \tag{7.27}$$

The growth rate is a smooth function of the angle θ, since $\gamma_{b,max} \sim (1/\omega_k)$ (see Fig. 7.4). The dependence of the growth rate on the absolute value of the wave vector is shown in Fig. 7.5. The maximum is achieved at $\omega_k \sim \omega_{LH}$ and $k_0 \sim \omega_{LH}/v_b$ and it will be assumed that the latter quantity is much less than r_D^{-1} and r_H^{-1}. With increasing y the graph of the maximum growth rate bends towards the region of large values of

$$k_0 R \sim (\omega_{LH}/v_b)(v_{T_e}/\omega_p)y \,. \tag{7.28}$$

At $k_0 R \sim \frac{1}{3}$, a strong Landau damping is switched on and the instability disappears. Furthermore, with an increase of y, the value of the growth rate itself is decreasing and the threshold $\gamma_b = v_{ci}/2$ of the instability may be inaccessible for large value of y. These effects allow us to restrict the discussion to the propagation of quasi-transverse oscillations only.

It was shown above that for $y > 1$ the major role is played by the scattering by ions, whereas for $y < 1$ the scattering by electrons becomes the most important. We will consider the region $y > 1$ first and examine the case $\omega_k \omega_H \ll \omega_p^2$. This condition is practically always satisfied in astrophysical applications [88, 89, 92]. The kinetic equation has the form (7.9), where γ_b is included in the Γ_k term, as well as Landau and collisional damping. Expression for γ_{nl} takes the form of a parabola (see (7.21)). It follows from the considerations above (see (7.15)) that for stationary solutions the surface Γ_k lies higher than γ_{nl} and is tangent to it at the points where the solution exists. Fig. 7.6 shows the dependence of Γ_k on the wave vector for a fixed value of y. Since γ_{nl} is a parabola, there exist two stable stationary solutions, corresponding to the curves 1 and 2 in Fig. 7.6. In both cases, the distribution of the oscillations is singular and has the form of a jet in k-space.

Let us begin by considering the first case. Here there exist two jets:

$$N_k = N_b(y)\delta(k - k_0(y)) + N_1(y)\delta(k - k_1(y)) \,. \tag{7.29}$$

The first stretches along the line of the maximum growth rate $k = k_0(y)$ and the second is located in the region of large k, where Landau damping becomes important. Substituting this solution in (7.15) yields

$$\gamma_L(k_0) + v_{ei} - \gamma_b(k_0) = \alpha k_0^2 (d/dy)(N_b + N_1) + \alpha(d/dy)(k_0^2 N_b + k_1^2 N_1) , \qquad (7.30)$$

$$\gamma_L(k_1) + v_{ei} = \alpha k_1^2 (d/dy)(N_b + N_1) + \alpha(d/dy)(k_0^2 N_b + k_1^2 N_1) , \qquad (7.31)$$

where

$$\alpha = \frac{\pi}{2Mn} \frac{\omega_p^2}{\omega_p^2 + \omega_H^2} (M/m)^{1/2} .$$

By substracting (7.30) from (7.31), we obtain

$$\alpha(k_1^2 - k_0^2)(d/dy)(N_b + N_1) = \gamma_L(k_1) - \gamma_l(k_0) + \gamma_b > 0 . \qquad (7.32)$$

Thus, the total number $N_b + N_1$ of waves increases with y, and the natural boundary conditions $N_k = 0$ cannot be satisfied for $y > y_0$, where $\gamma_b(y_0) = v_{ei} + \gamma_L$. Therefore, the distribution of the oscillations has the form of a single jet. In contrast to the case considered at the beginning of this section, plasmons are concentrated in the comparably low k-range. It can be seen in Fig. 7.7 that for a "narrow" beam, when $\Delta v \ll v_b$, the jet is located at the maximum of the growth rate $k_0 \simeq (\omega_k/v_b)(1 + \Delta v/v)$. For $\Delta v \sim v_b$, the precise location of the jet in the region of positive growth rates is determined by conditions (7.15). Since the obtained results are weakly dependent on k_0, we shall assume, in the following, that $k_0 \simeq \omega_k/v_b$. The onset of such a distribution of jets was confirmed by a numerical solution of (7.9). This result is related in an essential way to the axial symmetry of the growth rate.

The distribution of oscillations along the jet is described by the equation

$$\Gamma(k_0) = \alpha \left[k_0^2 \frac{dN_b}{dy} + \frac{d}{dy}(k_0^2 N_b) \right] = 2\alpha k_0 \frac{d}{dy} k_0 N_b . \qquad (7.33)$$
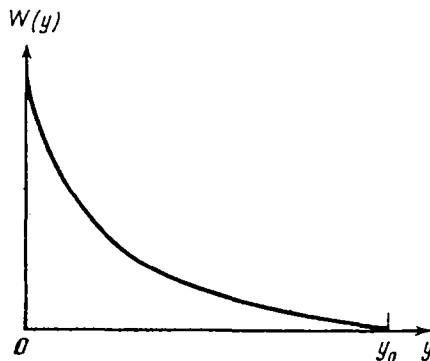

Fig. 7.7. The angular distribution of the oscillation energy density $W(y)$ at $y_0 = 20$.

Typically in astrophysical applications the collisional damping is negligible, Landau damping is also small along almost the whole jet. By taking this into account, Eq. (7.33) yields

$$N_b(y) = \frac{1}{2k_0\alpha} \int_y^{y_0} \frac{\gamma_b}{k_0(y')} \, dy'$$

$$= \frac{\gamma_b(0)v_b}{2\alpha k_0(y)\omega_{LH}} \left[\arctan y_0 - \arctan y \right], \tag{7.34}$$

where y_0 is the initial point of the jet. In a weakly collisional plasma the value y_0 is defined by Landau damping, which becomes significant for $k_z v_{T_e}/\omega_k \sim \frac{1}{3}$, i.e.

$$y_0 \approx v_b/3v_{T_i} \, .$$

For $y < 1$, the main nonlinear process is scattering by electrons. The corresponding equation describing the evolution of plasmons has the same form as (7.9), and γ_{nl} has been found, for example, in [82]:

$$\gamma_{nl} = \alpha \sqrt{\frac{m}{M}} \int \left(k^2 y \frac{\partial}{\partial y} \frac{N_{k'}}{y} + \frac{1}{y} \frac{\partial}{\partial y} y N_{k'} k'^2 \right) dk' \, . \tag{7.35}$$

It can be seen that γ_{nl} is a parabola as a function of k. Therefore, by repeating all the arguments used earlier, one can find that the spectrum also is built-up of a single jet, located along the line of the maximum growth rate. The equation for the jet-like spectrum coincides with (7.33) and, therefore expression (7.34) is valid up to the limit of applicability of the differential approximation $\omega_{LH} y^2 \sim k_z v_{T_e}$, i.e. $y \sim k_0 R$.

The energy density of oscillations in the inertial interval y^* and y_0 is

$$W = \sqrt{(m/M)} \int_{y^*}^{y_0} \omega_k N_b(y') \, dy'$$

$$\approx nT \frac{\gamma_b(0)(\omega_p^2 + \omega_H^2)}{\pi \omega_p^2 \omega_{LH}} \frac{v_b^2}{v_{T_e}^2} \left[g(y_0) - g(y) \right], \tag{7.36}$$

where

$$g(y) = \int_0^y \left[\arctan y_0 - \arctan y' \right] dy'$$

$$= \ln(1 + y^2) - y \arctan \left(\frac{y_0 - y}{1 + y_0 y} \right), \tag{7.37}$$

and the energy flux entering the plasma in this interval is

$$Q = nT \frac{\gamma_b^2(0)(\omega_H^2 + \omega_p^2)}{\pi \omega_p^2 \omega_{LH}} \frac{v_b^2}{v_{T_e}^2} \left[\phi(y_0) - \phi(y^*) \right] . \tag{7.38}$$

The plots of W, $\phi(y)$ are shown in Figs. 7.7 and 7.8. Here y^* is the boundary of the strong turbulence zone.
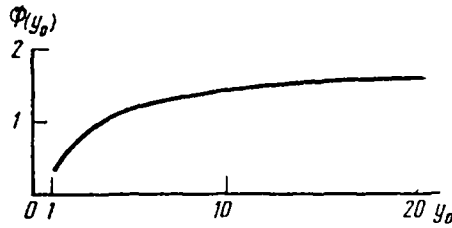
Fig. 7.8. The function $\phi(y_0)$, describing for $y^* \ll 1$ the energy flux into the plasma. At $y_0 \geq 10$, it is seen that the quantity Q is practically independent of y_0 and max $\phi(y_0) = 1.6$.

The estimates, presented in [87], are demonstrating that the interaction with the ion beam is considerably weak inside the strong turbulence zone and the energy deposition is defined by the weak turbulence theory.

Finally, let us discuss briefly the role of decay processes of the type $\omega_k \rightarrow \omega_{k_1} + \omega_{k_2}$. Their growth rate $\gamma_d \sim \omega_k(W/nT)(kv)^2$ is sufficiently large, and they may compete with the induced scattering (see [98,99]). Nevertheless, for $\omega < 2\omega_{LH}$ the decay processes are forbidden, because of the form of the dispersion law. Since the energy density in a jet increases with decreasing y, all the oscillation energy is, in effect, concentrated in the vicinity of ω_{LH} and, therefore, the role of the decay processes is small and they can be neglected.

7.2. Influence of inhomogeneity

It has been shown that singularity of the turbulent spectra is a consequence of the Fredholm structure of the kinetic equations. A small noise level causes a regularization of the spectral pattern, but does not change the integral parameters of the turbulence. Plasma inhomogeneity also breaks the Fredholm structure and its influence often can be more essential than the effect of external noise. If the inhomogeneity is strong enough it can suppress entirely the excitation of waves. Hence, we will consider below the influence of a sufficiently weak inhomogeneity in the case of the parametric excitation

$$\gamma_p/\omega \gg 1/kL . \tag{7.39}$$

Here L is a characteristic scale of the inhomogeneity and γ_p is a growth rate of the parametric instability. A Similar criterion exists for the case of the beam-plasma interaction [95]. In such a situation it can be restricted to only a consideration of the inertial interval.

The kinetic equation (1.41) must be modified in the following way:

$$\frac{\partial n_k}{\partial t} + \frac{\partial \omega_k}{\partial k}\frac{\partial n_k}{\partial r} - \frac{\partial \omega_k}{\partial r}\frac{\partial n_k}{\partial k} = (\gamma_{nl} - \Gamma_k)n_k . \tag{7.40}$$

Let us consider briefly the case of an isotropic plasma. Due to the smallness of the group velocities one can neglect the second term in (7.40) and consequently the convection of plasmons. To estimate the broadening of the jet-like spectra let us consider the third term in (7.40) as external noise and

use the results of Section 2. For a two-dimensional jet we obtain

$$\Delta k_\perp / k \sim \sqrt{\omega_p / \gamma_{nl} k L} \sim \sqrt{\omega_p / \gamma_p k L} \ . \tag{7.41}$$

One can see that the broadening of the singular spectra is small. It means that, as the effect of the noise terms, an inhomogeneity leads to a smoothing of the plasmon distribution, but does not change the integral features of the turbulence.

The situation changes drastically in the magnetoactive plasma. As was shown in this section, in the case of the excitation of Langmuir plasmons with the dispersion $\omega_k = \omega_p |\cos \theta| = \omega_p k_z / k$ nonlinear processes result in the "condensation" of the spectrum in the region of large wave vectors, where plasma damping is strong. A considerable change in the damping and, consequently, a significant modification in the spectrum results from just a slight broadening caused by an inhomogeneity $\Delta k / k \geq (k r_D)^2$.

Let us consider the steady state; for simplicity we will discuss the case of a strong magnetic field $\omega_H \gg \omega_p$. In this case $k \partial \omega_k / \partial k \sim r \partial \omega_k / \partial r$, but, due to the singularity of the spectra, the convection term $v_g \partial n_k / \partial r$ in (7.40) can be neglected. If we consider the case when the gradient of the density is parallel to the magnetic field and $\omega_p^2 < \omega_k \omega_H$, the plasmon distribution has to be axially symmetrical and $n_k \equiv n_k(x)$, $(x = \cos \theta)$. It is convenient to separate oscillations travelling in the direction of increasing concentration $n_k^+(y)$ and in the opposite direction $n_k^-(y)$, where $y \equiv |x|$. Generally speaking, they correspond to different nonlinear terms $\gamma_{nl}^\pm$. In the assumed case of a strong magnetic field $\omega_k \omega_H \gg \omega_p^2$ the third term in the kernel of the kinetic equation (7.2) dominates. Going over to the differential approximation we obtain (compare with (7.11))

$$\gamma_{nl}^\pm = k^2 y (d/dy) y C_0 + y (d/dy) y C_2 \pm 2 k y^2 (d/dy) y^2 C_1 \ ,$$

$$C_i = (\pi^2 / M n) \int k^{2+i} (n_k^-(y) + (-1)^i n_k^+(y)) dk \tag{7.42}$$

The narrowness of the distribution in k-space allows us to ignore the spatial migration of oscillations and to assume that $\partial / \partial k_y = x \partial / \partial k$. Consequently, the steady-state kinetic equation simplifies to

$$\pm y \frac{\partial \omega_k}{\partial z} \frac{\partial n_k^+}{\partial k} = (\gamma_{nl}^\pm - \Gamma_k) n_k^\pm \ . \tag{7.43}$$

The structure of the solution (7.43) is shown qualitatively in Fig. 7.9. Since oscillations drift away, steady-state conditions are obtained if $\gamma_{nl}^\pm > \Gamma_k$, i.e. if the curves $\gamma_{nl}^\pm$ intersect the curve Γ_k at two points and the distribution of the oscillations is no longer singular (see Fig. 7.9). In the case of oscillations travelling along the concentration gradient we find that n_k^+ for $k > k_+$ is of the order of the thermal noise n_k^0. The wave vector of n_k^+ decreases along the inhomogeneity, but it begins to rise in the region $\gamma_{nl}^+ > \Gamma_k$. The maximum of the distribution n_k^+ obviously coincides with the point κ_+ and then in the range $\gamma_{nl}^+ < \Gamma_k$ there is a rapid fall to the thermal noise level. A distribution n_k^- is of similar form, except that the fall in the range $k > k_-$ is steeper because of the strong Landau damping. Thus, the spectrum has the form of two jets representing waves travelling in opposite directions. A reduction in the gradient reduces the thickness of the jets and causes them to coalesce into one.
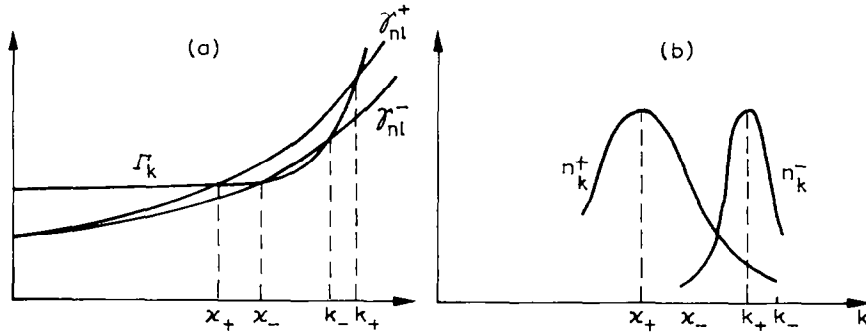
Fig. 7.9. (a) Dependences of γ_{nl}^{+}, γ_{nl}^{-} and Γ_k on the wave vector k. (b). Dependences on k of the number of waves n_k^{+} and n_k^{-} travelling in the direction of increasing and decreasing concentration, respectively.

We shall assume that the concentration profile is linear $\partial\omega_k/\partial z = \omega_k/L$. For simplicity, we shall consider fairly low oscillations obeying $y^2 \ll 1$. It can be assumed that $\gamma_{nl}^{+} = \gamma_{nl}^{-} \equiv \gamma_{nl}$, $k_{+} = k_{-} \equiv k_2$, $\kappa_{+} = \kappa_{-} \equiv k_1$. Since the dependence of γ_{nl} on k is known, Eq. (7.43) can be integrated, which gives

$$n_k^{+} = n_k^0 \exp \int_k^{k_2} (\gamma_{nl} - \Gamma_k) \frac{L}{\omega_k y} \, dk , \qquad n_k^{-} = n_k^0 \exp \int_{k_1}^{k} (\gamma_{nl} - \Gamma_k) \frac{L}{\omega_k y} \, dk , \tag{7.44}$$

where the limits of integration are selected in accordance with the qualitative nature of the solution described above and n_k^0 is the thermal noise level. Going over to dimensionless variables and integrating, we obtain

$$\ln n_k^{+}(y) = l \left[\frac{k_2^3 - k^3}{3} y \frac{d}{dy} y C_0 + (k_2 - k) \left(y \frac{d}{dy} y C_2 - 1 \right) \right.$$

$$\left. - \left(\frac{\pi}{2} \right)^{1/2} \frac{\omega_k}{\nu_{ei}} \left(\exp\left(-\frac{1}{2k_2^2} \right) - \exp\left(-\frac{1}{2k^2} \right) \right) \right] ,$$

$$\ln n_k^{-}(y) = l \left[\frac{k^3 - k_1^3}{3} y \frac{d}{dy} y C_0 + (k - k_1) \left(y \frac{d}{dy} y C_2 - 1 \right) \right.$$

$$\left. - \left(\frac{\pi}{2} \right)^{1/2} \frac{\omega_k}{\nu_{ei}} \left(\exp\left(-\frac{1}{2k^2} \right) - \exp\left(-\frac{1}{2k_1^2} \right) \right) \right] . \tag{7.45}$$

where $l = (L/r_D)(\nu_{ei}/\omega_k)$. Here the $n_k^{\pm}$ are normalized to n_k^0 and all the frequencies are normalized to ν_{ei}; k is understood to mean kr_D, whereas C_0, C_1, C_2 are still described by the formulas (7.42) but with other values of the coefficient before the integral $\pi^2/Mn \to \pi^2 n_k^0/Mn\nu_{ei}r_D^5$. Knowing the explicit dependence of n_k^{+} on the wave vector, we can integrate in Eq. (7.42) and obtain a closed system of equations. Obviously, the main contribution to the integral of n_k^{+} is the region of the maximum where $k \sim k_1$ and the integral of n_k^{-} is dominated by the region near $k \sim k_2$. Calculating the integral by the steepest descent method we shall arrive at a closed, but complicated system of

equations. It was studied in [94] and here we present only estimates. When the spectral broadening is small $\Delta k/k \ll (k r_D)^2$, the structure of the solution and the value of γ_L-region change slightly. Therefore, we shall be interested in the opposite limiting case. At the boundary of the validity of this condition $\Delta k/k \sim (k r_D)^2$ the width of the jets and the distance between them are of the same order of magnitude. The connection between Δk and the size of the density gradient L causing this broadening can be estimated in the same manner as the broadening due to thermal noise (see Section 2). From (7.43) we obtain

$$y^2 \omega_p / L \, n_k / \Delta k \sim (\partial^2 / \partial k^2)(\gamma_{nl} - \Gamma_k) \Delta k^2 n_k \, .$$

Substituting here

$$(\partial^2 / \partial k^2)(\gamma_{nl} - \Gamma_k) \sim v_{ei} r_D^2 / (k r_D)^4 \, , \tag{7.46}$$

we obtain the value $L = L_c$, when $\Delta k/k \simeq (k r_D)^2$ and

$$L_c \sim (\omega_p / v_{ei}) \, r_D y^2 / (k r_D)^5 \, . \tag{7.47}$$

At first sight the reason for the broadening of the spectra of an inhomogeneous plasma is obvious: the wave vector of oscillations travelling in a medium with an inhomogeneous concentration changes in accordance with the equation $\partial k_z / \partial t = - \partial \omega_k / \partial z$. However, if we estimate the change in the wave vector also during the oscillation life time v_{ei}^{-1}, we find that this change is considerably less than the broadening obtained above. The answer is as follows: in a homogeneous medium the contraction of the spectrum into a jet is due to the nonlinear processes, associated with Fredholm structure of the kinetic equations, and this is why the spectrum is so sensitive to a change in the structure of these equations. It follows that even a weak inhomogeneity can influence significantly the process of the "condensation" into jets.

With decreasing the value of L, n_k^+ and n_k^- diverge to the left and right of k_0. The collisionless damping increases in the case of n_k^-, whereas for n_k^+ we can ignore the term representing this damping. As a result, the ratio of N^- to N^+ decreases

$$N^- / N^+ \sim (L/L_c)^{1/4} \, ,$$

where L_c is given by (7.47). Landau damping and hence, a producing of fast electrons, is determined by the N^- waves propagating toward the direction of decreasing density. As a result, a very weak inhomogeneity generates a macroscopic current, which can be large enough [96].

We have shown that the effect of an inhomogeneity is to alter the structure of the equations, giving rise to an effective "noise" so that a transverse inhomogeneity should also deform the spectrum. Since in typical experiments such an inhomogeneity is considerably greater than the longitudinal one, and also because oscillations travel mainly across the magnetic field, this aspect is very important. We can easily show that if

$$L_\perp \leq (\omega_p / v_{ei}) r_D / (k r_D)^5 \tag{7.48}$$

the turbulence spectrum is greatly modified. However, an inhomogeneity results primarily in an angular change of the spectra, namely, their axial symmetry, but may not give rise to fast electrons.

Much more important can be a stochastic long-wavelength inhomogeneity (see [94, 98]). Such effects can be due to, for example, drift or magneto-acoustic oscillations which always occur in typical experiments. The scattering of oscillations by such an inhomogeneity results in diffusion in

k-space, so that the steady-state equation (7.40) can be written in the form

$$D_\perp \partial^2 n_k/\partial k^2 + D_\perp \Delta_\perp n_k = n_k(\Gamma_k - \gamma_{\mathrm{nl}}) \,. \tag{7.49}$$

Since such a low-frequency turbulence can naturally be assumed to be axially symmetric, the most important effect is the diffusion in the transverse direction. The diffusion coefficient $D_\perp$ can be obtained consistently from the kinetic wave equation, transferring to the differential approximation; but in our case it is sufficient to obtain simple estimates [97, 98]. Let the change in the concentration of the inhomogeneity be δn and the characteristic transverse wave vector be q. Then, the order of magnitude of the diffusion coefficient is $D_\perp \sim (\partial k_\perp/\partial t)^2 \tau$, where τ is the time for high-frequency oscillations to travel a distance q^{-1}, $\tau \sim (qv_{\mathrm{gr}})^{-1} \sim k_0/q\omega_k$, and $\partial k_\perp/\partial t$ is governed by the condition $\partial k_\perp/\partial t = -\nabla_\perp \omega_k$, so that the diffusion coefficient is

$$D_\perp \sim \omega_k q k_0 (\delta n/n)^2 \,.$$

Eq. (7.49) coincides with the stationary Schrödinger equation, n_k is similar to the ground state ψ-function in the potential $\Gamma_k - \gamma_{\mathrm{nl}}$. For small values of $\delta n/n$, $\Gamma_k - \gamma_{\mathrm{nl}}$ has a parabolic profile and the solution of (7.49) is a well-known one. After that it is possible to calculate C_0 and C_2 and finally to determine the spectrum. For higher values of $\delta n/n$ the variational principle can be used [98]; qualitative estimates are the following. A broadening of the jet due to the diffusion is δk, which can be determined from Eq. (7.49) exactly as has been done above

$$D_\perp/\delta k^2 \sim (\partial^2/\partial k^2)(\gamma_{\mathrm{nl}} - \Gamma_k)\delta k^2 \sim v_{\mathrm{ei}}/(kr_{\mathrm{D}})^2(\delta k/k)^2 \,. \tag{7.50}$$

A considerable increase in Landau damping occurs when $\delta k/k \geq (k_0 r_{\mathrm{D}})^2$, so that the intensity of the long-wavelength oscillations corresponding to the onset of significant heating of electron "tails" is given by

$$(\delta n/n)^2 \geq (v_{\mathrm{ei}}k/\omega_k q)(kr_{\mathrm{D}})^3 \,. \tag{7.51}$$

We can see that the fluctuation level defined by Eq. (7.51) is very low. In the case of characteristic parameters of tokamaks at frequencies of the order of the lower-hybrid one, low-frequency oscillations have a considerable influence on the spectra of the high-frequency turbulence even for $\delta n/n \leq 1\%$ and they increase considerably the number of fast electrons. It should be stressed that even if a transverse inhomogeneity dominates in the generation of fast electrons, an analysis of the longitudinal inhomogeneity is very important because it leads to the heating of the electrons and the generation of a current becoming anisotropic.

Up to now, we considered only the influence of external inhomogeneities. But an "internal inhomogeneity" can arise spontaneously, due to the development of the modulational instability. For two-dimensional jets, what is the case in a magnetized plasma, instability does not lead to collapse, but to the spectral broadening. This problem will be discussed in Section 9.

8. Langmuir turbulence under parametric excitation

We presented above a detailed study of turbulence spectra in the inertial interval and some results on the matching of these spectra with the pumping region. Unfortunately, for the two most common ways of Langmuir waves excitation: by a beam of charged particles or by a powerful

electromagnetic wave, it is difficult directly to apply this general theory. As was shown in the Section 6 the essential part of the turbulence spectra interacts with the particles if the beam is not strictly monochromatic. The inertial interval turns out to be a narrow one and the beam structure defines the jets pattern to a great extent. The situation is even worse for the case of parametric excitation. Usually most attention is concentrated on the first-order decay instability

$$\omega_0 \rightarrow \omega_k + k v_{T_i} ; \tag{8.1}$$

which is a decay of an electromagnetic wave into a plasmon and a strongly damped ion-sound wave. This process is quite similar to the induced scattering by ions, the basic nonlinear process in an isothermal plasma and the main object of the present survey. For $T_e \sim T_i$ the second-order decay instability, or, in other words, the aperiodic (two-stream) instability

$$2\omega_0 \rightarrow \omega_k + \omega_{-k} \tag{8.2}$$

has a growth rate which is lower only by a factor of two in the isothermal plasma. (The discussion of parametric instabilities and of their description one can find e.g. in [100–102]). One reason to neglect the latter one is that a description of this process is not a trivial matter – in addition to induced scattering by ions, an important role is played by the phase-dependent mechanism of amplitude limitation. The equations describing this process turn out to be quite different from the equations of standard weak turbulence theory, and the solutions of these equations have several remarkable features. In particular, the steady-state wave distribution in the region of the positive growth rate of the aperiodic decay instability of second order is a standing monochromatic wave, so that the narrowness of the region in which the growth rate for this instability is positive does not lead to any decrease in the energy deposited in the plasma. Nevertheless, on the basis of analysis and numerical simulation we believe that its contribution is small for any amplitude of the external field. We emphasize that this is a numerical smallness, due to the particular coefficients in the equations, rather than a smallness which is immediately obvious. The amplitude of the plasma waves which are excited and their distribution in k-space are governed essentially by the first-order decay instability.

1. Let us start with a consideration of the isotropic plasma case. An equation describing the excitation of Langmuir waves by a uniform high-frequency electric field $E_0 \cos \omega_0 t$ can be easily obtained from (1.32) by a change of variables,

$$a_k \rightarrow a_k + (k/8\pi e)\,(2m\omega_p/n_0)^{1/2}(E_0\,V\delta(k))\mathrm{e}^{\mathrm{i}(\omega_0 - \omega_p)t} . \tag{8.3}$$

It means that now the electric field in the plasma consists of two parts, an electric field of Langmuir waves and an HF-term corresponding to an electromagnetic wave. The coefficient in (8.3) is easily calculated from the relation between an electric field and canonical variables which was discussed in Section 1. The equation for a_k now takes a form

$$i(\partial a_k/\partial t) + \tilde{\omega}_k a_k$$

$$= V_k a^*_{-k}\mathrm{e}^{2\mathrm{i}(\omega_0 - \omega_p)} + \int T_{kk_1k_2k_3} a^*_{k_1} a_{k_2} a_{k_3}\delta(k + k_1 - k_2 - k_3)\,\mathrm{d}k_1\,\mathrm{d}k_2\,\mathrm{d}k_3 , \tag{8.4}$$

where the a_k are the normal wave amplitudes, which are related to the electric potential by

$$a_k = k\phi_k/(8\pi\omega_p)^{1/2} \,,$$

$$T_{kk_1k_2k_3} = \frac{\omega_p^2[(k_1k_2)(kk_3)G(\omega_k - \omega_{k_3}/|k - k_3|) + (kk_2)(k_1k_3)G(\omega_k - \omega_{k_2}/|k - k_2|)]}{4n_0 T_e kk_1k_2k_3} \,,$$

$$G(\omega/k) = \frac{L_{\omega k}}{1 - L_{\omega k}}; \quad L_{\omega k} = \frac{T_e}{Mn_0}\int \frac{k(\partial f_0/\partial v)}{kv - \omega}\,\mathrm{d}v \,,$$

$$\tilde{\omega}_k = \omega_k + \mathrm{i}\gamma + \omega_p \frac{(kE_0)^2}{32\pi n_0 T_e k^2} G\left(\frac{\omega_0 - \omega_k}{k}\right) \,,$$

$$V_k = \omega_p \frac{(kE_0)^2}{32\pi n_0 T_e k^2} G\left(\frac{\omega_0 - \omega_k}{k}\right) \,. \tag{8.5}$$

Here $\omega_k = 3/2\omega_p k^2 r_D^2$ is the dispersion part of the frequency of the Langmuir waves, and γ is their damping rate; we assume this damping to be collisional.

Eq. (8.4) holds if the external field is not too strong; the characteristic instability growth rate must be small in comparison with the damping rate of low-frequency beats:

$$E_0^2/8\pi n_0 T_e < kr_D\sqrt{(m/M)}\,(\gamma_s/\omega_s) \,, \tag{8.6}$$

where γ_s and ω_s are the ion-sound damping and frequency, respectively. Under this condition Eq. (1.30) is valid (see Section 1). In an isothermal plasma we have $\gamma_s \sim \omega_s$. As the temperature is reduced, the ratio γ_s/ω_s decreases, and when $T_i \ll T_e$ we have $\gamma_s/\omega_s \sim \sqrt{m/M}$. Linearizing (8.4) and assuming $a_k \propto \exp(-\mathrm{i}\Omega t)$, we find the instability growth rate to be

$$\Omega = \mathrm{Im}\,\tilde{\omega}_k \pm [1/4(\omega_0 - \mathrm{Re}\,\tilde{\omega}_k)^2 - |V_k|^2]^{1/2} \,. \tag{8.7}$$

We see that if condition (8.6) holds, waves are excited in two nonintersecting regions of k-space. The imaginary part of the Green function G reaches a maximum at $\omega_k + kv_{T_i} \sim \omega_0$, and an instability develops with a growth rate

$$\gamma_k = \omega_p((kE_0)^2/32\pi n_0 T_e k^2)\,\mathrm{Im}\,G((\omega_0 - \omega_k)/k) \,. \tag{8.8}$$

The imaginary part of G describes two processes: the conversion of the electromagnetic wave into Langmuir wave by ions, $\omega_0 \rightarrow \omega_k + kv_{T_i}$, and the decay of the electromagnetic wave into a plasma wave and a virtual ion-sound oscillation, $\omega_0 \rightarrow \omega_k + kc_s$, $c_s^2 = (T_e + 3T_i)/M$. Fig. 8.1 shows a plot of the function $\mathrm{Im}\,G$. In the case $T_e = T_i\,\max\mathrm{Im}\,G \simeq 1$ is reached for $\omega_0 - \omega_k = 3/2kv_{T_i}$; if $T_i \ll T_e$, we have $\max\mathrm{Im}\,G \sim \omega_s/\gamma_s$, and the maximum is reached at $\omega_0 - \omega_k \simeq kc_s$. When T_i/T_e decreases, the maximum of G becomes narrower, and this process becomes more "resonant". Near the surface (8.2) an aperiodic decay instability of the second order develops in the narrow region $|\omega_0 - \mathrm{Re}\,\tilde{\omega}_k| < 2|V_K|$. Its growth rate, which is easily derived from (8.7), is

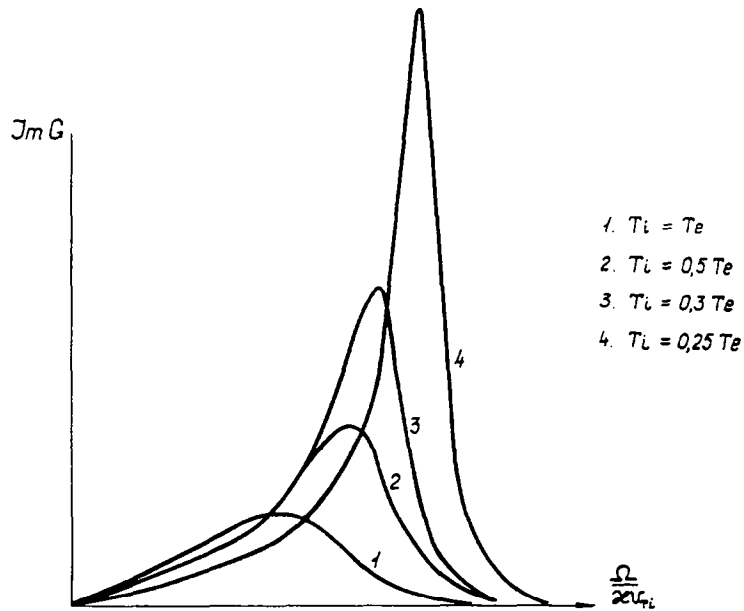$$\gamma = |V_k| = ((kE_0)^2/32\pi n_0 T_e k^2)|G(0)| = \omega_p(kE_0)^2/32\pi n_0(T_e + T_i)k^2 \,. \tag{8.9}$$

Fig. 8.1. Plot of the imaginary part of Green function $\operatorname{Im} G(x) = -\operatorname{Im} G(-x)$; $x = \Omega/kv_{T_i}$ for different values of ratio T_e/T_i.

The ratio of the growth rates for these processes is

$$v = T_e/(T_e + T_i)\,\max \operatorname{Im} G ;$$

in other words, up to $T_i = T_e$ the growth rate of the process (8.2) is numerically small in comparison with that for (8.1), so that it can be neglected in a qualitative analysis of the plasma heating. If we assume the wave phases to be random, we can simplify (8.4) considerably, converting to a statistical ensemble. This is done most simply for the process (8.1). Multiplying (8.4) by a_k^*, averaging over phases, and neglecting the rapidly oscillating terms, we find a kinetic equation for the number of quasi-particles (1.41).

2. We turn now to an analysis of process (8.2). At first, we neglect energy cascading through the spectrum, i.e. we assume that all waves lie near the surface (8.2). Since the initial wave is coherent, the sum of phases Φ_k for the excited waves a_k and a_{-k} is fixed; the energy flux into the plasma is proportional to Φ_k. Accordingly, in order to describe the turbulence we need to introduce, in addition to the number of waves n_k, the "anomalous" correlation functions $\sigma_k = \langle a_k a_{-k} e^{2i\omega_0 t}\rangle$. Equations for n_k and σ_k can be derived in the standard manner, by splitting the quaternary correlators into binary correlators [100, 103, 104]. Since near the surface (8.2) we have $\operatorname{Im} G(k, \omega_k - \omega_0) \ll 1$, we arrive at the following system of equations [105]

$$\tfrac{1}{2}(\mathrm{d}n_k/\mathrm{d}t) + \gamma n_k = \operatorname{Im} P_k \sigma_k^* , \qquad \tfrac{1}{2}(\mathrm{d}\sigma_k/\mathrm{d}t) + i\bar{\omega}_k \sigma_k = iP_k n_k , \tag{8.10}$$

where

$$P_k = V_k + \int S_{kk'} \sigma_{k'} \, dk' \,, \quad S_{kk'} = T_{k,-k,k',-k'} \,,$$

$$\omega_k = \tilde{\omega}_k + 2 \int \tilde{T}_{kk'} n_{k'} \, dk' \,, \quad \tilde{T}_{kk'} = T_{kk'kk'} \,.$$

The variables a_k are the normal variables of the linear problem, so that Eqs. (8.10) describe a broad class of physical phenomena. These equations have been studied in detail for the case of parametric excitation of spin waves in ferromagnets [103]; we will use those results here. We note first, that phase correlation in the pair a_k, a_{-k} is complete: $n_k = |\sigma_k|$. This is true even during the transient stage of the process. Furthermore, all the stable steady-state solutions of (8.10) lie on the surface $\bar{\omega}_k = 0$, i.e. waves are excited only at the surface, where the decay conditions (8.2) hold for frequencies renormalized due to the interaction. In particular, this circumstance implies that in a continuous medium there is no stabilization of the instability by a nonlinear frequency shift.

Before we turn to a further description of the properties of the solutions of (8.10) we note that the single-frequency nature of these solutions considerably simplifies the coefficients of nonlinear interaction:

$$\tilde{T}_{kk'} = \frac{\omega_p^2}{2n(T_e + T_i)} \frac{(kk')^2}{k^2 k'^2} \,, \quad S_{kk'} = \tilde{T}_{kk'} \,, \quad V_k = \omega_p \frac{(kE_0)^2}{32\pi n(T_e + T_i)k^2} \,. \tag{8.11}$$

The simplest solution of (8.10) is the monochromatic standing wave

$$n_k = n_0(\delta(k + k_0) + \delta(k - k_0)) \,; \quad \sigma_k = n_0 \exp^{-i\Phi_0} \,,$$

where the amplitude n_0 and the phase Φ_0 satisfy the conditions

$$V_{k_0} \sin \Phi_0 = \gamma \,, \quad 4S^2 n_0^2 = V_{k_0}^2 - \gamma^2 \,, \quad S = S_{k_0 k_0} \,.$$

We see from the Eqs. (8.10), (8.11) that we have $V_k \propto S_{k_0 k}$. It is known that in this case a monochromatic wave is the only stable steady-state at any level of the pump above the threshold. This steady state is established over a time $\sim (1/V_{k0}) \ln(V_{k_0}/Sf)$ as the waves grow from the thermal noise level f. To now take into account wave pumping through the spectrum due to induced scattering by ions, we write a_k as the sum of a monochromatic part A_k and a stochastic part $\tilde{a}_k$. Then singling out the coherent and incoherent parts of the dynamical equations we find that the appearance of waves off the resonant surface leads to the appearance in (8.10) of a nonlinear damping:

$$\gamma_{nl} = \int T_{kk'} n_{k'} \, dk' \,, \quad \langle \tilde{a}_k \tilde{a}_{k'} \rangle = n_k \delta(k - k') \,.$$

The waves which are excited at the resonant surface constitute the stochastic part of the pump, with a growth rate

$$\Gamma_k = T_{kk'} n_0 \,. \tag{8.12}$$

It has been shown above that the spectrum of waves excited due to processes (8.8) consists of a series of sharp peaks, spaced at intervals k_{dif}. As a result of the onset of the aperiodic decay instability, energy is evolved in an even more anisotropic manner, so that the wave spectrum also

consists of a series of peaks.

A numerical solution of the system (8.10) with the nonlinear damping derived above due to induced scattering shows (see Figs. 6.2 and 6.3) that there is only a series of peaks due to process (8.1). This circumstance is attributed to the finite width of the peaks and the comparatively slow decreasing of the imaginary part of the Green function $G_{k\Omega}$. Nevertheless, the simulation demonstrates that a "peak-kinetics" model, discussed above, provides a good coincidence with simulation of the exact equations. The presence of a coherent standing wave leads to only a slight additional spreading of the first few peaks. As in Section 4, we neglect the finite peak width and take into account only the interaction between the nearest neighbours. Furthermore, in the same approximation, we can set $\bar{\omega} = 0$ [105]:

$$\frac{1}{2}\frac{dn_0}{dt} = n_0(V_{k_0}\sin\Phi_0 - [\gamma + T(\tfrac{3}{4})N_1]), \qquad \frac{d\Phi_0}{dt} = V_{k_0}\cos\Phi_0 + 2Sn_0,$$

$$dN_1/dt = N_1(\gamma_{k_0} - \gamma + T(\tfrac{3}{4})n_0 - TN_2),\tag{8.13}$$

$$\vdots \qquad\qquad \vdots$$

$$dN_k/dt = N_k(-\gamma + T(N_{k-1} - N_{k+1})),\tag{8.14}$$

$$\vdots \qquad\qquad \vdots$$

$$(dN_n/dt) = N_n(-\gamma + TN_{n-1}),$$

$$n_k = \sum_{i=1} N_i\delta(\pm k_0 \mp ik_{dif}),$$

where

$$T = \max T((k - k')/k_{dif}) = T(\tfrac{3}{2}).$$

In Eqs. (8.13), (8.14) the peak positions are assumed fixed. Generally speaking, this is not actually true, and their coordinates are governed by the stability condition [103]. However, as the numerical results show, the peak shift is slight in comparison with the peak width and can be neglected.

3. Let us consider steady-state solutions of this system. If we neglect a term $T(\tfrac{3}{4})n_0$ in (8.13) due to the sharp dependence of the Green function $G(\xi)$, the peaks with even and odd indices will turn out to be unrelated. The amplitude of the next-to-last peak is always $\gamma/T \equiv N_c$. We see from (8.14) that the amplitude difference between two peaks with the same parity is N_c, so that if the total number of peaks is $2m$ the amplitudes of the first is

$$N_1 = mN_c,$$

The amplitude of the second peak is determined from the steady-state solution of (8.13):

$$(\gamma_{k_0} - \gamma)/T = N_2 < mN_c.$$

As the pump growth is increased, the amplitude of the odd peaks remains "frozen" while that of the "even" ones increases: when the pump level above threshold is described by

$$(\gamma_{k_0}^{(m)} - \gamma)/T = mN_c \, ,$$

the first and the second peak become equal in size, while the amplitude of the last peak varies in correspondence with N_c. Then a $(2m + 1)$th peak is created. In this situation, as follows from the considerations above, the amplitude of the second peak should be independent of the extent of the pump level above the threshold; it should be equal to mN_c. On the other hand, we see from (8.13) that this amplitude increases continuously with increasing γ_{k_0} (within small terms). This result means that the $(2m + 2)$th satellite is created immediately; etc. This result changes, of course, when the finite peak width is taken into account, but the results of a numerical simulation clearly show that the interval of pump levels above the threshold in which there exists an even number of peaks is much larger than that in which there is an odd number.

We can now write the amplitude of the first peak as

$$N_1 = [\gamma_k/\gamma]N_c \, , \tag{8.15}$$

where the bracket denotes the largest integer. For n_0 we have

$$n_0^2 = (1/4S^2)\,[V_{k_0}^2 - (\gamma + T\,(3/4)N_1)^2] \, ,$$

or, substituting the numerical values of the Green function for $T_i = T_e$:

$$n_0^2 = (1/4T^2)[(\gamma_{k_0}^2/4) - (\gamma + 0.37\gamma\,[\gamma_k/\gamma])^2] \, .$$

If we neglected the sign of the largest integer, we see that in the case

$$\gamma_k < \gamma/(0.5 - T\,(3/4)/T) \simeq 7.7\gamma$$

the second order decay instability is completely suppressed. When the pump is far above threshold we have

$$n_0 = \tfrac{1}{2}N_1[\tfrac{1}{4} - (T\,(3/4)/T)^2]^{1/2} \simeq 0.15N_1 \, ,$$

i.e. in this case we can in fact neglect its effect on process (8.1). Accordingly, the amplitude of the monochromatic pair excited by process (8.2) turns out to be far lower than that of the first peak. This occurs because of the large growth rate $\gamma_k = 2V_k$ for $T_i \sim T_e$ in (8.1), the greater nonlinearity due to the anomalous correlations, and the circumstance that the first peak causes quite nonlinear damping in the region $\omega_k \simeq \omega_0$. A numerical experiment [105] confirms these results well: the amplitude of the monochromatic standing wave is small, not only in the steady state, but also during the transient process.

Is there a change in the nonlinear decay of the wave distribution at the resonant surface $\bar\omega = 0$? For this case we can easily find the threshold for the creation of the second group of waves [106]:

$$S^2 n_0^2/\gamma^2 = (\gamma_k^2 V_{k_0}^2 - \gamma_{k_0}^2 V_k^2)/(SV_k - V_{k_0}S_{k_0 k})^2 \, ,$$

where γ_k is the total damping at point k and

$$\gamma_k = \gamma + (\omega_p^2/2n_0 T)\cos^2\theta\,[\mathrm{Im}\,G(3/4\cos\theta/2)]N_1 \, , \quad \cos\theta = (\mathbf{k}\mathbf{k}_0)/kk_0 \, .$$

Since $V_k \propto S_{kk_0}$, the threshold for creation of the second group of waves is again infinite under the condition

$$\gamma_k V_{k_0} > \gamma_{k_0} V_k \ .$$

Since $\mathrm{Im}\, G(3/4 \cos \theta/2) > \mathrm{Im}\, G(\tfrac{3}{4})$, this condition in fact holds.

4. One of the most important characteristics of RF-heating is the energy flux into the plasma, Q. For process (8.1) we have

$$Q_1 = 2\gamma_{k_0}\omega_p N_1 = 8 \frac{\gamma_{k_0}\gamma}{\omega_p}\left[\frac{\gamma_{k_0}}{\gamma}\right] n T_e \sim \frac{1}{2}\,\omega_p \left(\frac{E^2}{8\pi n_0(T_e + T_i)}\right)^2 n_0(T_e + T_i)\ .$$

Omitting the symbol telling us to take the integral part, we have $Q \propto E^4$. This result can also be found by simple estimates; it agrees with the conclusions reached in the diffusion approximation and has been confirmed in several experiments. The jumps in the energy flux found above should be particularly noticeable when the coefficient giving the excess of the pump level above threshold is ~ 1. As the numerical simulation shows, however, the finite peak width causes a pronounced overlapping of the peaks, so we can hardly expect to detect this effect experimentally. From (8.8) we find the energy flux into the plasma due to the second-order decay instability to be

$$Q_2 = 2\omega_p V_{k_0} n_0 \sin \Phi_0 = 2\omega_p n_0(\gamma + T(3/4)N_1)\ ,$$

$$Q_1/Q_2 = \gamma_{k_0} N_1/n_0(\gamma + T(3/4)N_1)\ .$$

Far above threshold we have

$$Q_1/Q_2 \simeq \gamma_{k_0}/T(3/4)n_0 \simeq (T/T(3/4))(N_1/n_0) \simeq 16.5\ .$$

Fig. 8.2 shows Q_1 and Q_2 as functions of time for the case $\gamma_{k_0}/\gamma = 3$. Although Q_2 does not vanish, because of the finite peak width it is small, not only in the steady state but also in the transient process.

Well above the threshold, $\gamma_{k_0}/\gamma > k_0/k_{\mathrm{dif}}$, with the energy absorption due to Langmuir collapse (see Section 6), no steady state is established. The energy evolved at $k \sim k_0$ is transferred by pulses to the long-wave region. This process was described in detail in previous sections. In this case we can essentially neglect the influence of the monochromatic wave. Fig. 8.3 shows Q_1 and Q_2 as functions of time. We see that here again we have $Q_1 \gg Q_2$. The oscillations of Q_2 are not as sharp, because of the additional phase mechanism which limits the wave amplitudes. The energy evolution in the plasma due to the process (8.1), on the other hand, is pulsed, and the pulses are separated by quite long-time intervals, $\gamma_{k_0}\tau \sim \ln(\gamma_k/Tf)$.

5. It is worth to note that if the pump is not coherent, the process (8.1) is greatly suppressed. If the spectral width $\Delta\omega$ exceeds $V_k n_0 \sim \omega_p E^2/32\pi n_0 T$, a growth rate for the process (8.1) drops $V_k n_0/\Delta\omega$ times. The growth rate of the instability (8.2) does not depend on the phase. It means that waves are excited by the different spectral components independently

$$\gamma = \int T_{kk_0} N_\omega \, \mathrm{d}\omega\ ,$$

where N_ω is related to the electromagnetic wave flux I as $I = I\, c\omega_p \int N_\omega \, \mathrm{d}\omega$. If $\Delta\omega$ is small in comparison with kv_{T_i}, the value of the growth rate practically does not change. When $\Delta\omega > kv_{T_i}$,
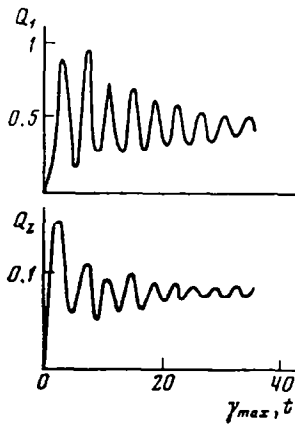
Fig. 8.2. Energy fluxes into the plasma due to the decay instabilities of first (Q_1) and second (Q_2) orders for the case $\gamma_k/\gamma = 3.2$.
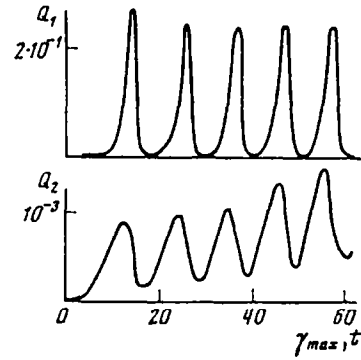
Fig. 8.3. Energy fluxes due to the decay instabilities of the first and the second orders for the case of a pump infinitely far above threshold.

the growth rate becomes a smooth function of k and differential approximation can be used also for the growth rate

$$\gamma \sim TN_\omega (kv_T)^2/\Delta\omega \ .$$

6. Let us discuss now an excitation of waves in a magnetized plasma. It occurs again as a result of two processes (see [107] and references therein) (8.1) and (8.2). The same arguments as above can be applied here. As a result, we can discuss only the process of conversion by ions. The absorption rate Q is

$$Q = \int \gamma_p \omega_k N_k \, dk \sim \gamma_p \bar{W} \ .$$

The energy of waves in the region of growth rate $\bar{W}$ can be estimated from the condition $\gamma_p \sim \gamma_{nl}$ or $\bar{W} \sim E_0^2/8\pi$. For the most interesting case $\omega\omega_H \ll \omega_p^2$, for example,

$$\gamma_p = \frac{\omega_p^4}{\omega_H^2\omega}\frac{E_0^2}{16\pi n_0 T}\,\mathrm{Im}\,G\left(\frac{\omega_0 - \omega_k}{kv}\right) \sim \frac{\omega_p^4}{\omega_H^2\omega}\frac{E_0^2}{16\pi n_0 T}$$

and

$$Q \sim (\omega_p^4/\omega_H^2\omega)(E_0^2/16\pi n_0 T)^2 n_0 T \ .$$

The numerical coefficient can be determined exactly only with the help of numerical simulation of the exact equations [108,109]. In an isotropic plasma all absorbed energy is transferred to the electrons, and within the scope of weak turbulence there is electron heating via collisional absorption. In the magnetized homogeneous plasma collisions are also important, but in this situation the inertial interval is very long and the wave frequency can change significantly $\Delta\omega \sim \omega$. Due to the conservation of the plasmon number a part of energy $\Delta\omega/\omega$ can be transferred to ions

via scattering by ions. Detailed calculations (see [110]) demonstrate that the ions can absorb up to 30% of energy. This pattern can be strongly affected by the density fluctuations. As shown in Section 7, even a very small fluctuation level strongly increases Landau damping. As a result, the interval of cascading is shortened, and the part of energy to be transferred to ions decreases. In Section 9 we will show that such fluctuations can arise as a result of modulational instability and all energy is typically transferred to a small group of accelerated particles.

9. Singular spectra of Langmuir turbulence and modification of weak turbulence approach

9.1. Introduction

We presented above a very detailed pattern of the weak turbulence of an isothermal plasma. The natural questions arise: how applicable is weak turbulence theory (WT) to real experiments? Does it work? These "naive" questions have recently become especially urgent. The increase of computational power makes possible a numerical simulation of the dynamic equations and direct comparison with WT predictions [111–114]. On the other hand, an active development of plasma diagnostics permits now to measure a very fine structure of the excited turbulence and to compare with the theoretical results and with numerical experiments. Especially the studies of the plasma turbulence induced in the ionosphere F-layer by powerful HF-radars [115–117] are well documented. It is accepted everywhere that the WT approximation is valid at the low turbulence level, precisely, typical growth rates must be smaller than the frequencies of interacting waves. The simulations of the dynamic equations, performed in the one-dimensional geometry [111] and in the two-dimensional geometry at low excesses above threshold [113], confirmed in very details WT results. But experiments and simulations demonstrate a lot of features inconsistent with WT predictions even at a low turbulence level. All simulations, cited above, dealt with the isotropic plasma case. For magnetized plasma turbulence, as was mentioned early, the range of the validity of WT must be broader. Nevertheless, experimental data, related to parametric heating, sometimes strongly contradict WT theory. For example, the measured width of the turbulence spectra does not exceed a few cascading steps in the wide range of the pump intensities for various experimental situations [118]. As we saw in the previous sections, within the WT approximation a very large $\Delta\omega \sim \omega$ width of the turbulent spectra must be expected. From our point of view this contradiction is a consequence of the singular character of Langmuir spectra and can be explained by the following reasons. It was shown that WT spectra have a singular, jet-like structure, being arranged on the lines, surfaces in k-space or even consisting of a set of quasi-monochromatic waves. Such a distribution can be unstable [119, 120] against the arising of spontaneous spatial modulations of the turbulence, which can lead, in principle, to a local growth of the intensity of the wave field and the necessity to improve the WT approach. Below we will discuss these problems in detail.

9.2. Modulational instability of singular WT spectra

We derived the kinetic wave equation in Section 1 using a small parameter

$$\gamma_{\mathrm{nl}}/\Delta\omega_k \ll 1 \ . \tag{9.1}$$

Here γ_{nl}^{-1} is a characteristic time of nonlinear interaction and $\Delta\omega_k$ is the mean difference of the frequences of interacting waves. Let us remind the approximations which we used to derive the kinetic equation

· The phases of the individual oscillations are random and are governed by Gaussian statistics. This assumption makes it possible to express correlation functions of a high order in terms of the pair ones. Condition (9.1) guarantees the randomness of the phases. Even if they are initially correlated, the rotation of the individual phases due to dispersion of frequency leads to the decay of the correlations.

· Turbulence is assumed to be uniform. It means that the conditions

$$\langle a_k a_{k'}^* \rangle = n_k \delta(k - k') \tag{9.2}$$

are satisfied.

As was mentioned above, the development of the modulational instability of the singular spectra breaks the homogeneity of the turbulence. Now it becomes $\langle a_k a_{k'} \rangle = n_{kk'}$. If the homogeneity is weak, $(kL \gg 1$, L- is a typical scale of inhomogeneity), $n_{kk'}$ is a very sharp function of $(k - k')$ and a smooth function of $(k + k')$. Hence we can introduce a density of plasmons, slowly varying in space:

$$n_{\tilde{k}}(r) = (1/(2\pi)^{3/2}) \int n_{\tilde{k},\kappa} \exp^{i\kappa r} d\kappa ; \quad \kappa = k - k' , \quad \tilde{k} = (k + k')/2 ,$$

and, starting from (1.32), obtain the following modification of (1.41) (we shall omit the sign of $\sim$ over k later):

$$\frac{\partial n_k}{\partial t} + \frac{\partial \tilde{\omega}_k}{\partial k} \frac{\partial n_k}{\partial r} - \frac{\partial \tilde{\omega}_k}{\partial r} \frac{\partial n_k}{\partial k} = \left(\gamma_k + \int T_{kk'} n_{k'} dk' \right) n_k . \tag{9.3}$$

Here $\tilde{\omega}_k$ includes a linear dispersion $\omega_k = \omega_p(1 + \frac{3}{2}k^2 r_D^2)$ together with a nonlinear frequency shift

$$\tilde{\omega}_k = \omega_k + 2 \int F_{kk'} n_{k'} dk' , \tag{9.4}$$

where $F_{kk'} = \mathrm{Re}\, T_{kk'kk'}$, $F_{kk'} = F_{k'k}$ and matrix element T_{kk,k_2k_3} is given by (1.33). Eq. (9.3) is closely connected with Vedenov–Rudakov equations (see for the corresponding discussion [121]); it was used also for the description of the narrow wave packet in [122, 123]. Without its right-hand part (9.3) describes a propagation of plasmons in inhomogeneous media (see [125]), the only difference is that the plasma frequency or refraction index can be spatially inhomogeneous due to the variation of a nonlinear frequency shift. It clarifies an action of the modulational instability: namely, a small disturbance of the wave field intensity change the trajectories of plasmons. It results in the additional focusing and a further local intensity growth. Of course, the presence of cascading can affect strongly the development of this instability. Eq. (9.3) does not include the diffraction effects; as a result it failed to describe the whole range of the maximal growth rate [121] and is useless for the description of the nonlinear stage of the modulational instability. For a singular jet-like spectra another approach can be used [120].

We restrict ourselves initially to a parametric excitation of Langmuir waves when the oscillations propagate in parallel to the external electric field (see Section 6), the direction of which we shall choose as the z-axis. Owing to the large difference between the group velocities along the z-axis

spatially nonuniform perturbations are suppressed in this direction and the modulational instability (MI) can develop only in directions perpendicular to the z-axis [120]. Therefore, we have

$$n_{kk'} = n_{k_z}(k_\perp, k'_\perp)\delta(k_z - k'_z) .$$

We shall change to a statistical description; the breaking up of the fourfold correlators into the pair correlators can be done also in a spatially nonuniform situation (the randomness of the individual phases is guaranteed by the large width of the packets along k_z):

$$n_{k_z}(\boldsymbol{r}_\perp, \boldsymbol{r}'_\perp) = (1/(2\pi)^2) \int n_{k_z}(k_\perp, k'_\perp) \exp\{i(\boldsymbol{k}_\perp \boldsymbol{r}_\perp - \boldsymbol{k}'_\perp \boldsymbol{r}'_\perp)\} \, \mathrm{d}\boldsymbol{k}_\perp \, \mathrm{d}\boldsymbol{k}'_\perp .$$

Finally, we obtain

$$((\partial/\partial t) + v + i(\tilde{\omega}_k - \tilde{\omega}_{k'}) + i\tfrac{3}{2}\omega_{\mathrm{p}}r_{\mathrm{D}}^2(\Delta_r - \Delta_{r'}))n_k(rr') . \tag{9.5}$$

We change here the definition of nonlinear frequency shift by including the imaginary part of the matrix element in it

$$\tilde{\omega}_k = \tfrac{3}{2}\omega_{\mathrm{p}}(kr_{\mathrm{D}})^2 + 2\int (F_{kk'} + iT_{kk'})n_{k'}(rr') \, \mathrm{d}k' ,$$

$$F_{kk'} = F_{k'k} = \mathrm{Re}\, T_{k_z k'_z k_z k'_z} , \qquad T_{kk'} = -T_{k'k} = \mathrm{Im}\, T_{k_z k'_z k_z k'_z} . \tag{9.6}$$

It is assumed that the scale of the spatial modulations is significantly larger than the wavelengths, therefore, we can neglect the $k_\perp$ dependence in the matrix elements. To simplify the notations we can drop in (9.6) and below the indices of k_z and the index $\perp$ of $r_\perp$. We note that the kernels $F_{kk'}$ and $T_{kk'}$ depend in this quasi-one-dimensional approximation only on $(\omega_k - \omega_{k'})/|k - k'| \simeq (|k - k'|)3/2\omega_{\mathrm{p}}r_{\mathrm{D}}^2$ and that to a good approximation they are difference operators. One can simplify Eq. (9.6) by noting that it has a solution of the form

$$n_k(r, r') = A_k(r)A_k(r') .$$

Here A_k satisfies the equation

$$i(\partial A_k/\partial t) + ivA_k + \tfrac{3}{2}\omega_{\mathrm{p}}r_{\mathrm{D}}^2 \Delta A_k + 2\int (F_{kk'} + iT_{kk'})|A_{k'}|^2 \, \mathrm{d}k' A_k = 0 . \tag{9.7}$$

In a transparent medium where $T_{kk'}$, $v = 0$ Eq. (9.7) transforms into a multi-component nonlinear Schrödinger equation. For a spatially uniform distribution of the oscillations we are led to the one-dimensional Eq. (1.41) by introducing $N_k = |A_k|^2$. In the general case (9.7) describes both the spectral transfer due to induced scattering and the effects of the modulational instability. For the 2D-jets this equation has a similar structure [120], only the integration over k must be performed along the two-dimensional jets and Δ – is a one-dimensional operator with a differentiation across the jet.

As was shown in previous sections, in case of a parametric excitation the Langmuir spectrum consists of a set of the quasi-monochromatic peaks. It is more convenient to change the envelopes of these peaks directly in (1.32):

$$\psi_{\mathrm{s}}(r) = \exp^{-ik_s r} \int a_{k_s} \exp^{ikr} \mathrm{d}k , \quad k_{\mathrm{s}} = k_0 = sk_{\mathrm{dif}} ,$$

here a_{k_s} is a part of a_k localized near k_s. For ψ_s one can easily find

$$i\psi_{0t} + 3/2\omega_p r_D^2 \Delta\psi_0 + F|\psi_0|^2\psi_0 = i(\gamma_0 - T|\psi_1|^2)\psi_0 \,,$$

$$i\psi_{1t} + 3/2\omega_p r_D^2 \Delta\psi_1 + F|\psi_1|^2\psi_1 = i(-\nu + T(|\psi_0|^2 - |\psi_2|^2))\psi_1 \,,$$

$$\vdots \tag{9.8}$$

$$i\psi_{nt} + 3/2\omega_p r_D^2 \Delta\psi_n + F|\psi_n|^2\psi_n = i(-\nu + T(|\psi_{n-1}|^2 - |\psi_{n+1}|^2))\psi_n \,,$$

In this derivation we used the fact that $F_{k_j k_{j-1}} = F(k_j - k_{j+1}) = F(k_{\text{dif}})$ is equal to zero while $F(2k_{\text{dif}})$ is small. The number of peaks is, as for homogeneous turbulence, determined by the ratio γ_0/ν. We also note that $F = -(\omega_p^2/4nT) \times G(0) \sim \omega_p^2/4nT$ is a positive quantity. If we consider only one of the coupled nonlinear Schrödinger equations (9.8), the sign of F defines the possibility of the modulational instability.

Eq. (9.8) can be obtained directly from (9.7) by putting

$$A_k(r) = \sum \psi_s \delta^{1/2}(k - k_0 + sk_{\text{dif}}) \,.$$

For the homogeneous case (9.8) is reduced to the satellite approximation with $n_s = |\psi_s|^2$.

Eq. (9.7) determines the spatially uniform stationary solutions of the form $A_k = A_k^0 \exp(i\Omega_k t)$, where A_k^0 and Ω_k are determined from the conditions

$$\Omega_k = \int F_{kk'}|A_{k'}^0|^2 \, dk' \,, \qquad \nu + \int T_{kk'}|A_{k'}^0|^2 \, dk' = 0 \,. \tag{9.9}$$

We consider the instability of (9.9) under small, spatially nonuniform perturbations

$$A_k = (A_k^0 + \delta A_k \exp(-i\Omega t + i\kappa r))\exp(i\Omega_k t) \,.$$

Linearizing (9.7) we obtain

$$\Omega\delta A_k - \tfrac{3}{2}\kappa^2 r_D^2 \omega_p \delta A_k + A_k^0 \int (F_{kk'} + iT_{kk'})A_{k'}^0(\delta A_{k'} + \delta A_{k'}^*) \, dk' = 0 \,,$$

$$-\Omega\delta A_k^* - \tfrac{3}{2}\kappa^2 r_D^2 \omega_p \delta A_k^* + A_k^* \int (F_{kk'} - iT_{kk'})A_{k'}^*(\delta A_{k'} + \delta A_{k'}^*) \, dk' = 0 \,.$$

Introducing the quantities

$$u_k = A_k^0(\delta A_k + \delta A_k^*) \,, \quad v_k = A_k^0(\delta A_k - \delta A_k^*)$$

and eliminating v_k, we obtain

$$\Omega\left(\Omega - 2i|A_k^0|^2 \int T_{kk'} u_{k'} \, dk'\right) = \tfrac{3}{2}\omega_p \kappa^2 r_D^2 \left(\tfrac{3}{2}\omega_p \kappa^2 r_D^2 + 2\int F_{kk'} u_{k'} \, dk' |A_k^0|^2\right) . \tag{9.10}$$

Notwithstanding the fact that Eq. (9.7) resembles the nonlinear Schrödinger equation qualitatively, the appearance of an MI is completely unexpected. The fact is that the spectral transfer (as we shall show in what follows) can effectively suppress the occurrence of local intensity maxima. It is impossible to study (9.10) in the general case and we restrict ourselves to considering a simpler physical situations.

If the linear damping of the waves is small, one can assume that the stationary distribution of the oscillations is uniform, $|A_k^0|^2 = \text{const} = N_0$. It was noted already that it is possible to take the kernels $T_{kk'}$ and $F_{kk'}$ as difference operators for $k \gg k_{\text{dif}}$

$$G((\omega_k - \omega_{k'})/|k - k'|v_{T_i}) \simeq G((k - k')/k_{\text{dif}}) .$$

In this case we easily get from (9.10) the dispersion equation

$$\Omega_{1,2} = -iT_q N_0 \pm ((T_q N_0)^2 + 3/2\omega_p \kappa^2 r_D^2 (3/2\omega_p \kappa^2 r_D^2 - 2F_q N_0))^{1/2}$$

$$= -iT_q N_0 \pm ((3/2\kappa^2 r_D^2 - F_q N_0)^2 + N_0(|T_q|^2 - |F_q|^2))^{1/2} . \tag{9.11}$$

Here we have

$$T_q = (1/(2\pi)^{1/2}) \int T(x) \exp^{iqx} dx , \qquad F_q = (1/(2\pi)^{1/2}) \int F(x) \exp^{iqx} dx ,$$

$$T(x) = T(k - k') , \qquad F(x) = F(k - k') .$$

The function T_q is a purely imaginary one due to its symmetry, $T_q = if(q)$. Similarly, F_q is purely real function. It is also clear that as $q \to 0$ $T_q \propto q$. We have from (9.11) for the uniform perturbations two branches of neutral-stable perturbations $\Omega = 0$ and $\Omega = 2f(q)N_0$. In the long-wavelength limit one of them changes into second sound. It is evident that the spatially nonuniform perturbations are unstable for $|T_q| < |F_q|$. A simple calculation gives for the Green function in the hydrodynamical approximation

$$T_q = i\pi T_0 \exp(-(\gamma_s/\Omega_q)|q|k_{\text{dif}}) \sin qk_{\text{dif}} ,$$

$$F_q = -\pi T_0 \exp(-(\gamma_s/\Omega_q)|q|k_{\text{dif}}) \sin |q|k_{\text{dif}} , \qquad T_0 = \omega_p^2/4nT .$$

It is clear that $|T_q| = |F_q|$ and there is no instability, it is stabilized by the induced scattering. We shall show that this fact is not accidental and is not connected with any actual approximation of the kernels. In the general case the function G in the matrix elements can be expressed in terms of the electron purmuttivity and therefore it is analytical in the upper half plane. Hence we have

$$\int_{-\infty}^{\infty} G(x) \exp^{iqx} dx = 0 , \quad q > 0 ,$$

whence also follows the relation $|T_q| = |F_q|$. An instability appears if we take into account the modulation which is always present, of the intensity of the turbulence along the jet. One can show it for a spectrum consisting of a set of identical satellites. We consider now perturbations which involve only even or only odd peaks. It is clear from the system (9.8) that then there is no interaction between the neighboring perturbed peaks and there appears separately a modulation instability of each excited peak.

9.3. Nonlinear stage of modulational instability

We start from the consideration of the parametric excitation of waves, more precisely, from the investigation of the nonlinear evolution of one quasi-monochromatic peak. It is described by the nonlinear Schrödinger equation, intensively studied recently. This evolution is strongly dependent

on the dimension of the problem. In the one-dimensional case MI results in a deep modulation and formation of a stable soliton with an amplitude comparable with the initial turbulence level. In 2-D and 3-D cases MI results in the formation of regions with an enhanced concentration of wave field and their collapse in a finite time. In fact, we must change to Langmuir collapse at large amplitudes. Independent of the dimension of the problem the characteristic evolution time is $(FN)^{-1}$. As was shown in Section 4–6, within the homogeneous model the energy is transferred from the excitation region by pulses, evolving at every instant of time only a few peaks. The velocity of such a pulse does not depend strongly on the noise level $v \sim TNk_{dif}$. A modulational instability with a characteristic growth rate FN must develop more quickly than the pulse is travelling a distance k_{dif}. So, the condition $FN < k_{dif}/v$, or $F < T$ is necessary for the MI to be suppressed. It is evident that the possibility of MI and the subsequent collapse depends on the ratio F/T, i.e. on the ratio of the electron temperature to the ion one. An elucidation of the actual value of this ratio, a detailed study of the development of MI, can be given by numerical simulations. It was carried out in [126] by using a system (9.8) written in dimensionless variables:

$$\gamma_0 t \to t , \quad k \to k_{dif} k , \quad F|\psi_j|^2 \to \gamma_0|\psi_j|^2 , \quad v/\gamma_0 \to v , \quad 2r^2\gamma_0/3r_D^2\omega_p \to r^2 ,$$

$$i\psi_{0t} + \Delta\psi_0 + |\psi_0|^2\psi_0 = i\psi_0(1 - v - \bar{T}|\psi_1|^2) ,$$

$$\vdots \tag{9.12}$$

$$i\psi_{jt} + \Delta\psi_j + |\psi_j|^2\psi_j = i\psi_j(- v + \bar{T}(|\psi_{j-1}|^2 - |\psi_{j+1}|^2)) . \tag{9.12}$$

Here $\bar{T} = T/F = \Omega/2\gamma_s$. It will be shown in what follows that this ratio determines whether it is possible that a MI can develop.

Under actual physical conditions the region of cascading is small (not more than 10 steps of spectral transfer) and in the small k-range there exists an energy sink caused by Langmuir collapse. One used a "running" boundary conditions bounded two last peaks

$$\psi_n = \psi_{n-1}$$

to simulate the finite size of the region in k-space and the energy absorption via collapse. The number of peaks was varied up to ten; axially symmetrical distributions were considered and a boundary condition $\partial\psi/\partial r = 0$ was used. The size of the computing region over r was $L = 10$, much larger than the typical size of MI, $L \sim 1$ for $|\psi|^2 \sim \gamma_0/F$.

Of most interest are the cases where one is well above threshold; therefore, one started from calculations for $v = 0$. The evolution of the oscillations depended strongly on the parameter $\bar{T}$. We show in Fig. 9.1 the evolution in time of the maximum amplitude of the separate peaks. The appearance of MI and then of Langmuir collapse is clear and it occurs typically not in the directly excited peak, but in the scattered ones. The first scattered peak collapses at $\bar{T} = 1$. When $\bar{T}$ increases, the oscillations are transferred along the spectrum and the collapse occurs after multiple scattering. Fig. 9.1 corresponds to $\bar{T} = 1.4$. The spatial distribution of the intensities of the oscillations in the various satellites is shown in Fig. 9.2. When the intensity of the collapsing satellite starts to exceed the intensity of the neighboring ones significantly, one can neglect the interaction with them and the growth of the electric field is described by the well-studied nonlinear Schrödinger equation. It means that in the collapse a finite energy is absorbed and it serves as an efficient dissipation mechanism [124]. The number of spectral transfer steps $kr_D\sqrt{m/M}$ can in
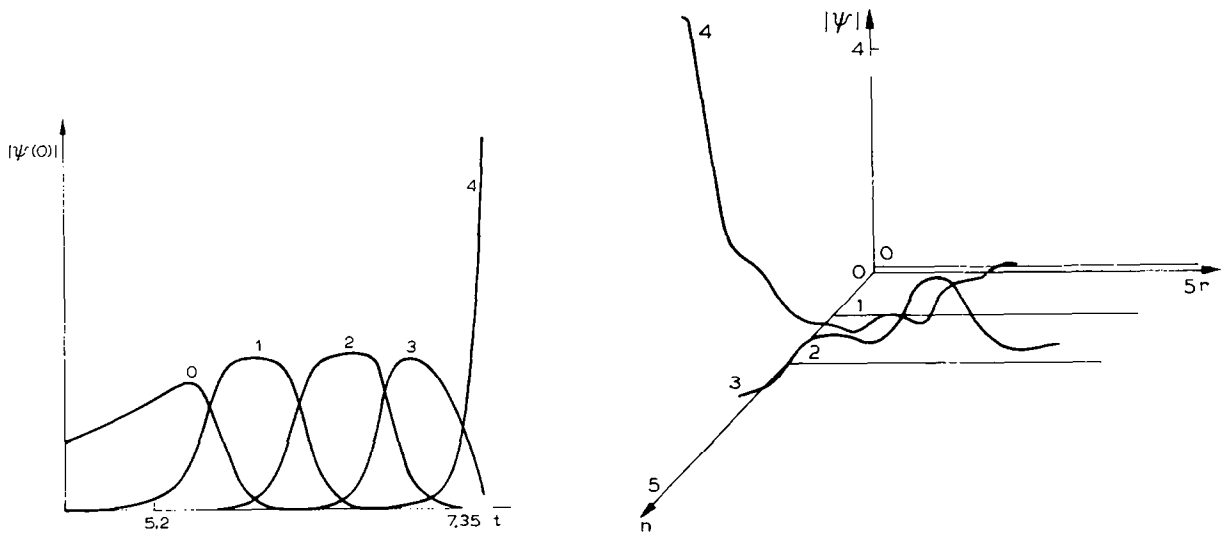
Fig. 9.1. Temporal evolution of the amplitudes of the different modes in the center of the packets for $\tilde{T} = 1.4$. One can see a stage-by-stage energy transfer along the modes corresponding to the weak-turbulence description. A field singularity develops in the fourth peak after a finite time.

Fig. 9.2. Spatial distribution of the amplitudes of the different modes at the moment immediately before the collapse for the calculations represented in Fig. 9.1.

practice not be larger than ten. This means that already for $\tilde{T} \sim 3$, which corresponds to $T_e = 3T_i$, calculations show that the modulational instability does not manage to develop and the transfer to the small k region, the collapse region, is described by the weak turbulence theory. It has the nature of a periodic splitting of the oscillation pulses (solitons), as is very clearly seen in numerical experiments. If the initial stationary uniform distribution of peaks is considered, the calculations show it to be stable for $\tilde{T} > 3$ in the range of about 10 peaks. In that case the perturbations manage to be carried to the boundary of the interval before the collapse manages to occur.

At finite excesses above threshold the spectra consist of $n \sim \gamma_0/\nu$ satellites. Numerical calculations show that if the peak with number n_c in which the collapse develops is closer than $(\gamma_0/\nu)k_{dif}$ to the excitation source, the process looks the same as for $\nu = 0$. If, on the other hand, $n_c \geq \gamma_0/\nu$, the collapse does not occur. The dynamics of the peaks is nonstationary, in agreement with Sections 5 and 6, and changes from being periodic just above threshold to be rather entangled. As was told above, the self-focussing and the collapse are very efficient dissipation mechanisms and it means that cascading practically terminates at $n = n_c$. For an isothermal plasma one can conclude therefore that for an isothermal plasma not more than a few cascadings can occur.

Even in the situation when collapses are absent, modulational instability is able to change the dynamics of turbulence. In the paper [113], mentioned above, it was shown that the results of the two-dimensional dynamical simulations were the same as WT predictions. Unfortunately, the authors of [113] were restricted by the limited computational resources to obtain a long-time detailed study. It is easy to perform it within the system (9.12) [126]. In Fig. 9.3 comparative results
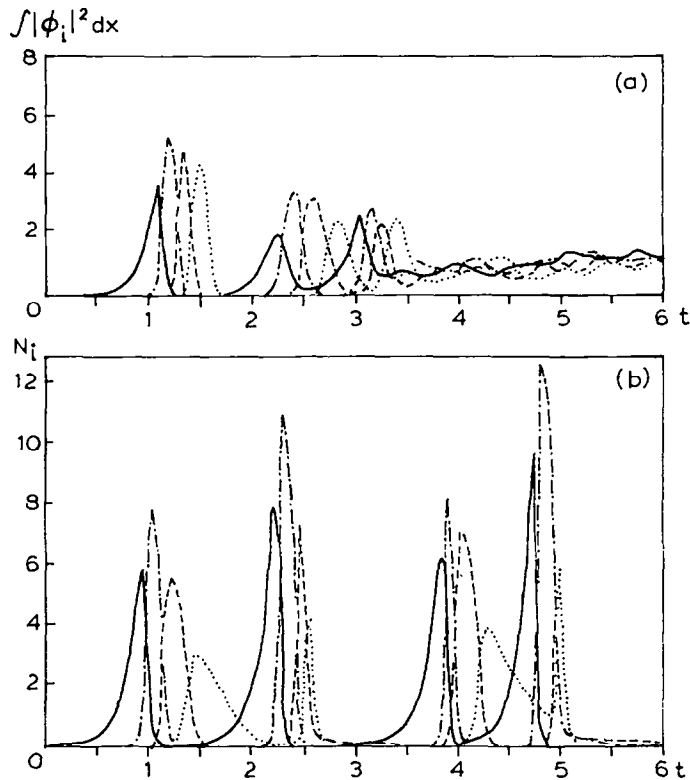
Fig. 9.3. (a) Evolution of the integral intensity $\int |\psi_i|^2 dx$ for two-dimensional turbulence when one is well above threshold. We show in the figure the intensities of the first four peaks; $\tilde{T} = 3.7$, $\gamma_0/\nu = 13$. (b) Evolution of the peak intensities in the satellite approximation [Eqs. (4.4)] for the parameters corresponding to Fig. 9.3(a).

are shown for the temporal evolution of the oscillations in the framework of (4.4) and (9.12). In the first curve we show the evolution of the intensity of the peaks in (4.4) and in the second one – the evolution of the integral intensity $\int |\psi_j|^2 dx$. It is clear that when the first few pulses split, the results of the calculations are practically the same. However, when time goes on the gaps between the temporal maxima start to become less distinct and a stationary solution is reached. This is not surprising since the system (9.12) is not Hamiltonian. Eqs. (9.12) are local and the transfer rates in different points along the x-axis are different. The nonlinear interaction correlates x but since the growth rates of the spectral transfer and of the MI are comparable, the total intensity of the peaks does not drop to zero and stationarity is reached. There occurs then an appreciable deformation of the spatial distribution of the waves as compared to the initial stage of the process. We see that the development of MI can greatly accelerate the onset of the steady state, and the stationary intensity and, hence, the absorption rate well correspond to WT results. Let us discuss in more details simulation results within the dynamical equations (see e.g. Figs. 9.4 and 9.5 taken from [113]). In Fig. 9.4 time-averaged spectral distributions are presented and in Fig. 9.5 – a few "snap-shots" of the spectral evolution. One can see that turbulence really takes a peak-like structure, justifying
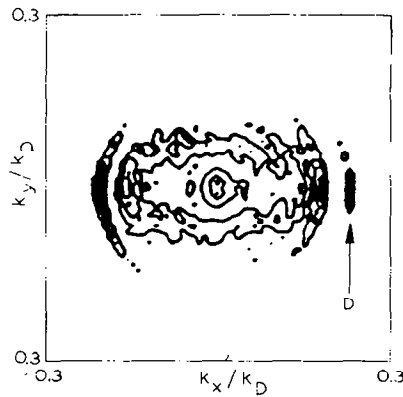
Fig. 9.4. Langmuir spectra averaged over time excited by a monochromatic driver at the point labeled by D, obtained by a numerical simulation of Eqs. (1.11), (1.25). Three steps of cascading are clearly demonstrated.
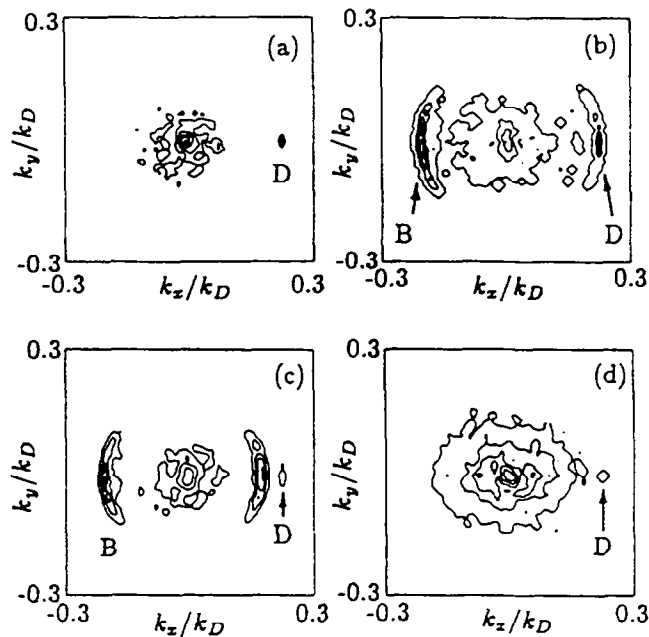

Fig. 9.5. Instantaneous wave number spectra for the simulations presented in the Fig. 9.4. A nonstationary cascading – splitting of pulses from the pump region (described above) is sharply pronounced.

results of the previous sections. Nonstationary behavior also corresponds to the pattern outlined above. For the results presented in Figs. 9.4 and 9.5 excitation was performed in one mode; three consequent cascadings are clearly pronounced. The spectrum consists of counter-propagating waves and the modulation instability along the longitudinal direction is suppressed. The matrix elements describing the induced scattering are smooth functions in the perpendicular direction and

sharp ones – along the jets. As a result an arising modulational instability is one-dimensional and the collapse is absent. Two-dimensional simulations, described early, enlightened another problems of utilization of WT results. When the ion-sound damping is small, a build-up of powerful ion-sound waves takes place, especially in the small k region. It turns out the conversion on ion-sound plasmons to become an important process [127, 128] and to lead to the necessity to take into account the sound nonlinearities. An even larger amount of cascades can be seen in Fig. 9.6, taken from the paper [129]. This figure presents an averaged spectrum of parametrically excited Langmuir turbulence. Let us underline that in [129] two-dimensional simulations were performed and real number of cascades can be smaller.

We see that Langmuir spectra with multiple cascading can be observed only in a plasma with very weak ion-sound damping. Such a situation can be realized in the powerful laser interaction with high-Z targets. In this case $c_s = \sqrt{ZT_e/M}$ might be substantially larger than the ion thermal velocity even for $T_e \sim T_i$ and only weak Landau damping on the electrons is important. Recently anomalously high "red-shifted" spectra were observed in experiments with gold foils [130].

Let us discuss briefly an excitation of Langmuir waves by electron or ion beams. As we saw, turbulence spectra represents a two-dimensional jet (see Section 6). An arising modulational instability in the transverse direction is one-dimensional and results only in the broadening of spectra along the line of the maximal growth rate. For the quasi-monochromatic beams this spreading can be comparable with the size of the growth rate region and can lead to a drop in the energy deposition [131, 132], therefore a modification of WT considered in this section is desirable. For the "wide" beams, when the broadening is small in comparison with the size of growth rate, the WT approximation is valid, at least, for the calculation of the deposition rate and an evaluation of the relaxation length.
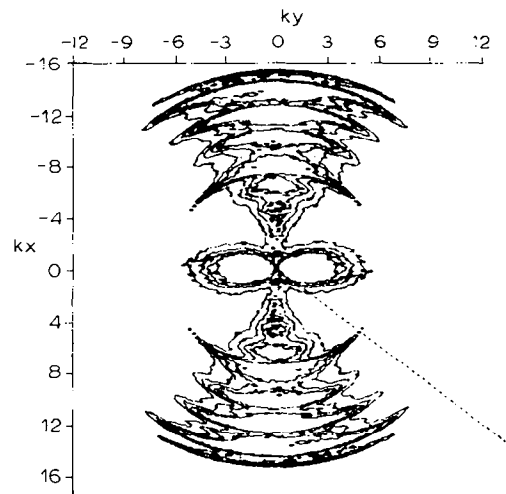

Fig. 9.6. Spectra averaged over time of parametrically excited Langmuir turbulence obtained during a simulation of two-dimensional dynamic equations in Ref. [129].

9.4. Turbulence of magnetized plasmas

A weak magnetic field ($\omega_H \ll \omega_p$) affects the turbulence spectra qualitatively little. The situation changes drastically for $\omega_H > \omega_p$ when the dispersion law of magnetized Langmuir oscillations has the form $\omega_k = \omega_p \cos|\theta|$, where θ is the angle between the wave vector and the magnetic field. In this case, as it was shown in Section 7, the spectra are axially isotropic and take the form of jet $n_k = n(\theta)\delta(k - k_0)$. An energy transfer along the jet leads to the condensation of the oscillations in the large k region which is stopped only by Landau damping, while k_0 is determined by the condition $\gamma_L(k_0) \simeq (k_0 r_D)^2 v_{ei}$ (v_{ei} is the collisional damping rate). The modulational instability of this singular spectra can develop only across the jet; i.e. it is essentially one-dimensional. As was mentioned already, one-dimensional MI does not lead to the collapse but only to a broadening of the jet. However, even a small broadening of the spectrum, $\Delta k/k \sim (k_0 r_D)^2$, leads to a steep increase of Landau damping (in the same way, as density fluctuations do), so that MI can lead also to a significant growth of the absorption in this case. An analytical description of the problem is quite difficult and to elucidate the general physical picture one has to use a numerical simulation. In [126] a numerical calculation was performed within the one-dimensional system (9.12) with $\nabla^2 \psi_j = \psi_{xxj}$ and with adding a term $\hat{\gamma}_k \psi_j$ simulating Landau damping. In the k-representation the operator $\hat{\gamma}_k$ is equal to

$$\hat{\gamma}_k = \begin{cases} \alpha k^2, & k > 0, \\ 0. \end{cases}$$

The magnitude of α was chosen such that for a modulation broadening Δk corresponding to being above threshold by an amount of order unity, $\alpha(\Delta k)^2$ was of order ν. Numerical experiments showed that the nature of the evolution of the system and its integral characteristics were not sensitive to the value of α. Before going over to a description of the numerical calculations we discuss what information we hope to get from them. The assumption of strong dissipation occurring thanks to the simultaneous action of the MI and of the damping $\hat{\gamma}_k$ is not obvious. It is possible, in principle, that there are situations when together with a broadening there is a significant shift to the region of negative k and the effective absorption is small. The calculations [126] showed that although such a shift does occur, a significant part of energy is contained in "Landau damping" region and that its role increases when the pumping growth rate increases. The width of the spectrum $\Delta\omega$ can be used as a good indicator of the efficiency of the damping. In the discrete numerical model its role is played by the effective number $\bar{n}$ of excited peaks,

$$\bar{n} = \frac{\sum_k k \int_{-\infty}^{\infty} |\psi_k|^2 \, dx}{\sum_k \int_{-\infty}^{\infty} |\psi_k|^2 \, dx}. \tag{9.13}$$

In the framework of the uniform "peak-kinetics" model $\bar{n}$ increases when the damping ν decreases, on average as $\bar{n} \sim 1/\nu$. In Fig. 9.7 we show the results of evaluating n for the model (4.4). Including the damping $\hat{\gamma}_k$ leads to the fact that the magnitude of $\bar{n}$ ceases to increase and reaches saturation. The effective decrease in the width of the spectrum is very clear in Fig. 9.3, where the spectral
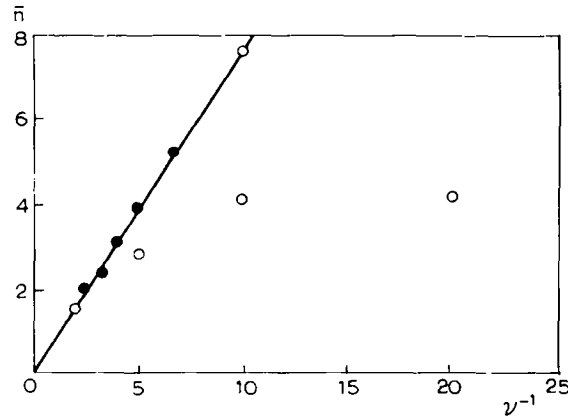
Fig. 9.7. Width of the spectrum (the number of satellites) as a function of the damping for the turbulence model of a magnetized plasma. The results of the calculations carried out using Eq. (9.13) are indicated by crosses. The asterisks show the results when Landau damping is included.

densities of the intensity of the different satellites, averaged over time, are shown. This result is reasonable. As to order of magnitude, the effective damping must be equal to the growth rate of the modulational instability, $\gamma_{\text{mod}} \sim F|\psi|^2 \sim FN$. Since we have for the number of peaks

$$\bar{n} \sim \gamma_{\text{p}}/\nu_{\text{eff}} \sim \gamma_{\text{p}}/(\nu + \hat{\gamma}_k) \sim \gamma_{\text{p}}/f|\psi|^2 \ ,$$

it is clear that when the growth rate increases, $\bar{n}$ reaches a constant value. More precisely, we can write for the steady state

$$T(N_{k-1} - N_{k+1}) = FN_k \ .$$

Assuming the change in intensity from the peak to the peak to be small,

$$N_{k-1} - N_{k+1} = -2\,\mathrm{d}N_k/\mathrm{d}k \ ,$$

we get $N_k = N_0 e^{-(F/2T)k}$, $N_0 = \gamma_{\text{p}}/T$, i.e. the width of the spectrum is $\bar{k} \sim 2T/F$, or, in dimensional variables, $\Delta\omega = (2T/F)kc_s$, and is independent of the magnitude of the growth rate. Let us emphasize that similar to the case of an isotropic plasma, the absorption rate, defined by the first peak, can be described by WT formulas.

We have thus shown that the WT description of Langmuir turbulence of isothermal plasma is valid when it is not too far above the threshold of pumping. The main reason is that the jet-like spectra are unstable under the development of the modulational instability. It was shown also that a constructive modification of the WT approach by the introduction of an effective damping can be done. This modification provides an adequate description of the experimental situations.

PART II. LANGMUIR TURBULENCE OF NONISOTHERMAL PLASMA

10. Introduction

In a plasma with different electron and ion temperatures $T_e \gg T_i$ – a so called nonisothermal plasma, there occurs a modification of the mechanism defining the turbulence spectra. In a nonisothermal plasma the decay interaction involving ion-sound waves is the main nonlinear process

$$\omega_k^l = \omega_{k_1}^l + \Omega_{k_2}^s, \quad k = k_1 + k_3, \tag{10.1}$$

where $\omega_k^l = \omega_p(1 + \frac{3}{2}k^2 r_D^2)$, $\Omega_k^s = c_s k$ are the frequencies of Langmuir and ion-sound oscillations; $c_s = \sqrt{T_e/M}$ is the ion-sound velocity. In contrast to the case of isothermal plasmas, discussed in part I, low-frequency motions are not forced, there are an additional degrees of freedom. The frequencies of the Langmuir waves are higher than Ω_k and the decay process (10.1) is a variant of the classical problem of the interaction of high- and low-frequency collective motions of the continuous media. The appearance of additional degrees of freedom associated with ion-sound substantially complicates the picture of the nonlinear interaction and makes it essentially impossible to carry out anything approaching a thorough analysis of the corresponding kinetic equations. In this situation it is important to combine analytic methods with numerical simulations in order to develop relatively simple models for the plasma description in particular cases.

It would seem that the scattering Langmuir waves by ion-sound can smooth a turbulence spectra in comparison with the one arising due to induced scattering (described in Part I). A qualitative analysis of the decay kinetic equations shows, however, that Langmuir waves with near colinear wave vectors are interacting more strongly. It gives rise to the appearance of anisotropic spectra and we start with an investigation of the main characteristics and conditions of the onset of jet-like spectra, which can be established under the anisotropic excitation of waves. Section 11 is devoted to the isotropic spectra corresponding to the wide over angle excitation of Langmuir waves. At the end of this part it will be shown that Kolmogorov–Richardson ideas can be used in the problem of l's interaction and that Kolmogorov spectra will be obtained.

In a nonisothermal plasma there appear two new parameters – the ratio of the ion-sound damping $\gamma_s = \sqrt{(\pi m/8M)} k c_s$ to the collisional Langmuir damping γ_s/ν_{ei} and the ratio γ_s/Ω_s. A change of various turbulence regimes is defined by these parameters. In particular, ion-sound oscillations are "induced" under the condition

$$\nu_{ei} < \gamma_{nl} < \gamma_s \tag{10.2}$$

and it is possible to use again an induced scattering approximation. A limiting case of the strong damping of Langmuir waves

$$\Omega_s \sqrt{(\pi m/8M)} \equiv \gamma_s \ll \gamma_{nl} \ll \nu_{ei}, \Omega_s \tag{10.3}$$

occurs at the narrow parameter range and it will not be considered. It is worth to note that such a situation can be realized in laser plasmas (see for example [133]).

11. Jet-like spectra

The system of kinetic equations (1.50)–(1.52), describing the decay processes, in the absence of excitation and damping $\Gamma_k = v_{\rm ei} - \gamma_k \equiv 0$, $\gamma_s \equiv 0$ conserves the total energy

$$E = \int (\omega_k N_k + \Omega_k n_k) \, dk \tag{11.1}$$

and the total number of plasma-wave quanta

$$N = \int N_k \, dk \,, \tag{11.2}$$

but it generally leaves the number of ion-sound waves arbitrary.

An important feature of (1.50)–(1.52) is that the kernels of the integral equations are not homogeneous functions of the moduli of the wave vectors k, k_1, k_2. The reason for this situation lies in the different ways in which the frequencies ω_k and Ω_k vary with the wave vector. As a result, a characteristic scale arises in k-space:

$$k_{\rm dif} = \tfrac{2}{3} r_{\rm D}^{-1} \sqrt{(m/M)} \,. \tag{11.3}$$

The quantity $k_{\rm dif}$ represents the maximum change in the wave vector of a plasma-wave quantum in a single interaction event. Generally speaking, the existence of this characteristic interaction size should have the consequence that the spectra lack scale invariance. In other words, the turbulence spectra would be "cut up" as functions of k analogously to the induced scattering case (see Part I). Another important circumstance is the strong angular dependence of the matrix element $|V_{k,k_1 k}|^2$. It can be seen from (1.50)–(1.52) that Langmuir waves with parallel k interact more efficiently (it corresponds to the maximum of the impulse received by ion-sound quanta for each l's interaction event). It is natural that there occur one-dimensional jet-like spectra under the anisotropic source of waves γ_k. The onset problem, however, is a rather more difficult task than in the isothermal plasma due to the appearance of new integrand terms like $\sim \int N_{k_1} n_{k_2} \, dk_1 \, dk_2, \int N_{k_1} N_{k_2} \, dk_1 \, dk_2$ in the kinetic equations. These terms look like "own noise" and, in principle, could lead to the smoothing of the singular distributions and to the isotropization of spectra. A more detailed investigation shows (see below) that Langmuir spectra remain jet-like ones, at least, under the anisotropic excitation of waves.

Let us derive the equations describing the distribution of oscillations along one-dimensional jets [134]. Setting $N_k = N_\kappa \delta(k_\perp)$ and $n_k = n_\kappa \delta(k_\perp)$ in (1.50)–(1.52), we find the differential-difference equations

$$(\partial N_\kappa / \partial t) + 2\Gamma_\kappa N_\kappa$$

$$= 4\alpha [n_{2\kappa-1}(N_{-\kappa+1} - N_\kappa - N_\kappa N_{-\kappa+1} + n_{-2\kappa-1}(N_{-\kappa-1} - N_\kappa) + n_{-\kappa-1} N_\kappa] \,,$$

$$(\partial n_{2\kappa-1}/\partial t) + 2\gamma^{\rm s}_{2\kappa-1} n_{2\kappa-1} = 2\alpha [n_{2\kappa-1}(N_\kappa - N_{-\kappa+1}) + N_\kappa N_{-\kappa+1}] \,, \tag{11.4}$$

$$(\partial n_{-2\kappa-1}/\partial t) + 2\gamma^{\rm s}_{-2\kappa-1} n_{-2\kappa-1} = 2\alpha [n_{-2\kappa-1}(N_{-\kappa-1} - N_\kappa) + N_\kappa N_{-\kappa-1}] \,.$$

It follows immediately from (11.4) that the interaction couples plasma waves whose wave vectors differ by k_{dif}. For simplicity we set $N_\kappa = N_{-\kappa}$ and $n_\kappa = n_{-\kappa}$. When $\Gamma_\kappa = \gamma_\kappa^s \equiv 0$, there is a continuum set of integrals of motion:

$$N_\kappa - 2(n_{2\kappa+1} - n_{2\kappa-1}) = f(\kappa) , \tag{11.5}$$

where the function $f(\kappa)$ is defined by the initial conditions. The existence of an infinite set of integrals of motion for different wave vectors make the dynamics of Langmuir-sound waves highly nontrivial. In particular, there is no energy pumping to large k. Infact, let us assume that at $t = 0$ Langmuir oscillations are excited for $\kappa < \kappa_0$ and ion-sound ones – for $\kappa < 2\kappa_0$, therefore $f(\kappa) \equiv 0$ for $\kappa > \kappa_0$. Then it follows from (11.5) that Langmuir waves with $\kappa > \kappa_0$ cannot appear during the further evolution in time. It is evident that these considerations are valid also if one include damping and excitation of waves. A remarkable feature of (11.4) takes place: thermodynamic equilibrium cannot be reached due to the one-dimensional character of the Γ's interaction (although a relaxation to a Rayleigh–Jeans distribution is possible within the initial system (1.50)–(1.52)).

If the characteristic length for changes in N_κ, n_κ is much larger that k_{dif}, it can be converted to the differential approximation in (1.4) analogously to Section 3 of

$$\frac{\partial N_k}{\partial t} + 2\Gamma_k N_k = 4\alpha k_{\text{dif}} \frac{\partial}{\partial k}\left(N_k^2 + k_{\text{dif}} n_{2k} \frac{\partial N_k}{\partial k}\right), \tag{11.6}$$

$$\frac{\partial n_{2k}}{\partial t} + 2\gamma_{2k}^s n_{2k} = 2\alpha\left(N_k^2 + k_{\text{dif}} n_{2k} \frac{\partial N_k}{\partial k}\right). \tag{11.7}$$

11.1. Steady-state spectra

The simplest way to analyse steady-state solutions of (11.4) is to adopt the differential approximation, according to which (11.6), (11.7) become

$$\Gamma_k N_k = 2k_{\text{dif}} \frac{\text{d}}{\text{d}k} \gamma_{2k}^s n_{2k} , \qquad \gamma_{2k}^s n_{2k} = \alpha\left(N_k^2 + k_{\text{dif}} n_{2k} \frac{\text{d}N_k}{\text{d}k}\right). \tag{11.8, 11.9}$$

In solving (11.8), (11.9) it will be assumed that the width of the growth rate γ_k is small, $\Delta k \ll k_0$, so one can distinguish an excitation region ($k \sim k_0$) and an inertial interval, in which $\gamma_k \ll \nu_{\text{ei}}$. In this case, even if the excitation level is above the threshold by an amount corresponding to $\gamma_{k_0}/\nu_{\text{ei}} \gg 1$, the properties of the solutions of (11.8), (11.9) do not depend on the structural details of the growth rate and are governed by its integral characteristics. Eqs. (11.8), (11.9) can be integrated most simply in the limiting cases $\nu_{\text{ei}} \gg \gamma_k^s$ and $\nu_{\text{ei}} \ll \gamma_k^2$. In the first of these cases, Eq. (11.9) can be simplified as follows for the inertial interval:

$$\gamma_k^s = \alpha k_{\text{dif}} (\text{d}N_k/\text{d}k) \quad (n_{2k} \neq 0) . \tag{11.10}$$

integrating (11.10) over the inertial range ($k > k_0$, $\gamma_k \sim 0$) and taking into account the finite size of the jet, we obtain

$$N_k = \sqrt{(\pi m/8 M)}\, c_s/\alpha k_{\text{dif}}(k^2 - \tilde{k}^2) . \tag{11.11}$$

Substituting (11.11) into (11.8), (11.9), we obtain in the inertial interval

$$n_{2k} = (\nu_{ei}/12\alpha k_{dif}^2)((k - \tilde{k})^2/k)(k + 2\tilde{k}) , \tag{11.12}$$

and for $k > k_0$, where $\gamma_k \simeq 0$, we find $n_{2k} = N_k = 0$. It follows from (11.12) that the spectral distributions of n_{2k} and N_k are nonzero in the respective intervals

$$\tilde{k} < k \le k_0 , \qquad 2\tilde{k} < k \le 2k_0 . \tag{11.13}$$

As was noted above, there is no pumping of energy toward high frequencies. It will be shown below, that the "violet shift" is due exclusively to the fact that the spectra are not one dimensional.

Let us calculate the value of $\tilde{k}$ corresponding to the end of the interval filled by Langmuir waves. For this purpose we can use an equation of Langmuir quanta, which follows from (11.8), (11.9):

$$\int_{\tilde{k}}^{k_0} \Gamma_k N_k \, dk = 0 . \tag{11.14}$$

Finding the width of the growth rate γ_k from

$$\int \gamma_k \, dk \simeq \gamma_{k_0} \Delta k , \tag{11.15}$$

the length of the jet turns out to be

$$k_0 - \tilde{k} \simeq 3(\gamma_{k_0}/\nu_{ei}) \Delta k . \tag{11.16}$$

According to (11.13), the spectrum reaches "zero" when the excitation level is

$$\gamma_{k_0}/\nu_{ei} \le k_0/\Delta k . \tag{11.17}$$

Eqs. (11.11), (11.13) completely determine the one-dimensional spectrum. Let us calculate the total energy densities of Langmuir and ion-sound waves from these equations:

$$W_1 = \int_{\tilde{k}}^{k_0} \omega_p N_k \, dk \simeq n_0 T_e \left((m/M) \, \Delta k/k_{dif}\right)^2 (\gamma_{k_0}/\nu_{ei})^2 k_0 r_D ,$$

$$W_s = \int_{\tilde{k}}^{k_0} \Omega_{2k} n_{2k} \, dk \simeq n_0 T_e (\nu_{ei}/\omega_{pi})(\Delta k/k_{dif})^2 (\gamma_{k_0}/\nu_{ei})^2 k_0 r_D (m/M)^{1/2} . \tag{11.18}$$

Eqs. (11.8), (11.9) thus lead to an extremely high ion-sound level:

$$W_s/W_1 \sim (\nu_{ei}/\omega_{pi})(\Delta k/k_{dif})(\gamma_{k_0}/\nu_{ei}) . \tag{11.19}$$

The physical meaning of this result is quite simple. The number of Langmuir quanta does not change in a decay event, and number of ion-sound quanta increases by one. Therefore,

$$n_s/N_1 = W_s\omega_p/W_1\Omega_s \simeq (k - \tilde{k})/k_{dif} . \tag{11.20}$$

For large excesses above threshold,

$$n_s/N_1 \sim k/k_{dif} . \tag{11.21}$$

Finally, the energy flux into the plasma is

$$Q^1 = \int_{\tilde{k}}^{k_0} v_{ei} N_k \omega_p \, dk \simeq v_{ei} n_0 T_e (m/M) (\Delta k/k_{dif})^2 (\gamma_{k_0}/v_{ei})^2 k_0 r_D \,, \tag{11.22}$$

$$Q^s = \int_{\tilde{k}}^{k_0} \gamma_{2k}^s n_{2k} \Omega_{2k} \, dk \simeq v_{ei} n_0 T_e (m/M)^{3/2} (\Delta k/k_{dif})^3 (\gamma_{k_0}/v_{ei})^2 (k_0 r_D)^2 \,,$$

$$Q^s/Q^1 \simeq \sqrt{(m/M)} \, k_0 r_D (\Delta k/k_{dif}) (\gamma k_0/v_{ei}) \,. \tag{11.23}$$

We turn now to the opposite limiting case $\gamma_k^s \gg v_{ei}$. It is easy to see that this case corresponds to the approximation of induced scattering for Langmuir waves (see Part I). Eliminating the ion-sound oscillations from (11.8), (11.9) by means of

$$\gamma_{2k}^s n_{2k} = \alpha N_k^2 \,, \tag{11.24}$$

we find

$$\Gamma_k = 4\alpha k_{dif} (dN_k/dk) \,. \tag{11.25}$$

Working by analogy with the procedure above, we can easily find from (11.25) the densities of the Langmuir and ion-sound waves and also the energy flux into the plasma. For the spectral density N_k, e.g. we have

$$N_k = (v_{ei}/4\alpha k_{dif})(k - \tilde{k}) \,, \quad k_0 - \tilde{k} = \Delta k (\gamma_{k_0}/v_{ei}) \,. \tag{11.26}$$

The energy flux is correspondingly

$$Q^1 \sim (\gamma_{k_0}^2/\omega_p) n_0 T_e (\Delta k/k_{dif})^2 \,. \tag{11.27}$$

The relative contribution of the ion-sound waves is also determined by (11.19) and (11.23). At a sufficiently high excitation level above the threshold,

$$\gamma_{k_0}/v_{ei} \gtrsim k_0/\Delta k \,, \tag{11.28}$$

in both cases ($v_{ei} \gg \gamma_k^s$, $v_{ei} \ll \gamma_k^s$), jets reach the region $k \simeq 0$. In this case the effect of collapse must be taken into account by introducing an effective damping at small k. Even further above the threshold, at which the collapse occurs directly in the excitation region ($k \sim k_0$), the effect of the collapse is much more complicated, and the effect of the intense sound must be taken into account.

To conclude this section, it should be noted that steady-state solutions of kinetic equations can be found not only in the differential approximation but also in the opposite one the satellite approximation. It corresponds to the excitation of waves by a "narrow" growth rate with the characteristic size less than k_{dif}. The corresponding distributions N_k and n_k are a set of δ-function peaks, which fall off away from the growth-rate region corresponding to $k \sim k_0$ (it is assumed that $\Delta k \ll k_{dif}$) into the region of small values of k and are separated from each other by distances of k_{dif} and $2k_{dif}$, respectively. The envelope of these peaks is described by the differential approximation.

11.2. Time-dependent spectra and the validity of the one-dimensional description

The steady-state distributions of Langmuir and ion-sound oscillations were derived above. There appears the problem of their onset and dynamics. It is impossible to obtain an analytical solution of this problem and one has to use numerical simulations. It was shown in [134] that within the one-dimensional model at sufficiently low excesses above threshold $\gamma_{k_0}/\nu_{ei} \gg k_0/\Delta k$, in which case the waves are damped before they reach the region $k \sim 0$, the steady-state distributions are in fact established in a time of the order of $(20\text{--}40)\gamma_{k_0}^{-1}$. Fig. 11.1(a, b) show a typical steady-state spectrum for $\nu_{ei} \simeq \gamma_{2k}^s$. As expected, in the case of "narrow" excitation $\Delta k \leq k_{dif}$ the densities N_k, n_k consist of a sequence of decreasing peaks spaced at intervals of k_{dif} for Langmuir waves and $2k_{dif}$ for the ion-sound waves. In the case $\Delta k \geq k_{dif}$ the N_k, n_k are smooth functions modulated with $\sim k_{dif}$. In the case $\gamma_{k_0}/\nu_{ei} \gg k_0/k_{dif}$ no steady-state spectra are established. The behavior of N_k and n_k is essentially nonstationary and it varies depending on the ratio of damping rates ν_{ei}/γ_k^s. In all these cases there occurs a wave accumulation at $k \sim 0$ - the formation of a condensate.

We turn now to the two most interesting cases.

1. With a "doubly infinite" excitation level, $\gamma_{k_0} \gg \gamma_{2k}^s$, $\gamma_{k_0} \gg \nu_{ei}$, we can neglect by the wave damping. Converting to the differential approximation, we obtain

$$N_\kappa - 2\frac{\partial n_{2\kappa}}{\partial \kappa} = f(\kappa), \qquad \frac{\partial n_{2\kappa}}{\partial \tau} = 2\alpha' \left(N_\kappa^2 + n_{2\kappa}\frac{\partial N_\kappa}{\partial \kappa} \right); \qquad (11.29, 11.30)$$
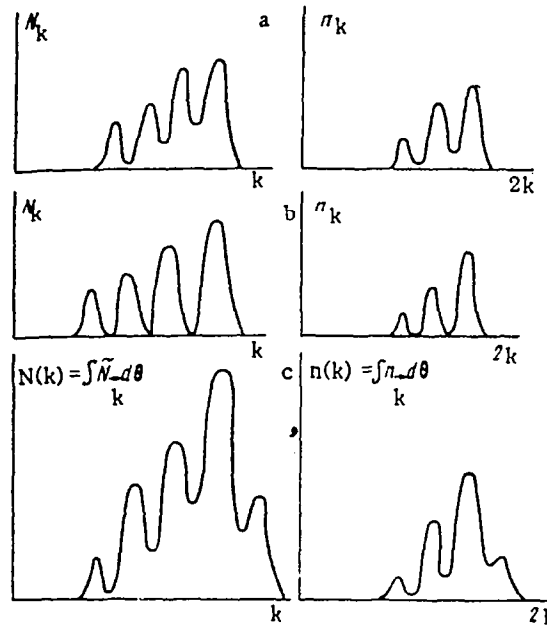

Fig. 11.1. (a) Steady-state one-dimensional distributions of N_k and n_k for $\Delta k \simeq 2k_{dif}$; $\gamma_{k_0}/\nu_{ei} = 2.7$; $\gamma_{2k}^s \sim \nu_{ei}$; (b) the same, for $\Delta k \simeq 0.8 k_{dif}$; $\gamma_{k_0}/\nu_{ei} = 2.7$; $\gamma_{2k}^s \simeq \nu_{ei}$; (c) average characteristics of the two-dimensional spectra $N(k) = \int N_k d\theta$, $n(k) = \int n_k d\theta$ for the case of a "narrow beam", with $\gamma_{max}/\nu_{ei} = 2.7$; $\gamma_{2k}^s \sim \nu_{ei}$.

where $\tau = \gamma_{k_0} t$, $\kappa = k/k_{\text{dif}}$, $\alpha' = \alpha \gamma_{k_0}^{-1}$. We now seek solutions which satisfy the initial condition $N_\kappa = n_{2\kappa} = 0$ at $t = 0$. Then from (11.29), (11.30) we find

$$\frac{\partial n_{2\kappa}}{\partial \tau} = 4\alpha' \left[2\left(\frac{\partial n_{2\kappa}}{\partial \kappa}\right)^2 + n_{2\kappa} \frac{\partial^2 n_{2\kappa}}{\partial \kappa^2} \right], \qquad N_\kappa = 2\frac{\partial n_{2\kappa}}{\partial \kappa} . \qquad (11.31, 11.32)$$

Eq. (11.31) can be rewritten in the form

$$\partial n_{2\kappa}^2/\partial \tau = (8\alpha'/3)(\partial^2 n_{2\kappa}^3/\partial \kappa^2) . \qquad (11.33)$$

An equation of this type arises, for example, in the study of the nonlinear filtering of a liquid or gas. Strictly speaking, Eq. (11.31) holds only for $0 < \kappa < \kappa_0$. We will formally construct its solution for an arbitrary $\kappa < \kappa_0$ and the condition will be imposed

$$n_{2\kappa} = 0 \;\; \kappa \to -\infty .$$

Eq. (11.33) is satisfied by the family of self-similar solutions

$$n_{2\kappa} = (\tau^{2\beta-1}/\alpha') \Phi(\kappa/\tau^\beta) ,$$

where $\Phi(\xi)$ is a smooth function of the dimensionless variable $\xi = \kappa/\tau^\beta$, and the self-similarity exponent β is determined from the boundary condition. It should be naturally to assume that for excitation of plasma waves in the inertial interval a solution with a constant flux of Langmuir quanta will be established. The value of this flux is determined at the boundary of the interval. According to (11.32) it corresponds to the condition

$$(\partial n_{2\kappa}/\partial \kappa)|_{\kappa=\kappa_0} = \text{const} > 0 . \qquad (11.34)$$

Precisely, this solution was realized during the numerical simulation of the exact equations (1.50)–(1.52) (see Fig. 11.2). It follows from condition (11.34) that self-similarity exponent $\beta = 1$ and the solutions of Eqs. (11.31) and (11.32) under these conditions are

$$n_{2\kappa} = \begin{cases} \dfrac{\gamma\kappa_0}{\alpha} \left[2t\gamma_{k_0} + \dfrac{(\kappa - \kappa_0)}{2} \right], & \kappa_0 - 4t\gamma_{k_0} < \kappa \leq \kappa_0 , \\[4mm] 0 , & \kappa < \kappa_0 - 4t\gamma_{k_0} , \end{cases} \qquad (11.35)$$

$$N_\kappa = \begin{cases} \dfrac{\gamma\kappa_0}{\alpha} , & \kappa_0 - 4t\gamma_{k_0} < \kappa \leq \kappa_0 , \\[4mm] 0 , & \kappa < \kappa_0 - 4t\gamma\kappa_0 . \end{cases} \qquad (11.36)$$

Fig. 11.2 shows the numerical solution of (11.4) for the case $\nu_{ei} \equiv \gamma_{2k}^s \equiv 0$ at three successive times.
    The plot of the N_k envelope is reminiscent of the propagation of a shock wave at a constant velocity

$$\nu_0 = 4\gamma_{k_0} k_{\text{dif}} . \qquad (11.37)$$

(see (11.35), (11.36)) into the region of small wave numbers. The exact solution differs from (11.36) only in a small region. The n_{2k} envelope is also essentially the same as the line segment in (11.35) everywhere; it moves parallel to itself at the same velocity ν_0. The ratio of the integral intensities of
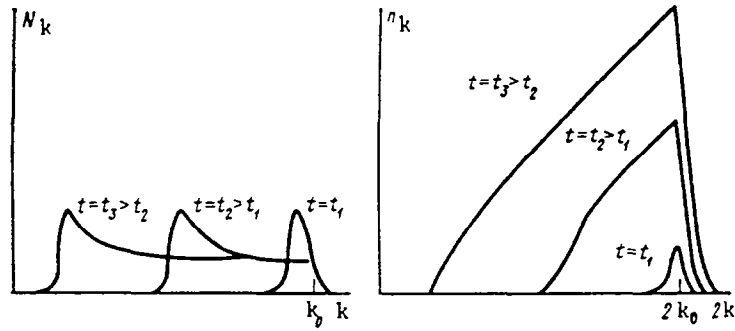
Fig. 11.2. Time-dependent one-dimensional spectra for a "double-infinite" excitation level ($\gamma_{k_0} \gg \nu_{ei}$; $\gamma_{k_0} \gg \gamma_k^s$) at three successive times.

the ion-sound and Langmuir waves increases linearly with the time in this case. For the parameter regions $\gamma_{k_0}/\gamma_{2k}^s \gg 1$, $\gamma_{k_0}/\nu_{ei} \gg 1$, the self-similar solutions in (11.35), (11.36) thus give a good description of the behavior of the N_k and n_{2k} spectral distributions.

2. If $\gamma_{2k}^s \gg \gamma_{k_0}$ and $\gamma_{k_0} \gg \nu_{ei}$, we can ignore the damping of the plasma waves and the terms containing n_k. Then Eq. (11.4) for N_k is the same as the kinetic equation describing the evolution of Langmuir waves due to induced scattering by the strongly damped ion-sound. The time-dependent solutions of this equation were studied in detail in Sections 3–6, where it was shown that these solutions correspond to a sequence of solitons with an amplitude $N_k \sim (\gamma_{k_0}/\alpha)\ln[\gamma_{k_0}/(\alpha N_0)]$ which are travelling along a chain of peaks at a constant velocity $v_0 \sim \gamma_{k_0} k_{dif}$ (cf. (11.37)) toward small values of k. The results of a numerical simulation of (11.4) for these parameters show that the N_k spectrum is approximately the same as that found in part I, while the level of the ion-sound is $n_{2k} \sim \gamma_{k_0}/\gamma_{2k}^s N_k$, as follows from (11.4).

After investigation of the one-dimensional spectra it is necessary to examine their stability with respect to three-dimensional perturbations, i.e. the excitation of waves outside the jets (external stability). According to [134], the waves lying within the cone $\theta < \theta_0$ are unstable. The cone angle θ_0 depends on the excess above threshold of the wave pumping. At $\nu_{ei} \gg \gamma_{2k}^s$ there is

$$\theta_0 \simeq (\gamma_k^s/\nu_{ei})(\Delta k/k_{dif})^2(\gamma_{k_0}/\nu_{ei})^2 ,$$ (11.38)

and in the opposite case $\gamma_k^s \gg \nu_{ei}$:

$$\theta_0 \simeq \tfrac{1}{4}(\nu_{ei}/\gamma_k^s)(\Delta k/k_{dif})^2(\gamma_{k_0}/\nu_{ei})^2 .$$ (11.39)

The jets are thus unstable with respect to three-dimensional perturbations, but if the excitation level is only slightly above threshold the instability region in the inertial interval is extremely narrow and is localized near the jets. On this basis one can expect a stabilization of an external instability of the one-dimensional jets by a small angular broadening, as it was in the case of induced scattering. These qualitative considerations were tested [134] in a series of numerical simulations of the exact equations (1.50)–(1.52) in the case of excitation of waves by a relativistic electron beam with the angular spreading $\Delta\theta$ (for the corresponding dependences of the growth rate γ_b see Section 6).

According to the numerical simulations, the wave spectra are anisotropic in all cases. In the region where the energy is concentrated ($\gamma_b \neq 0$), the N_k and n_k distributions correspond to a single two-dimensional jet, whose position is essentially the same as the line of the maximum beam growth rate. In the inertial region, the waves are concentrated in rather narrow angular intervals near $\theta = 0$ and $\theta = \pi$. The width of jets is governed by the properties of the kinetic equations and the parameters of the problem, γ_k^s, ν_{ei} and γ_{max}. The width remains, however, much smaller than $\pi/2$ at $\Delta\theta < 1$. A slight broadening with respect to the angle θ is thus sufficient to keep the solutions corresponding to narrow jets. The wave distribution along these jets can take quite different forms, depending on γ_k^s/γ_{max} and ν_{ei}/γ_{max}. The results of the numerical simulations for several typical cases are represented in Figs. 11.3–11.5. In the first series of calculations $\Delta\theta$ was taken to be $10°$ (a "narrow" beam). At this case in the inertial interval waves are concentrated in the narrow regions near $\theta = 0$ and $\theta = \pi$, and they take the form of a sequence of decreasing peaks (see Fig. 11.3). Comparison of the numerical solution of (11.4) reveals good agreement with the one-dimensional model (Fig. 11.1) Increasing of $\Delta\theta$ up to $20–25°$ (a "broad" beam) we find that quasi-one-dimensional jets were spread out (both for steady-state cases $\gamma_{max}/\nu_{ei} = 2$ 5, $\nu_{ei} \simeq \gamma_{2k}^s$ and for double-infinite cases $\gamma_{max} \gg \nu_{ei}$; $\gamma_{max} \gg \gamma_{2k}^s$) forming a complex relief which approached a quasi-isotropic distribution (Fig. 11.4). Nevertheless, even for an instability-cone angle of order unity, the ratio of the wave intensities of $\theta = 0$ and $\theta = \pi/2$ was two or three orders of magnitude, as can be seen from Fig. 11.5, which shows the N_k and n_k distributions for several fixed values of k.
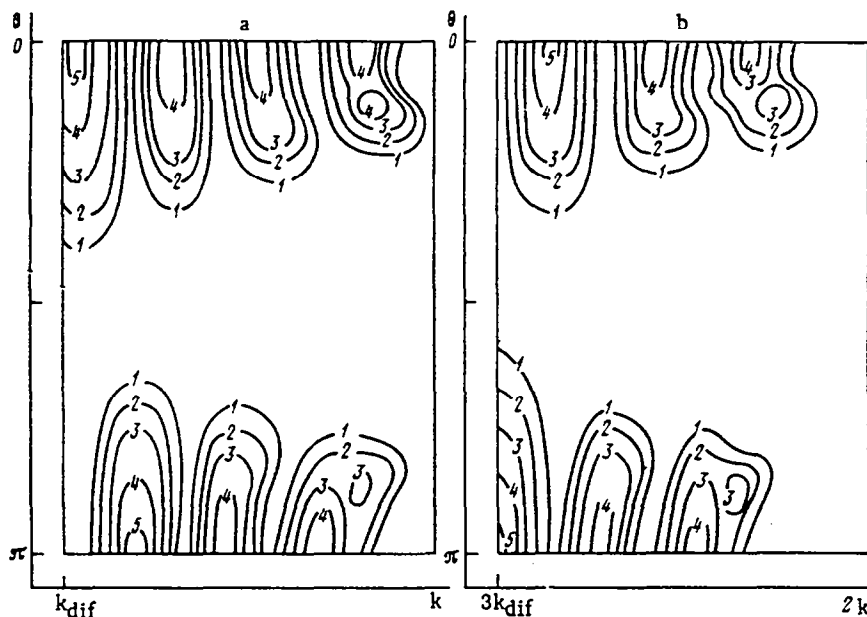

Fig. 11.3. Lines of constant value of the function: (a) $\ln(N_k/N_0)$, (b) $\ln(n_k/n_0)$, for the case of a "narrow beam" and for an excitation level far above the threshold $\gamma_{max}/\nu_{ei} = 15$; $\gamma_{2k}^s/\nu_{ei} \sim 0.1$ with $t \sim 20\gamma_{max}^{-1}$.
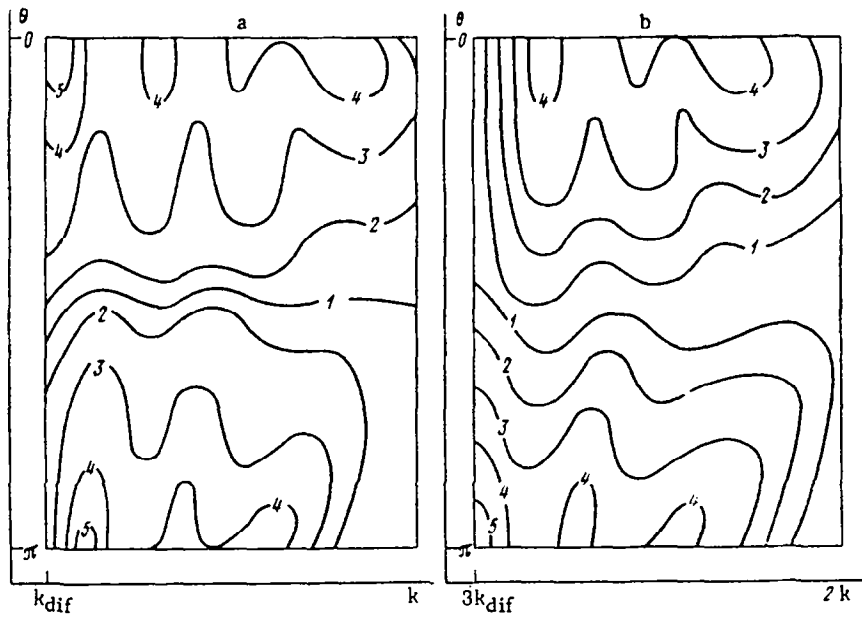
Fig. 11.4. Lines of constant level of the function (a) $\ln(N_k/N_0)$ and (b) $\ln(n_k/n_0)$ for a "broad beam" and for a "double-infinite" excitation level.
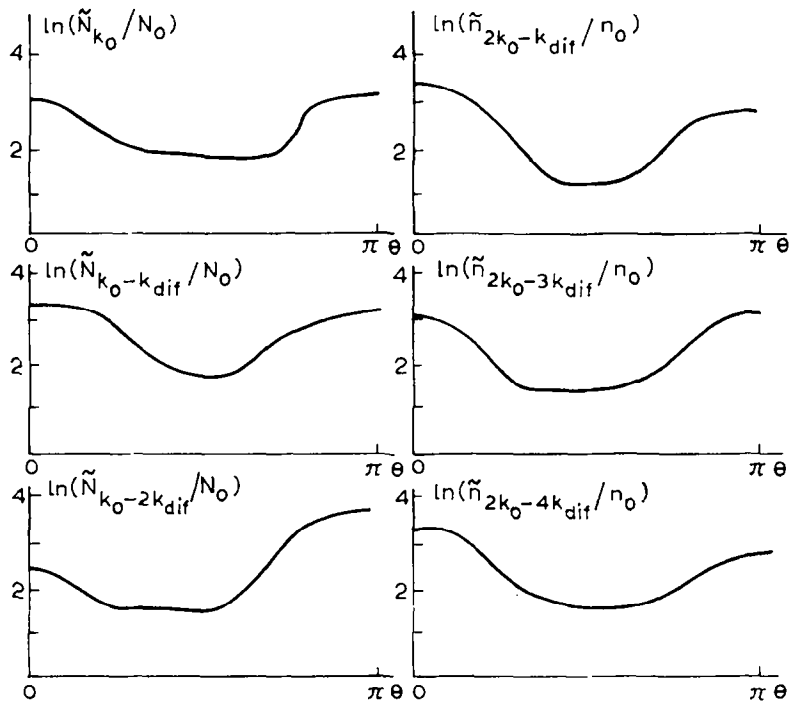
Fig. 11.5. Angular variation of spectral distributions for several fixed values of the modulus of the wave vector.

It follows from these results that for an excitation of waves uniform over angle (or close to uniform) an isotropic approximation must be used. It occurs, for example, at the decay of an electromagnetic wave into two Langmuir oscillations [135]. The anomalous absorption of laser radiation in a plasma corona is determined mainly by this nonlinear process.

12. Isotropic approximation

Taking the average of (1.50)–(1.52) over angles it can be found that

$$
\left(\frac{\partial}{\partial t} + 2\Gamma\right) N_k = U^2 \int_{k-k_{\text{dif}}}^{k} \left[\frac{(k^2 - k_1^2)^2 - k_{\text{dif}}^2(k^2 + k_1^2)}{2k_1 k k_{\text{dif}}^2}\right]^2 \left(\frac{k^2 - k_1^2}{k_{\text{dif}}}\right)^2
$$

$$
\times \left\{(N_{k_1} - N_k)n\left(\frac{k^2 - k_1^2}{k_{\text{dif}}}\right) - N_k N_{k_1}\right\} \frac{k_1 \, dk_1}{k k_{\text{dif}}}
$$

$$
+ U^2 \int_{k}^{k+k_{\text{dif}}} \left[\frac{(k_1^2 - k^2)^2 - k_{\text{dif}}^2(k_1^2 + k^2)}{2k_1 k k_{\text{dif}}^2}\right]^2 \left(\frac{k_1^2 - k^2}{k_{\text{dif}}}\right)^2
$$

$$
\times \left\{n\left(\frac{k_1^2 - k^2}{k_{\text{dif}}}\right)(N_{k_1} - N_k) + N_k N_{k_1}\right\} \frac{k_1 \, dk_1}{k k_{\text{dif}}} ; \tag{12.1}
$$

$$
\left(\frac{\partial}{\partial t} + 2\gamma^s\right) n_k = U^2 \int_{\frac{k-k_{\text{dif}}}{2}}^{\infty} \frac{(2k_2^2 + k k_{\text{dif}} - k^2)^2}{8k_2(k_2^2 + k k_{\text{dif}})}
$$

$$
\times [N(\sqrt{k_2^2 + k k_{\text{dif}}})(n_k + N_{k_2}) - N_{k_2} n_k] \, dk_2 ;
$$

$$
U^2 = \frac{\omega_p}{12\pi M n_0 c_s r_D^2} . \tag{12.2}
$$

Let us first consider the case of strong ion-sound damping $\gamma_k^s \gg \nu_{\text{ei}}$ (induced-scattering approximation) when it is possible to neglect terms proportional to n_k (Fig. 12.1). Shortened equations

$$
\frac{\partial N_k}{\partial t} = N_k \int_{k-k_{\text{dif}}}^{k+k_{\text{dif}}} T_{kk'} N_{k'} \, dk' \tag{12.3}
$$

differ from their analog (1.41) at first by the bounded integration region $(k \pm k_{\text{dif}})$ which is determined on the decay conditions and also by the qualitatively different kernel $T_{kk'}$ (for comparison of the kernels see Fig. 12.2), for example, $|T(k, k + k_{\text{dif}})| \neq |T(k, k - k_{\text{dif}})|$. Furthermore, in a nonisothermal plasma $T_{kk'}$ is a nonanalytic function and the problem of the existence of a steady-state solution is not a trivial one. It is not difficult to show that, in contrast to the isothermal plasma case, a solution corresponding to a set of infinitely narrow peaks $N_j \delta(k - jk_{\text{dif}})$ is unstable. It is natural to apply numerical simulations of Eqs. (12.1), (12.2) in this unclear situation [135]; some typical results of these calculations are shown in Fig. 11.2. The spectral distribution is a set of narrow peaks, as in an isothermal plasma. In precisely the same way, the relaxation to the steady-state requires a very long time, much longer than the reciprocal growth rates involved. It occurs also that at the reducing of the damping rate within a broad interval (from unity to hundred)
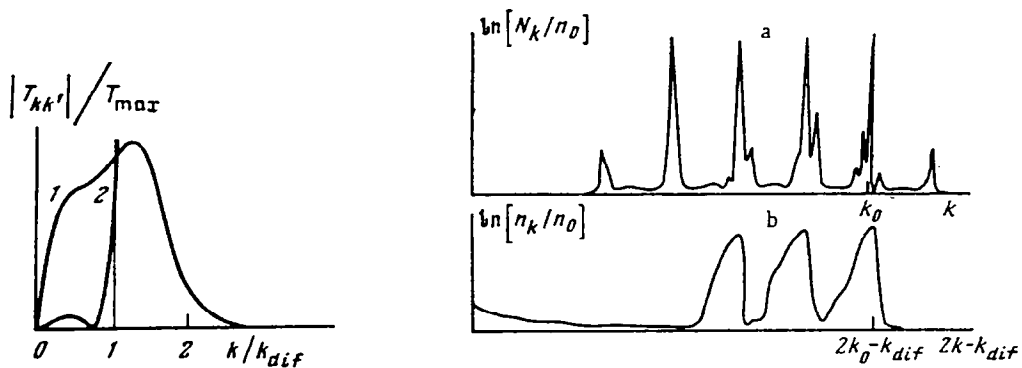
Fig. 12.1. The induced-scattering matrix element $|T_{kk'}|/T_{max}$, averaged over angles. Curve 1, isothermal plasma; curve 2, nonisothermal plasma.

Fig. 12.2. Steady-state wave distribution for three-times excess above threshold. The initial value $n_0 = 2 \times 10^{-3}$.

the Langmuir spectrum remains essentially the same; there is only an increase in the sound level (n_k is also a set of a sharp peaks). Another characteristics of these results, which confirms the validity of the induced-scattering approximation, is the lack of pumping toward large k.

12.1. Transition to Kolmogorov situation

Let us consider the situation well above threshold, in which one can ignore the damping of both Langmuir and ion-sound oscillations everywhere except for very small values of k. In the long-wave part of the spectrum, a strong nonlinear dissipation due to Langmuir collapse comes into play. For acoustic waves, on the other hand, the inhomogeneity of the plasma and collisional damping becomes important. The regions of damping and pumping are thus separated in k-space, and we find the ordinary Kolmogorov problem of the turbulence spectra in the inertial interval. The spectra of the isotropic turbulence of a nonisothermal plasma were found in [137, 138] (see below) under the assumption that these are smooth distributions. If the wave excitation occurs in a narrow region in k-space, we cannot expect on the face of it that we will find a continuous wave distribution. Furthermore, one can see that Eqs. (12.1), (12.2) have satellite solutions. To determine the structure of the turbulence, a numerical simulation was carried out in [135]. As we can see in Fig. 12.3, there is a good coincidence between the results of these numerical simulations at the infinite excess above threshold $\Gamma = \gamma^s = 0$ and analytic dependences derived in Section 13.

The case of strong damping of Langmuir waves, in the approximation opposite to the induced-scattering approximation, is intermediate between the two discussed above. Fig. 12.4 shows the results of numerical calculations for this situation. The spectrum is seen to take the form of a smoothy varying pedestal with sharp peaks. As the growth rate is increased and the damping rate of the ion-sound decreased, the peaks become blurred, and a transition to the Kolmogorov situation takes place.
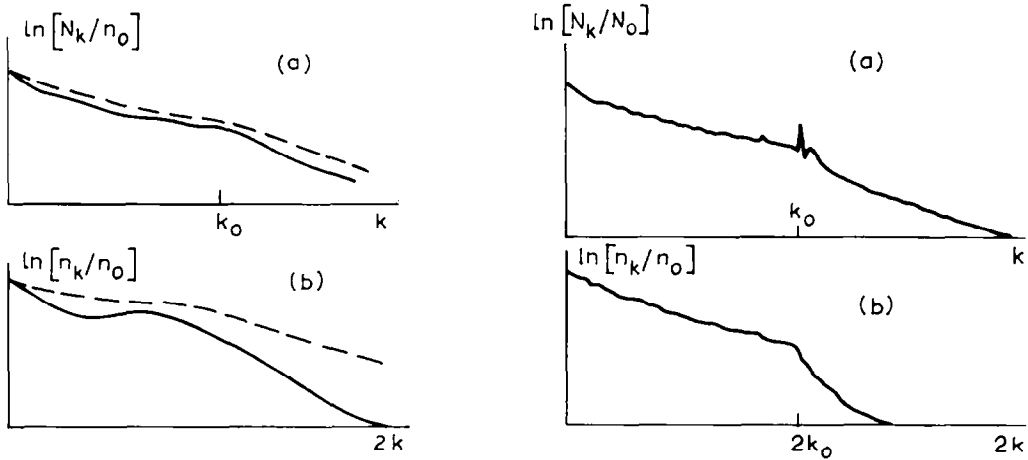
Fig. 12.3. Distribution of Langmuir and ion-sound waves for an infinite excess above the threshold, $\Gamma = \gamma = 0$. The dashed curves show spectra derived analytically by means of conformal mapping. The deviation from Kolmogorov spectra at $k > k_0$ results from Landau damping introduced in the numerical simulations and from the slower relaxation of the spectra at $k > k_0$.

Fig. 12.4. Steady-state wave distributions for five-times excess above threshold, $\Gamma = 100\gamma_{2k_0}$, $n_0 = 2 \times 10^{-3}$.

13. Kolmogorov spectra in nonisothermal plasmas

In nonisothermal plasmas the situation differs from the usual Kolmogorov case [136] by the absence of scale invariance and the presence of a characteristic length of the decay interaction k_{dif}. But for smooth spectra, as we know already, it is possible to change to the differential approximation and obtain scale invariant isotropic equations [137]. For this purpose it is necessary to expand the δ-functions of the frequencies in (1.50)–(1.52) as a series in Ω_k and to assume that N_k, n_k are isotropic:

$$\partial n_k/\partial t = \int R_{k|k_1 k_2}\, dk_1\, dk_2\ , \qquad \partial N_K/\partial t + \mathrm{div}_k p_N = 0\ , \tag{13.1, 13.2}$$

$$\partial \varepsilon_k/\partial t = -\,\mathrm{div}_k\, \omega_k p_N + \int (\Omega_k R_{k|k_1 k_2} - \Omega_{k_1} R_{k_1|kk_2})\, dk_1\, dk_2\ , \tag{13.3}$$

where

$$R_{k|k_1 k_2} = 2\pi|V_{kk_1 k_2}|^2 (N_{k_1}^2 + n_k \Omega_k (\partial N_{k_1}/\partial \omega_{k_1}))\delta_{k-k_1+k_2}\delta(\omega_{k_1} - \omega_{k_2})\ :$$

and

$$p_N = (k/k)\int \Omega_{k_2}/\omega_k\, R_{k_2|kk_1}\, dk_1\, dk_2$$

is the density of Langmuir quanta flux, $\varepsilon = \omega_k N_k + n_k \Omega_k$. Eqs. (13.1)–(13.3) have solutions in the form of Rayleigh–Jeans distributions which cause the fluxes of quanta $P_N = 0$ and energy $P_\varepsilon = 0$ to vanish ($R_{k|k_1,k_2} = 0$). We shall consider solutions with constant fluxes P_N and P_ε. The constancy of these fluxes corresponds to the power-law solutions:

$$N_k = Ak^x , \qquad n_k = Bk^x \omega_k / \Omega_k . \tag{13.4}$$

The turbulence spectra corresponding to a constant flux of the number of Langmuir waves are realised in the range $k < k_0$, whereas the spectra corresponding to $P_\varepsilon = $ const are realised in the range $k > k_0$; these fluxes are directed in opposite ways: P_N to the long-wavelength oscillations, where Langmuir waves are dissipated by collapse, and P_ε to the range of short waves, where the dissipation of ion-sound due to Landau damping by electrons is important. These spectra have the following form in the above-mentioned regions:

$$\begin{aligned} \varepsilon_k^l &= \omega_p A_1 / k^2 , & \varepsilon_k^s &= 3/2\omega_p r_D^2 B_1 , & k &< k_0 , \\ \varepsilon_k^l &= \omega_p A_2 / k^3 , & \varepsilon_k^s &3/2\omega_p r_D^2 B_2 / k , & k &> k_0 , \end{aligned} \tag{13.5}$$

where the constants A_1, B_1 and A_2, B_2 are deduced from the constancy of the fluxes P_N and P_ε and from the condition of their matching with the growth region. The condition for P_N can be written in the form:

$$P_N \sim \gamma \Delta k k_0^2 N_{k_0}$$

and hence it follows from (13.2) that

$$A_1 \sim B_1 \sim n_0 T (\gamma / \omega_p)(\Delta k / k_{dif}^2) .$$

The quantities A_2 and B_2 are determined from the continuity of the energy flux of the ion-sound waves P_s at $k = k_0$. We can easily see why such a flux appears for $k < k_0$. This is due to the fact that as a result of the transfer of Langmuir waves to the region $k \approx 0$ and their dissipation in this region, ion-sound is generated and accumulated. We recall that for $k < k_0$, where $P_N = $ const,

$$P_\varepsilon = 3/2\omega_p (kr_D)^2 P_N + P_s = 0 ,$$

i.e.

$$P_s = -3/2\omega_p (kr_D)^2 P_N ,$$

and is directed toward higher values of k. For a similar reason in the region $k > k_0$, where $P_\varepsilon = $ const and $P_N = 0$, the energy flux of the ion-sound waves is identical with P_ε. Hence, it follows from the condition of continuity of P_s at $k = k_0$ that

$$A_2 \sim B_2 \sim n_0 T (\gamma / \omega_p)(\Delta k k_0 / k_{dif}^2) .$$

In conclusion we have to say that all spectra (13.5) are local.

We see that in the most interesting three-dimensional case those occurs a degenerate situation, namely, the coincidence of Kolmogorov and thermodynamic spectra. As a result, there is no plasmon cascading over k-space. This problem was investigated in [138]. It was shown that in such

a degenerate situation the Kolmogorov spectra are slightly different from the power ones. For example, for $k < k_0$ they are (in dimensional variables):

$$N_k = y/k_2 \sqrt{P/U^2 k_{\mathrm{dif}}} \; ; \qquad n_k = z/k k_{\mathrm{dif}} \sqrt{P/U^2 k_{\mathrm{dif}}} \; . \tag{13.6}$$

Asymptotically, $y \simeq (\ln k^2)^{1/2}$, $z \simeq y + 4/y$; $y \gg 1$. Since z, y vary logarithmically, the spectra differ little in a form from (13.5), although, unlike the latter, they ensure a nonzero flux into the small k region.

Acknowledgments

References

[1] V.E. Zakharov, J. Appl. Mech. Tech. Phys. 4 (1965) 35.
[2] V.E. Zakharov, Sov. Phys. JETP 24 (1967) 457.
[3] V.E. Zakharov and N.N. Filonenko, Sov. Phys. Dokl. 170 (1966) 1292.
[4] V.E. Zakharov and N.N. Filonenko, J. Appl. Mech. Tech. Phys. 5 (1967) 62.
[5] A.M. Balk and V.E. Zakharov, Plasma Theory and Nonlinear and Turbulent Processes in Physics (World Scientific, Singapore, 1986).
[6] V.E. Zakharov, V.S. L'vov and G. Falkovich, Kolmogorov Spectra of Turbulence I (Springer, Berlin, 1992).
[7] A.A. Galeev and R.Z. Sagdeev, in: Basic Plasma Physics, Vol. 1, eds., A.A. Galeev and R.N. Sudan (North-Holland, Amsterdam, 1983).
[8] V.E. Zakharov, S.L. Musher and A.M. Rubenchik, Phys. Rep. 29 (1985) 286.
[9] D.F. Dubois and M.V. Goldman, Phys. Rev. Lett. 28 (1972) 218.
[10] W.L. Kruer and E.J. Valeo, Phys. Fluids 16 (1973) 675.
[11] J.A. Fejer and Y.Y. Kuo, Phys. Fluids 16 (1973) 1490.
[12] B.N. Breizman, V.E. Zakharov and S.L. Musher, Sov. Phys. JETP 37 (1973) 658.
[13] V.E. Zakharov, S.L. Musher and A.M. Rubenchik, Sov. Phys. JETP 42 (1975) 80.
[14] P. Cheung and D.F. Dubois, J. Geophys. Res. 97 (1992) 10.575.
[15] P. Stubbe, H. Kohl and M. Rietveld, J. Geophys. Res. 97 (1992) 6285.
[16] V.E. Zakharov, Sov. Phys. JETP 35 (1973) 908.
[17] V.E. Zakharov, Basic Plasma Physics, Vol. 2 (North-Holland, Amsterdam, 1983).
[18] V.D. Shapiro and V.I. Shevchenko, Basic Plasma Physics, vol. 2 (North-Holland, Amsterdam, 1983).
[19] P. Robinson and D.L. Newman, Phys. Fluids B 1 (1989) 2319.
[20] M.V. Goldman, D.L. Newman and F.W. Perkins, Phys. Rev. Lett. 70 (1993) 4075.
[21] D.F. Dubois, D. Russell and H. Rose, Reduced description of strong Langmuir turbulence from kinetic theory, Phys. Plasmas, submitted.
[22] G.W. Hammet and F.W. Perkins, Phys. Rev. Lett. 64 (1990) 3019.
[23] D.F. Dubois, H. Rose and D. Russell, Phys. Rev. Lett. 61 (1988) 2209.
[24] V.E. Zakharov, S.L. Musher and A.M. Rubenchik, Phys. Rep. 129 (1985) 286.

[25] B.B. Kadomtsev, Plasma Turbulence (Academic Press, London, 1965).
[26] A.A. Galeev and R.Z. Sagdeev, Basic Plasma Physics, Vol. 1 (North-Holland, Amsterdam, 1982).
[27] V.N. Tsytovich, Theory of Turbulent Plasma (Consultants Bureau, New York, 1977).
[28] V.E. Zakharov and V.S. L'vov, Radiophys. Quantum Electron. 18 (1976) 1084.
[29] S.L. Musher, A.M. Rubenchik and B.I. Sturman, Plasma Phys. 20 (1978) 121.
[30] A.M. Rubenchik, I.Ya. Rybak and B.I. Sturman, Sov. Phys. JETP 40 (1975) 678.
[31] B.N. Breizman, V.E. Zakharov and S.L. Musher, Sov. Phys. JETP 37 (1973) 658.
[32] A.A. Galeev and R.Z. Sagdeev, Basic Plasma Physics (North-Holland, New York, 1983).
[33] V.N. Tsytovich, Theory of Turbulent Plasma (Consultants Bureau, New York, 1977).
[34] B.N. Breizman, in Reviews of Plasma Physics, Vol. 15, ed. B.B. Kadomtsev (Consultants Bureau, New York, 1990).
[35] V.D. Shafranov, in Reviews of Plasma Physics, Vol. 3, ed. M.A. Leontovich (Consultants Bureau, New York, 1967).
[36] H.C. Chen and J.A. Fejer, Phys. Fluids 18 (1975) 1809.
[37] A.M. Rubenchik, I.Ya. Rybak and B.I. Sturman, Sov. Phys. JETP 40 (1975) 678.
[38] A.M. Rubenchik, I.Ya. Rybak and B.I. Sturman, Sov. Phys. Tech. Phys. 21 (1976) 412.
[39] B.N. Breizman, V.M. Malkin and O.P. Sobolev, Sov. Phys. JETP 37 (1973) 658.
[40] W.L. Kruer and E. Valeo, Phys. Fluids 16 (1973) 675.
[41] V.E. Zakharov, S.L. Musher and A.M. Rubenchik, Sov. Phys. JETP Lett. 19 (1974) 151.
[42] D.F. Dubois and M.V. Goldman, Phys. Rev. Lett. 28 (1972) 218.
[43] V.E. Zakharov, S.L. Musher and A.M. Rubenchik, Sov. Phys. JETP 42 (1975) 80.
[44] V. Volterra, Leçons su 'la théorie mathématique de la butte pour la vie (Gauthier Villars, Paris, 1931).
[45] G. Picard and J.T. Johnston. Phys. Rev. Lett. 48 (1982) 1610.
[46] B.N. Breizman, Sov. Phys. JETP 48, Zh. Eksp. Teor. Fiz. 72 (1977) 518.
[47] V.E. Zakharov, S.L. Musher and A.M. Rubenchik, Phys. Rep. 129 (1985) 286.
[48] D.F. Dubois and M.V. Goldman, Phys. Rev. Lett. 28 (1972) 218.
[49] E.J. Valeo and W.L. Kruer, Phys. Fluids 16 (1973) 675.
[50] V.E. Zakharov, S.L. Musher and A.M. Rubenchik, Sov. Phys. JETP 42 (1975) 80.
[51] V.E. Zakharov, Sov. Phys. JETP 35 (1972) 908.
[52] V.E. Zakharov, Sov. Phys. JETP 33 (1971) 538.
[53] V.E. Zakharov, S.L. Musher and A.M. Rubenchik, Sov. Phys. JETP Lett. 19 (1974) 151.
[54] S.V. Manakov, Sov. Phys. JETP 40 (1975) 269.
[55] V.E. Zakharov, in: Basic Plasma Physics, Vol. 2, eds., A.A. Galeev and R.N. Sudan (North-Holland, New York, 1983).
[56] A. Dyachenko and V.E. Zakharov et al., Physica D 52 (1991) 78.
[57] D. Cheung and D. Dubois, J. Geophys. Res. 97 (1992) 10.575.
[58] D. Cheung and A. Wong, Phys. Fluids 28 (1985) 1538.
[59] D. Karfidov, A. Rubenchik, K. Sergeichev and I. Sychev, Sov. Phys. JETP 71 (1990) 892.
[60] B.N. Breizman in: Reviews of Plasma Physics, Vol. 15, ed. B.B. Kadomtsev (Consultants Bureau, New York, 1990).
[61] B.N. Breizman and V.V. Mirnov, Geomagnetizm i Aeronomiya 10 (1970) 34 (in Russian).
[62] B.N. Breizman, V.E. Zakharov and S.L. Musher, Sov. Phys. JETP 37 (1973) 658.
[63] V.E. Zakharov, S.L. Musher and A.M. Rubenchik, Sov. Phys. JETP 42 (1975) 80.
[64] G.I. Marchuk, Methods of Numerical Mathematics (Springer, Berlin, 1982).
[65] Ya.B. Zeldovich, E.V. Levich and R.A. Syunyaev, Sov. Phys. JETP 35 (1972) 733.
[66] V.E. Zakharov, S.L. Musher and A.M. Rubenchik, Sov. Phys. JETP Lett. 19 (1974) 151.
[67] S.L.J. Musher, Comput. Phys. 43 (1981) 250.
[68] E.J. Valeo, C. Oberman and F.W. Perkins, Phys. Rev. Lett. 28 (1972) 340.
[69] D.F. Dubois and M.V. Goldman, Phys. Rev. Lett. 28 (1972) 218.
[70] V.E. Zakharov, S.L. Musher, A.M. Rubenchik and B.I. Sturman, Institute of Automation and Electrometry, Siberian Branch of Russian Ac. Sci., Novosibirsk, Preprint 29 (1977).
[71] S.L. Musher and A.M. Rubenchik, Sov. J. Plasma Phys. 1 (1975) 536.
[72] V.S. L'vov, Wave Turbulence under Parametric Excitation (Springer, Berlin, 1992).

[73] A.A. Galeev and R.Z. Sagdeev, Basic Plasma Physics, Vol. 1 (North-Holland, Amsterdam, 1982).
[74] V.E. Zakharov, S.L. Musher and A.M. Rubenchik, Phys. Rep. 229 (1985) 286.
[75] L.D. Landau and E.M. Lifshitz, The Classical Theory of Fields (Pergamon, Oxford, 1971).
[76] E.A. Kuznetsov and N.N. Noskov, Sov. Phys. JETP 48 (1978) 57.
[77] V.N. Tsytovich, The Theory of Turbulent Plasma (Consultants Bureau, New York, 1974).
[78] I.Ya. Shapiro, Sov. J. Plasma Phys. 11 (1985) 412.
[79] A.M. Rubenchik, I.Ya. Rybak and B.I. Sturman, Sov. Phys. JETP 40 (1975) 678.
[80] A.M. Rubenchik, I.Ya. Rybak and B.I. Sturman, Sov. Phys. Tech. Phys. 21 (1976) 412.
[81] B.I. Sturman, Radiophys. Quantum Electron. 17 (1976) 1348.
[82] B.I. Sturman, Sov. Phys. JETP 44 (1976) 322.
[83] A. Rogister and G. Hassellberg, Phys. Fluids 19 (1976) 108.
[84] I.Ya. Shapiro, Sov. J. Plasma Phys. 11 (1985) 412.
[85] I.Ya. Rybak, Sov. J. Plasma Phys. 7 (1981) 360.
[86] S.L. Musher, A.M. Rubenchik and B.I. Sturman, Plasma Phys. 20 (1978) 1131.
[87] S.L. Musher, A.M. Rubenchik and I.Ya. Shapiro, Sov. Phys. JETP 63 (1986) 519.
[88] V. Formisano, Plasma Astrophysics, ESA, SP-261 (1981) 145.
[89] V. Formisano, A.A. Galeev and R.Z. Sagdeev, Planet. Spa. Sci. 21 (1981) 526.
[90] S.L. Musher and B.I. Sturman, Sov. Phys. JETP Lett. 22 (1975) 265.
[91] V.D. Shapiro, V.I. Shevchenko, G.I. Solov'ev, V.P. Kalinin, R. Bingham, R.Z. Sagdeev, M. Ashour-Abdalla, J.J. Dawson and J.J. Su, Phys. Fluids B 5 (1993) 3148.
[92] O.L. Vaisberg, A.A. Galeev, G.N. Zastenker, S.I. Klinov, M.N. Nozdrachev, R.Z. Sagdeev A.Yu. Sokolov and V.D. Shapiro, Sov. Phys. JETP 85 (1983) 716.
[93] A.B. Mikhailovskii, Theory of Plasma Instabilities, Vol. 2 (Consultants Bureau, New York, 1974).
[94] B.D. Ochirov and A.M. Rubenchik, Sov. Phys. JETP 54 (1981) 79.
[95] B.N. Breizman, in: Reviews of Plasma Physics, ed. B.B. Kadomtsev (Consultants Bureau, New York, 1991).
[96] B.D. Ochirov and A.M. Rubenchik, Proc. Internat. Conf. on Plasma Phys., Sweden, Göteborg, Vol. 2 (1982) 111.
[97] K. Nishikawa and D.D. Ryutov, J. Phys. Soc. Japan 41 (1976) 1757.
[98] B.D. Ochirov and A.M. Rubenchik, Sov. J. Plasma Phys. 1 (1985) 101.
[99] L.V. Krupnova and V.T. Tikhonchuk, Sov. Phys. JETP 50 (1979) 917.
[100] V.E. Zakharov, S.L. Musher and A.M. Rubenchik, Phys. Rep. 229 (1985) 286.
[101] V.P. Silin and V.T. Tikhonchuk, Parametric Plasma Turbulence (North-Holland, Amsterdam, 1986).
[102] K. Nishikawa and M. Wakatani, Plasma Physics: Basic Theory with Fusion Applications (Springer, Berlin, 1990).
[103] V.E. Zakharov, V.S. L'vov and S.S. Starobinets, Sov. Phys. Usp. 17 (1975) 896.
[104] V.V. Vas'kov and A.V. Gurevich, Sov. Phys. JETP 39 (1974) 821.
[105] S.L. Musher and A.M. Rubenchik, Sov. J. Plasma Phys. 1 (1975) 536.
[106] V.V. Zautkin, V.E. Zakharov, V.S. L'vov, S.L. Musher and S.S. Starobinets, Sov. Phys.-JETP 62 (1972) 1782.
[107] M. Porkolab, Physica B and C 82 (1976) 186.
[108] I.Ya. Shapiro, Sov. J. Plasma Phys. 11 (1985) 412.
[109] A.M. Rubenchik, I.Ya. Rybak and B.I. Sturman, Sov. Phys. JETP 40 (1975) 678.
[110] S.L. Musher, A.M. Rubenchik and B.I. Sturman, Plasma Phys. 20 (1978) 1131.
[111] G.L. Payne, D.R. Nicholson and M.-M. Shen, Phys. Fluids B 1 (1989) 1737.
[112] D.F. Dubois, H.A. Rose and D. Russell, Phys. Rev. Lett. 66 (1991) 1970.
[113] P.A. Robinson, D.L. Newman and A.M. Rubenchik, Phys. Fluids B 4 (1992) 2509.
[114] A. Haussen, E. Mjølhus, D.F. Dubois and H.A. Rose, J. Geophys. Res. 97.A8 (1992) 125.
[115] J.A. Fejer, M.P. Sulzer and F. Djuth, J. Geophys. Res. 96.A5 (1991) 985.
[116] P.Y. Cheung and D.F. Dubois et al., J. Geophys. Res. 97.A7 (1992) 10 575.
[117] P. Stubbe et al. Proc. "Nonlinear modification of ionosphere", Santa-Fe, 1993.
[118] M. Porkolab, Physica B and C 82 (1976) 186.
[119] A.A. Vedenov and L.I. Rudakov, Sov. Phys. Dokl. 9 (1965) 1073.
[120] V.S. L'vov and A.M. Rubenchik, Sov. Phys. JETP 45 (1977) 67.
[121] V.E. Zakharov, S.L. Musher and A.M. Rubenchik, Phys. Rep. 229 (1985) 286.

[122] A.M. Rubenchik, Radiophys. Quantum Electron. 17 (1976) 249.
[123] A. Hasegawa, Phys. Fluids 13 (1971) 517.
[124] V.E. Zakharov, Sov. Phys. JETP 35 (1973) 908.
[125] V.N. Tsytovich, Theory of Turbulent Plasma (Consultants Bureau, New York, 1977).
[126] A.M. Rubenchik and E.G. Shapiro, Sov. Phys. JETP 76 (1993) 48.
[127] A.A. Galeev, R.Z. Sagdeev, V.D. Shapiro and V.I. Shevchenko, Sov. Phys. JETP 46 (1977) 711.
[128] J. Dawson and W. Kruer, Phys. Fluids 15 (1972) 446.
[129] D.F. Dubois, A. Haussen, H. Rose and D. Russell, Phys. Fluids B 5 (1992) 2616.
[130] B. Bauer et al., Bull. Amer. Phys. Soc. 38 (1993) 1912.
[131] V.E. Zakharov, V.S. L'vov and A.M. Rubenchik, Sov. Phys. JETP Lett. 25 (1977) 8.
[132] B.N. Breizman, in: Reviews of Plasma Physics, Vol. 15, ed. B.B. Kadomtsev (Consultants Bureau, New York, 1990).
[133] M.V. Goldman, D. Newman, D. Russel, D.F. Dubois, H. Rose, R. Drake and A. Rubenchik, New regimes of radiation driven Langmuir turbulence near the decay instability threshold, Phys. Fluids submitted.
[134] S.L. Musher, B.I. Sturman and I.Ya. Rybak, Sov. J. Plasma Phys. 5 (1979) 34.
[135] A.V. Kanashov, A.M. Rubenchik and I.Ya. Rybak, Sov. J. Plasma Phys. 8 (1982) 329.
[136] V.E. Zakharov in: Handbook of Plasma Physics, Vol. 2, eds. A. Galeev and R. Sudan (Elsevier, New York, 1984).
[137] V.E. Zakharov and E.A. Kuznetsov, Sov. Phys. JETP 48 (1978) 458.
[138] A.V. Kanashov and A.M. Rubenchik, Sov. Phys. Dokl. 25 (1980) 631.
[139] V.E. Zakharov, S.L. Musher and A.M. Rubenchik, Phys. Rep. 229 (1985) 286.